Fusaric acid alters global N^6-methyladenosine RNA methylation and PI3K/AKT signalling in U87MG cells

By

MCAYLIN MATADIN

BSc. Biology (Hons) (UKZN)

Submitted in fulfilment of the requirements for the degree of

Master of Medical Science

Discipline of Medical Biochemistry

School of Laboratory Medicine and Medical Sciences

College of Health Sciences

University of KwaZulu-Natal

2024

DECLARATION

I, _Mcaylin Matadin___, Student Number: __218027696__ declare that:

i. The research reported in this dissertation, except where otherwise indicated, is my original work.

ii. This dissertation has not been submitted for any degree or examination at any other university.

iii. This dissertation does not contain other person's data, pictures, graphs or other information, unless specifically acknowledged as being sourced from other persons.

iv. This dissertation does not contain other person's writing, unless specifically acknowledged as being sourced from other researchers. Where other written sources have been quoted then:

a. Their words have been re-written, but the general information attributed to them has been referenced.

b. Where their exact words have been used, their writing has been placed inside quotation marks and referenced.

v. Where I have reproduced a publication of which I am an author, co-author or editor, I have indicated in detail which part of the publication was actually written by myself alone and have fully referenced such publications.

vi. This dissertation does not contain text, graphics or tables copied and pasted from the internet, unless specifically acknowledged, and the source is in the dissertation and in the reference sections.

Student Signed: _____  _____ Date: _05 / 12 / 24_ __

ACKNOWLEDGEMENTS

Dr T. Ghazi

I wish to extend my deepest gratitude to you for your unwavering guidance, invaluable expertise, and encouragement throughout the course of this research. Your dedication and insightful feedback have been instrumental in shaping this thesis. Thank you for the endless support.

Prof. A.A. Chuturgoon

I am equally indebted to you for your exceptional mentorship, thought-provoking discussions, and constructive critique that continually inspired me to strive for academic excellence.

Ms. Neha Jivan

Thank you for your support, compassion, patience, and encouragement throughout this journey. Your belief in my abilities, even during the most challenging times, has been a source of immense strength and motivation.

My family and friends

Your steadfast support, patience and belief in me have been the foundation of my journey. Your encouragement kept me motivated during the most challenging times, and for that, I am eternally grateful.

My fellow master's students for 2024

I would also like to thank my fellow master's students, whose camaraderie, shared experiences, and collaborative spirit made this endeavour both enriching and enjoyable. The stimulating conversations and shared challenges have been invaluable.

The College of Health Sciences (CHS)

I express my sincere appreciation to the college for funding this project and providing the necessary resources. Your support has enabled me to undertake this research, and your commitment to fostering academic growth is deeply appreciated.

This work is a testament to the collective support and mentorship I have received, and I am truly grateful to all who contributed to its success.

PRESENTATIONS

Fusaric acid alters global N^6-methyladenosine RNA methylation and PI3K/AKT signalling in U87MG cells

Matadin, M., Chuturgoon, A.A., Ghazi, T.

College of Health Sciences Research Symposium (27th September 2024), University of Kwa-Zulu Natal, Durban, South Africa – 1st Prize Poster Presentation

ABBREVIATIONS

Akt	Protein kinase B
AMPK	AMP-activated protein kinase
ALKBH5	AlkB homologue 5
APS	Ammonium persulphate
ATP	Adenosine triphosphate
BCA	Bicinchoninic acid
BSA	Bovine serum albumin
BDNF	Brain-derived neurotrophic factor
BME	Bovine mammary epithelial cells
CBP	CREB-binding protein
CCM	Complete culture media
CCR4 - NOT	Carbon catabolite repression – negative on tata - less
cDNA	Complementary DNA
CLIP	Crosslinking immunoprecipitation
CO_2	Carbon dioxide
CRE	Cyclic-AMP-response element
CREB	Cyclic-AMP-response element binding protein
C_T	Cycle threshold
Cu^{2+}	Cupric ions
Cu^{+}	Cuprous ions
$CuSO_4$	Copper sulphate
dH_2O	Distilled water

DMSO	Dimethyl sulfoxide
DMEM	Dulbecco's modified eagle medium
DON	Deoxynivalenol
EGFR	Epidermal growth factor receptor
ELISA	Enzyme-linked immunosorbent assay
FA	Fusaric acid
FAO	Food and Agriculture Organization of the United Nations
FBS	Fetal bovine serum
FHB	*Fusarium* head blight
FOXO	Forkhead box transcription factors
FTO	Fat mass and obesity-related protein
GBM	Glioblastoma multiforme
GDP	Gross domestic product
GPCRs	G-protein-coupled receptors
H_2O_2	Hydrogen peroxide
HDAC	Histone deacetylase
HDAC1	Histone deacetylase
$HepG_2$ cells	Hepatocellular carcinoma cells
HNRNP	Heterogeneous nuclear ribonucleoprotein
hr	Hour
HRP	Horse-radish peroxidase
IC_{50}	Half-maximal inhibitory concentration
IGF1	Insulin-like growth factor 1
IGF2BP	Insulin-like growth factor 2 mRNA-binding proteins

IRS 1	Insulin receptor substrates 1
IRS 2	Insulin receptor substrates 2
KCl	Potassium chloride
m6A	N^6-methyladenosine
MAPK	Mitogen-activated protein kinase
$MgCl_2$	Magnesium chloride
METTL3	Methyltransferase-like 3
METTL14	Methyltransferase-like 14
METTL16	Methyltransferase-like 16
min	Minute
mRNA	Messenger RNA
mTOR	Mammalian target of rapamycin
mTORC2	Mammalian target of rapamycin complex 2
MTT	3-(4,5-dimethylthiazol-2-yl)-2-5-diphenyltetrazolium bromide
MYC	MYC proto-oncogene, BHLH transcription factor
NA	Nicotinic acid
NXF1	Nuclear RNA export factor
OH-	Hydroxyl
OTA	Ochratoxin
PA	Picolinic acid
P - Akt	Phosphorylated protein kinase B
PBS	Phosphate buffered saline
PCR	Polymerase chain reaction

PDK1	Phosphoinositide-dependent protein kinase 1
PH	Pleckstrin homology interaction domains
PI3K	Phosphatidylinositol-4,5-biphosphate 3-kinase catalytic subunit alpha
PIP2	Phosphatidylinositol 4,5-biphosphate
PIP3	Phosphatidylinositol (3,4,5)-triphosphate
PTEN	Phosphatase and tensin homologue
qRT - PCR	Quantitative real-time polymerase chain reaction
RBD	Relative band density
RBM15	RNA-binding motif protein 15
RBM15B	Putative RNA-binding protein 15 B
Rfc	Relative-fold change
RNA	Ribonucleic acid
RT	Room temperature
RTK	Receptor tyrosine kinase
SA	South Africa
SAM	S-adenosylmethionine
SD	Standard deviation
SDS	Sodium dodecyl sulphate
SDS - PAGE	Sodium dodecyl sulphate-polyacrylamide gel electrophoresis
TEMED	Tetramethylethylenediamine
Tris	Tris (hydroxymethyl) aminomethane
TrkB	Tropomyosin receptor kinase B
TTBS	Tris-buffered saline with Tween 20

U87MG	Uppsala 87 malignant glioma
V	Volts
VIRMA	Vir-like m6A methyltransferase-associated protein
WTAP	Wilms tumor 1 associated protein
XIST	X - inactive specific transcript
YTHDF1/2/3	YTH domain family proteins 1/2/3
YTHDC1/2	YTH domain containing proteins 1/2
ZC3H13	Zinc finger CCCH domain-containing protein 13

TABLE OF CONTENTS

LIST OF FIGURES

LIST OF TABLES

ABSTRACT

Mycotoxins are a global concern due to the extensive damage and loss they cause in the agricultural sector. Mycotoxins are transferred from animal feed into animal-derived consumables, such as eggs, milk and meat presenting a danger to humans. The picolinic acid derivative Fusaric acid (FA), produced by various species of *Fusarium*, poses a significant risk to both animal and human health because of its toxicological effects on various tissues. It is noted for its unusually potent phytotoxicity in plants and shows prevalence in causing hepatotoxicity, genotoxicity and nephrotoxicity in humans. However, the effects on arguably the most important organ in the human body, the brain, remains incompletely understood. The study set out to investigate the cytotoxic effects of FA on U87MG human glioblastoma cells by monitoring alterations in global m6A RNA methylation as well as gene and/or protein expression levels of the m6A complex and the *PI3K/Akt* pathway. Methods comprised of (i) culture of U87MG cells; (ii) MTT assay (IC_{50}: 180 µg/ml FA, 24 hrs) which was then used for subsequent treatments; (iii) ELISA; (iv) qRT-PCR (quantify mRNA expression of *METTL3, METTL14, YTHDF1, YTHDF2, YTHDF3, FTO, WTAP, YTHDC1, YTHDC2, ALKBH5, BDNF* and *CREB*); (v) western blot (protein expression of *BDNF, P-AKT, P-CREB* and *PI3K*). FA caused an upregulation (2.1059-fold; p = 0.0150) of global m6A RNA methylation in U87MG cells relative to the control. FA caused a downregulation of mRNA expression for *METTL3* (0.2605-fold; p = 0.0007); *METTL14* (0.4137-fold; p = 0.0068); *WTAP* (0.2740-fold; p = 0.0004); *YTHDF1* (0.7170-fold; p = 0.0793); *YTHDF2* (0.6269-fold; p = 0.0224); *YTHDC1* (0.9867-fold; p = 0.0008); *YTHDC2* (0.0570-fold; p = 0.0003); *FTO* (0.4534-fold; p = 0.0039); *ALKBH5* (0.0066-fold; p = 0.0004); *BDNF* (0.0106-fold; p = 0.0006) and *CREB* (0.9172-fold; p = 0.0003). However, *YTHDF3* (1.335-fold; p = 0.0647) was upregulated. FA increased protein expression of *BDNF* (1,205-fold; p = 0.0173) and *P-CREB* (1.5537-fold; p = 0.0002) and decreased protein expression of *PI3K* (0.8411-fold; p = 0.0346) and *P-Akt* (0.8274-fold; p = 0.0614). The observed increase in global m6A, despite downregulation of 'writers' and 'erasers' underscores a complex interplay of compensatory mechanisms resulting from FA exposure. The differential expression of m6A 'readers', particularly the upregulation of *YTHDF3* and downregulation of *YTHDF1*/*2* and *YTHDC1/2*, suggests selective stabilization of survival-related transcripts to counteract FA-induced neurotoxicity. FA exposure resulted in the upregulation of *BDNF* and *P-CREB* protein levels which indicates a compensatory mechanism aimed at preserving neuroprotective signalling despite transcriptional repression. *PI3K* and *P-AKT* were downregulated indicating a suppression of growth and survival pathways which are potentially linked to oxidative stress and energy conservation under toxic stress.

Keywords: Fusaric acid, fungi, genotoxicity, global m6A RNA methylation, mycotoxin, protein

INTRODUCTION

Agriculture is one of the largest industrial sectors on the planet. Agronomic crops provide essential food, grains, fibre and oils that feed entire human populations and livestock. Since 2000, Sub-Saharan Africa has pioneered agricultural developments worldwide, showing an agricultural growth increase of 4.3% annually (Jayne and Sánchez, 2021). An example of an agricultural product is cereals, which are a staple source of breakfasts in almost every single household and provide a source of nutrition and energy. However, these commodities are not safe from damage and loss, as food contamination is one of the leading causes of product defection (Bianchini & Stratton, 2019). An estimated 100 million euros was lost due to the Hungarian wheat epidemic in 1998 due to mycotoxin exposure, which are by-products of fungi that affect large scale crops (Milićević et al., 2010). Furthermore, findings from the Food and Agriculture Organization of the United Nations (FAO) approximate that a quarter of agronomic crops used for cereal worldwide have been contaminated and lost due to mycotoxins (Winter & Pereg, 2019).

A mycotoxin is classified as a naturally occurring secondary metabolite. Fungi belonging to the genera *Penicillium*, *Fusarium*, *Alternaria* and *Aspergillus* are known to produce a variety of mycotoxins. They are a global concern as they reproduce and grow rapidly, causing major toxic responses (mycotoxicosis) upon ingestion (Kebede et al., 2020). As of 2007, 300-400 mycotoxins have been identified and documented (Berthiller et al., 2007). However, recent estimations of mycotoxins in nature bring the value between 300 – 20, 000, with a possibility of even 300, 000 (Lee & Ryu, 2017).

Fusarium is a highly economically relevant genus of phytopathogenic fungi. Cereals constituted with barley, maize, oats or wheat are commonly the victims of infection from *Fusarium* species (Subramaniam et al., 2009). They cause a condition called *Fusarium* head blight (FHB) in grain and crop, such as wheat and barley, and have been shown to reduce total grain yield by up to 50%, as well as negatively affect the grain quality (Bottalico & Perrone, 2002). *Fusarium* is also unique unlike other fungi, such as *Penicillium* or *Aspergillus*, as it requires specialised morphological identification (Hassan et al., 2019). This makes the *Fusarium* species extremely hard to identify compared to other fungal species. When a plant is infected, the secondary metabolites of *Fusarium* become an unprecedented risk and exposure triggers public health concerns for their toxic properties. Mycotoxins are transferred from animal feed into animal-derived consumables, such as milk, eggs and meat, which now present a danger to humans.

The picolinic acid derivative Fusaric acid (FA), produced by various species of *Fusarium*, poses a significant risk to both animal and human health because of its toxicological effects on various tissues. Interestingly, it was also the first fungal phytotoxin to be successfully separated from a

contaminated host plant for its unusually potent phytotoxicity and shows prevalence in causing hepatotoxicity, genotoxicity, nephrotoxicity, and neurotoxicity (Niehaus et al., 2014). The FA mycotoxin was initially identified during the 1960's due to its exceptional ability to inhibit dopamine-beta-hydroxylase activity (Nagatsu et al., 1970). The 5-butyl side chain of FA has been noted to increase lipophilicity, which aids in cell membrane penetration (Devnarain et al., 2017). The carboxylic acid group of FA also donates protons, giving the compound its acidic characteristics (Liu et al., 2016). The chelate-forming ability FA possesses also disrupts cellular processes and biological functions by conjugating with metals such as copper, manganese, iron and zinc (Arumugam et al*.,* 2021). There have been previous studies conducted trying to explain the pathway of action FA undertakes however fundamental knowledge regarding its cellular toxicity remains incompletely understood. Four possible methods for explaining its cytotoxic effects found by Ruiz et al. (2015) include metal ion chelation, cell membrane potential alterations, ATP (adenosine triphosphate) synthesis inhibition or electrolyte leakage. According to a study by Pavlovkin, Mistrik & Prokop (2004), their findings on the mechanisms of FA toxicity are due to oxidative stress, membrane permeability, DNA (deoxyribose nucleic acid) damage, mitochondrial dysfunction and apoptosis. Newer research by Jiao et al. (2013) reported DNA fragmentation, accumulation of hydrogen peroxide and chromatin condensation in FA-induced treatments on plant cell cultures, indicating that there could be a programmed cell death signal in FA toxicity.

FA also has detrimental effects on animals. In a study conducted on zebrafish, FA was shown to have a direct influence on malforming notochords (Yin et al., 2015). Findings from Porter et al. (1995) show how FA induced neurotoxicity in mammalian brain tissue. Two separate studies, Ruiz et al. (2015) and Bacon et al. (2006), have also found that FA has toxic cellular effects on bacteria. With regards to the effect of FA on humans, multiple defects have been documented to date in a plethora of human systems. Its significant cytotoxicity has been reported in fibroblast, colon and breast cancer cells (Fernandez-Pol et al. 1993). Hepatocellular carcinoma (HepG2) cells, a well-researched malignant liver cell line, have been documented to show damage to DNA and post-translational disruptions of P53 due to FA (Ghazi et al., 2017). It also presents genotoxic effects in human lymphocytes and human cervical carcinoma cells (Mamur et al., 2020). The nervous system in humans is also greatly affected due to FA inhibition of the enzyme dopamine β-hydroxylase (Reddy et al*.*, 1996). Coupling these effects, FA is also documented causing skin and gastrointestinal complications and embryo developmental issues (Mézes, 2008). Abnormally high FA concentrations have carcinogenic effects on the nervous system, kidney, reproductive organs and liver of humans (Mamur et al., 2020). However, the effects on arguably the most important organ in the human body, the brain, remains incompletely understood.

When the brain is considered, it only constitutes 2% of an organism's total body mass, however it requires a substantial amount of consistent energy (Magistretti & Allaman, 2015). Despite having

glucose as its main source of energy, the brain also efficiently makes use of neuronal substrates and blood-derived substrates (Magistretti & Allaman, 2015). This poses an adverse effect of making the brain susceptible to oxygen and glucose deficiency, demonstrating that FA can cross the blood-brain barrier and initiate neurotoxic effects (Behrens et al., 2015). It was discovered that FA has detrimental impacts through various channels such as oxidative stress induction and disruption of ion homeostasis but most importantly its interference with neurotransmitter systems. Research regarding FA's neurotoxic effects is mainly found in *in vivo* and *in vitro* models, but very little research has been done on the impact of FA on humans.

The most prevalent messenger RNA (mRNA) modification is N6-methyladenosine (m6A) methylation (Weiner & Schwartz, 2021). It controls RNA (ribonucleic acid) stability, translation, processing as well as splicing, which all play crucial roles in human diseases such as cancer (Wang et al., 2020). The m6A modification is governed by three groups of enzymes with reversible capability. The initiating group are methyltransferases known as 'writers' and the terminating group are demethylases which are known as 'erasers'. The most important 'writers' of this complex are Wilm's tumour 1 associated protein (*WTAP*), methyltransferase-like 14 (*METTL14*) and methyltransferase-like 3 (*METTL3*) which catalyses the formation of m6A (Oerum et al., 2021). The 'readers' are RNA binding proteins which include insulin-like growth factor 2 mRNA binding protein (*IGF2BP*), heterogeneous nuclear ribonucleoprotein (*HNRNP*), YTH domain family proteins 1/2/3 (*YTHDF1/2/3*), and YTH domain containing proteins 1/2 (*YTHDC1/2*). (Liao et al., 2018; Zhao et al., 2020). The 'erasers' that remove the N-methyl groups of m6A and terminate the process are comprised of fat mass and obesity-related protein (FTO) and alkB homologue 5 (*ALKBH5*) (Oerum et al., 2021).

The m6A RNA methylation process is an essential component of mammalian development and is the most highly researched epigenetic modification of RNA bases. It accounts for more than 60% of every posttranscriptional RNA modification documented (Zhang et al., 2020). The m6A RNA modification is positioned at the nitrogen atom, sixth position of adenosine (Li et al., 2021). FA's relationship and how it influences m6A writers and erasers has been found to be complex. A study by Ghazi et al. (2022) found that while FA enhances *METTL3* and *METTL14* expression levels, the expression of *WTAP* was decreased. *WTAP* is a crucial element that forms the writer complex that mediates the nuclear localization of the *METTL3-METTL14* complex. This indicates a nuanced regulatory mechanism wherein FA not only promotes methylation by increasing methyltransferase levels but also potentially alters the localization and assembly of the methylation machinery.

Phosphoinositide 3-kinase (*PI3K*), protein kinase B (*Akt*) and mammalian target of rapamycin (*mTOR*) make up the *PI3K/AKT/mTOR* signalling pathway, which is an extremely important for

the growth, migration, survival and proliferation of cells. With regards to cancer cells, this pathway develops hyperactive tendencies and causes dysregulated cell proliferation and growth (Peng et al*.,* 2022). The pathway is activated when a ligand, e.g. insulin-like growth factor 1 (*IGF1*), binds to a receptor on the cell membrane (e.g. tyrosine kinase) (Miricescu et al., 2021). When the specific receptor is stimulated it activates *PI3K* (Miricescu et al., 2021). *PI3K* in turn catalyses the phosphorylation of phosphatidylinositol 4,5-bisphosphate (*PIP2*) at the 3' position of the inositol ring, which produces phosphatidylinositol (3,4,5)-trisphosphate (*PIP3*). Utilizing the pleckstrin homology interaction domains (*PH* domains), PIP3 serves by gathering two protein kinases and moves them to the plasma membrane (Miricescu et al., 2021). Two groups make up the *PH* domains, being *AKT* (protein kinase B) as well as phosphoinositide-dependent protein kinase 1 (*PDK1*). Upon arrival of the PH domains to the cell membrane, the intracellular enzyme mTOR complex 2 (*mTORC2*) causes *AKT* phosphorylation on Ser473 which allows for the phosphorylation of Thr308 by *PDK1*. Target proteins found in the cellular membrane are phosphorylated by activated *AKT*, which in turn terminates cellular membrane connectivity, resulting in different target proteins in the cytosol and cell nucleus becoming phosphorylated (Miricescu et al., 2021). This in turn leads to cell proliferation, cell survival and cell growth (Lim et al., 2014).

Mycotoxins pose a severe threat to global agriculture and health, contaminating crops and infiltrating food supplies with toxic secondary metabolites. These compounds can cause devastating health effects, including hepatotoxicity, genotoxicity, and neurotoxicity, contributing to diseases in humans and animals. Among these, FA is an underexplored mycotoxin with demonstrated toxic effects on various tissues, yet its mechanisms of action, particularly in the brain, remain poorly understood. Investigating FA's impact on critical pathways like m6A RNA methylation and *PI3K/Akt* signalling is essential for unravelling its cellular toxicity. This study is motivated by the need to fill gaps in understanding FA's neurotoxic effects and its broader implications on public health, providing valuable insights for science, agriculture, and medical research.

CHAPTER 1

LITERATURE REVIEW

1.1 Mycotoxins

A mycotoxin can be defined as a secondary metabolite of filamentous fungi that develop mycotoxicosis when eaten by higher animals. The most common moulds (Figure 1.1) that produce these mycotoxins are the *Penicillium*, *Aspergillus, Claviceps* and *Fusarium* genera (Yiannikouris and Jouany, 2002). Contamination of human foods or animal feeds could occur at any process in crop agriculture with non-specific environmental conditions, making crop contamination risk extremely high (Bhatnagar et al., 2004). The versatility of mycotoxins is their greatest advantage, affecting crop development in every geographic region with various climates (Kuiper-Goodman, 2004). Due to the alarming risk mycotoxins can present to the agricultural sector and global gross domestic product (GDP), research into mycotoxins has been of great importance currently.

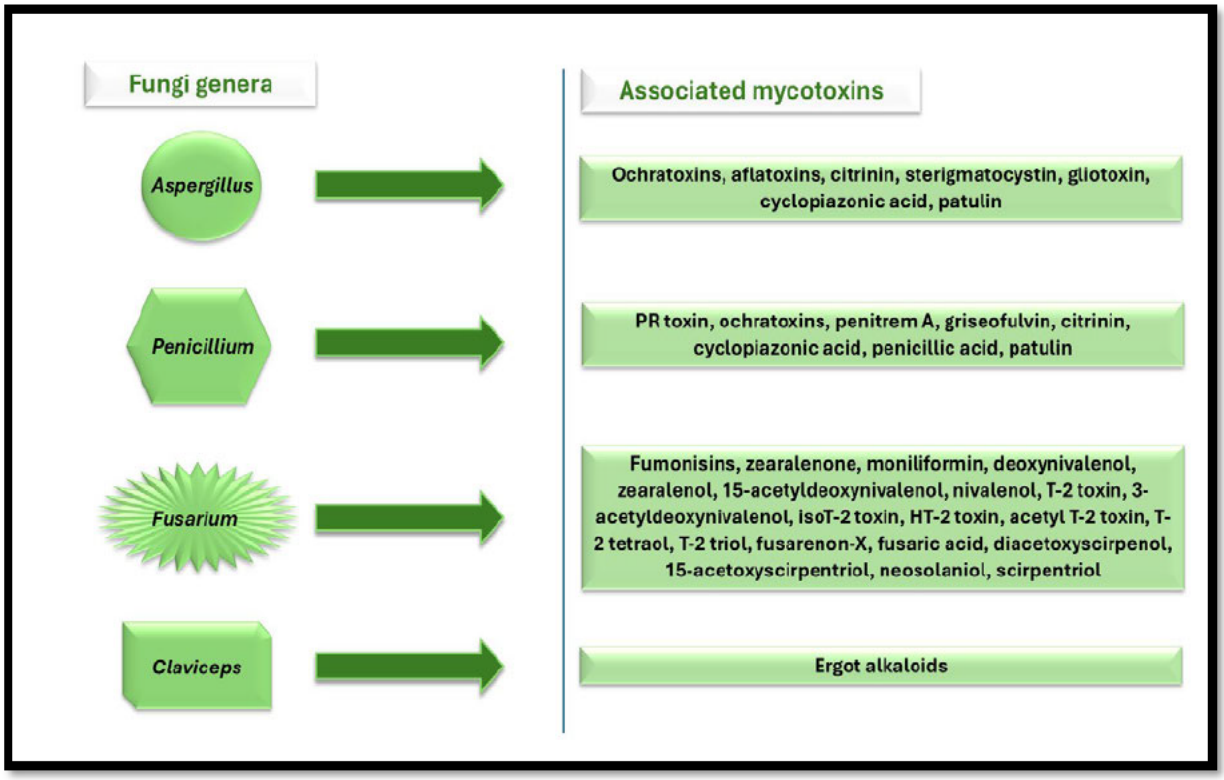

Figure 1.1 The most relevant fungal strains and their secondary metabolites (Composed by author, adapted from DeVries et al., (2002)).

Presently, more than 300 mycotoxins have been documented, yet a select few present risk to the economy (El-Sayed, 2022; Miller, 1995). These few have the capability of causing detrimental effects on livestock, humans and crops as well as major health and economic disadvantages (Peraica et al., 1999). A research study in India (2004 – 2005) set to discover the incidence rate of the most prevalent mycotoxins (T-2 toxin, aflatoxin and fumonisins) found in finished seeds and livestock feed and presented astounding results. 824 out of the 984 samples analysed tested positive for contamination (Murthy et al., 2005). Another study in China (2002 – 2003) assayed six mycotoxins (fumonisins, deoxynivalenol (DON), zearalenone, ochratoxin (OTA), aflatoxin and T-2 toxin) and presented an even higher contamination rate of 90% (Liu et al., 2016). Fumonisins, aflatoxins, ochratoxins and trichothecenes (Figure 1.2) seem to have the highest prevalence of all mycotoxins that are food contaminating.

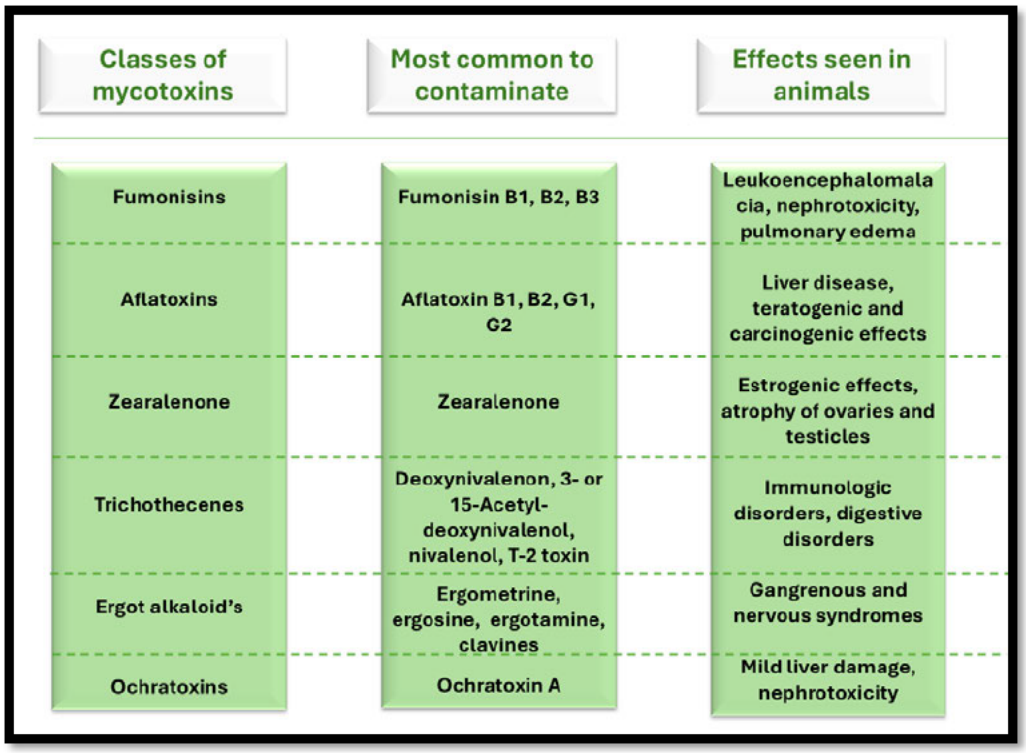

Figure 1.2: The most relevant mycotoxins and their effects upon ingestion (Composed by author, adapted from Binder (2007)).

The first incident involving mycotoxin exposure (aflatoxin; *Aspergillus flavus*) occurred in 1960 due to the Turkey X epidemic that claimed the lives of 100 000 turkey poults (Bennett and Klich, 2003). The cause was confirmed to be contaminated feed (peanut meal) (Peraica et al., 1999). Mycotoxin research has significantly increased since, yet remains a massive issue, with outbreaks still continuing to occur at a global scale (Peraica et al., 1999; Shephard, 2016; Yiannikouris and Jouany, 2002). Methods have been developed to try to curb their spread like product screening, but due to their natural mode of contamination, their production is unavoidable.

While mycotoxins are primarily known for their harmful effects, they also serve positive purposes to the filamentous fungi that produce them, such as defence against microbes (Palumbo et al., 2008). They are brought about by an adaptive response to nutrient supply and environmental factors (Zain, 2011). It is thought that these mycotoxins are produced as a form of toxic self-defence or as a means of decaying cellular membranes (Stack et al., 2014). Mycotoxins are noted for having relatively low molecular weights and varying chemical structures, giving each unique characteristics and biochemical outcomes (Yiannikouris and Jouany, 2002). There are many pathways a mycotoxin can affect humans and animals. Ingesting foods that are contaminated, mycotoxin accumulation and transfer from animal-derived products (eggs and packaged milk etc.) to humans, contact with the skin as well as spore-borne inhalation are all successful exposure methods (Bennett and Klich, 2003; Zain, 2011). Once ingested, mycotoxin exposure leads to a disease called mycotoxicosis (Zain, 2011). This disease is prevalent in developing countries since they lack the necessary tools and methods to properly handle and store food. An example of such a country is South Africa (SA), which is highly dependent on crops (maize, barley etc.) as dietary staples (Bennett and Klich, 2003).

1.2 The *Fusarium* mycotoxin: Fusaric acid

The *Fusarium* species are a dynamic and versatile fungal group, having over 1000 different species that can be found on various types of plant material (Nelson et al., 1994; Bouarab, 2009). These species produce a wide range of mycotoxins (Figure 1.3). They contribute to the structure of water biofilms and are found in soils all over the world (Elvers et al., 1998). They possess an advantaged ability to reproduce highly efficiently and grow on a plethora of substrates (Burgess, 1981). Cases reported range from completely different climate zones, showing how adaptive the species truly is. They have been recorded infecting rice in Taiwan, Thailand and Japan, cereal crops in North America and Western Europe and wheat in China (Bouarab, 2009).

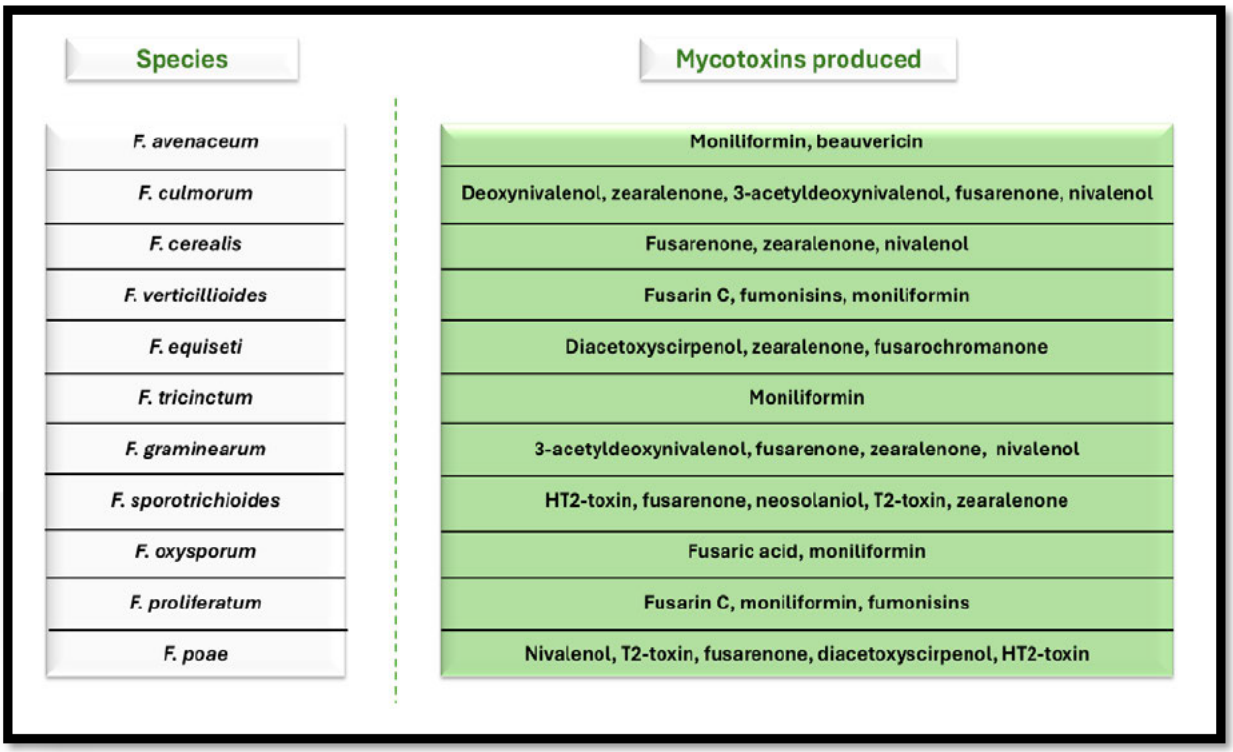

Figure 1.3: The different species of *Fusarium* and the mycotoxins they produce (Composed by author, adapted from Mirza et al. (2015))

The food-borne mycotoxin, Fusaric acid (FA; 5-n-butyl-pyridine-2-carboxylic acid or 5-butylpicolinic acid) is a secondary metabolite that frequently contaminates agricultural commodities (Yin et al., 2015; Terasawa & Kameyama, 1971). Only seven members belonging to the *Fusarium* species are documented to produce FA (Fairchild et al., 2005). During a study in 1934 a crystalline compound was found and extracted from a well-known fungus called *Gibberella fujikuroi*. In the 1960's, this extract was found to be FA, being noted for its exceptional ability to inhibit the function of dopamine-beta-hydroxylase (Nagatsu et al., 1970; Brown et al., 2012). Currently, it is the highest recorded mycotoxin present in food belonging to the *Fusarium* species, proving that investigating its toxicity may prove beneficial to mycotoxin research collectively (Bacon et al., 1996).

FA is an extremely harmful phytotoxin. It normally targets crops such as maize and barley (Voss et al., 1999) and has a direct role in developing plant diseases (Bacon et al., 1996). The compounds molecular weight is 179.2157 g/mol, and its chemical formula is $C_{10}H_{13}NO_2$ (Singh et al., 2017). The 5-butyl side chain of the compound has cell membrane penetration abilities as it increases its lipophilicity (Devnarain et al., 2017). The 5-butyl chain is fused to the chelating structure of picolinic acid (PA) (Bochner et al., 1980). The carboxylic acid group of Fusaric acid has the tendency to donate protons and gives acidic qualities to the compound (Liu et al., 2016). The chelate-forming ability Fusaric acid possesses also disrupts cellular processes and biological

functions by conjugating with metals such as zinc, copper, iron and manganese (Arumugam et al., 2021). Most of FA's weak acid characteristics are caused by a hydroxyl (OH-) group in its structure, which also serves as a proton donor.

The exact quantities of FA present in livestock feeds and agricultural produce varies extensively (Voss et al., 1999). Streit et al. (2013) found FA at an average concentration of 643 µg/kg when naturally occurring in feed samples. However, findings by Bacon et al. (1996) showed FA concentration in maize fluctuated between 20-1080 mg/ml. Feed samples were reported by Chen et al. (2016) to contain concentrations between 2.5-18 µg/kg of FA. Another study by Shimshoni et al. (2013) found FA at a concentration of 765 µg/kg in corn taken from silos in Israel. The host plant susceptibility and the virulence of the fungal strain has a direct effect on the quantity of FA produced (Singh et al., 2017). An extremely virulent strain of *Fusarium* coupled with an immunocompromised plant will typically yield a greater amount of FA (Singh et al., 2017)

FA is composed of a physiological metabolite derivative of picolinic acid coupled with the fungal fermentation of *Fusarium* and tryptophan (Stack et al., 2003). The molecular formula of PA is $C_6H_5O_2N$. Also known as 2-picolinic acid or 2-pyridine carboxylic acid, it has a six-membered ring structure (Figure 1.4) and is an isomer of nicotinic acid (NA) (Grant et al., 2009). Copper, iron, zinc, and cadmium can all be effectively chelated by PA (Fernandez-Pol et al., 1977), hence, it is highly researched due to its anti-proliferative effects (Grant et al., 2009). The chelation of the mentioned metal ions by PA is an essential component of cell development and may offer a method via which this substance inhibits cell proliferation (Grant et al., 2009).

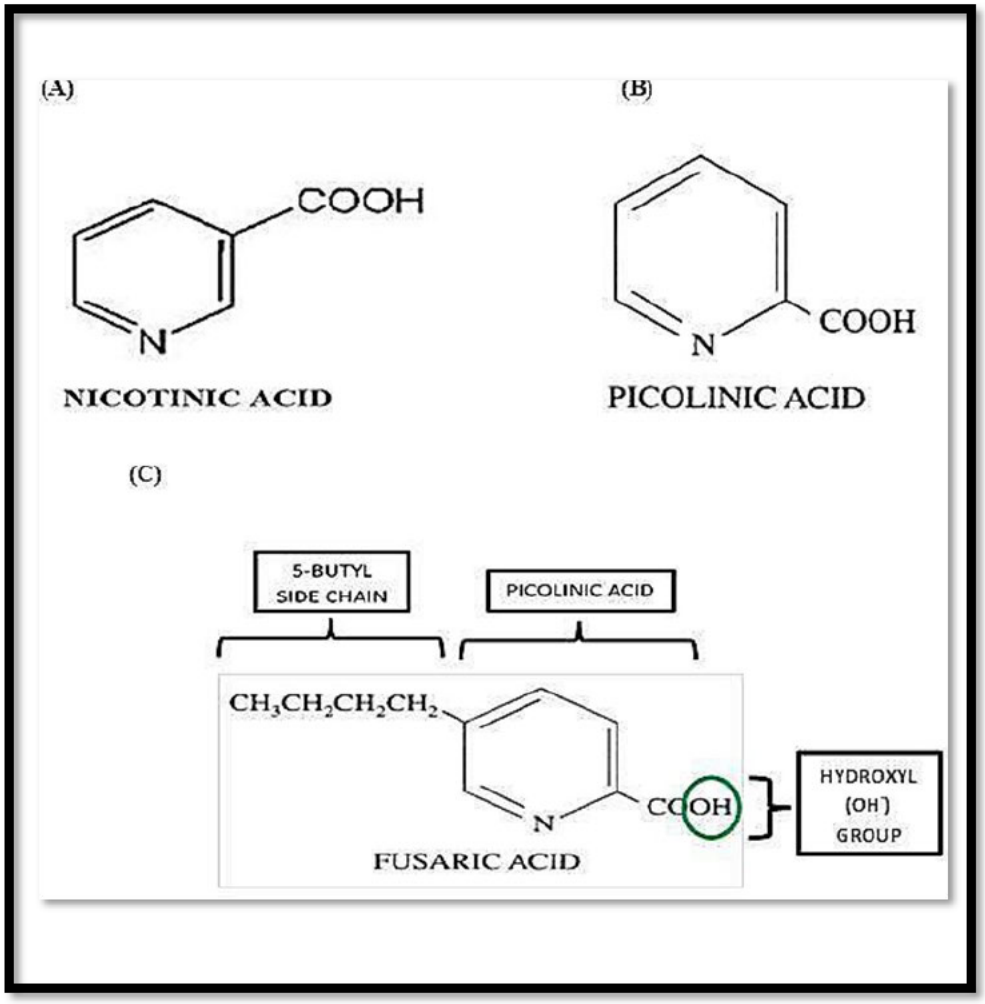

Figure 1.4: Difference in chemical structures of (A) NA, (B) PA and (C) FA (May et al., 2000)

1.3 Biosynthesis of Fusaric acid

FA is derived from a polyketide and is a secondary product (Srivastava et al., 2020). In the *Fusarium* genome, the biosynthetic process genes can be found clustered next to each other. These involve genes which are programmed to code for transcription factors, specific enzymes and transport proteins (Brown et al., 2015). Findings from Neihaus et al. (2014) show that the FA biosynthesis gene cluster (*FUB*) holds five genes in the *F. verticillioides* and *F. fujikuroi* species. However, findings from Brown et al. (2015) report no transporter genes or transcription factors were accounted for, rather the *FUB* cluster presented 12 genes (*FUB1* to *FUB12*) (Figure 1.5) in a total of seven other *Fusarium* species (Brown et al., 2015). FA production was found to be due to two transcription factors and nine *FUB* genes (Brown et al., 2015).

FA has the ability to contribute to the phytotoxic properties of the fungi, yet not interfering with the virulence ability, as seen in *F. oxysporum* as well as *F. verticillioides* when infecting cacti and crops (Brown et al., 2015). The pathway in which FA is produced initiates with the conversion of three acetate molecules to triketide by polyketide synthase, which then combines with oxaloacetate to produce FA. (Iqbal et al., 2024). Glutamine is synthesized and releases nitrogen, which is needed for FA production (Brown, et al., 2015). It should be noted that the purpose polyketide precursors serve to FA has not been discovered. (Brown et al., 2015; Niehaus et al., 2014). Certain genes contained within the *FUB* cluster such as *FUB2* have also not been researched thoroughly, and hence where its function is not known (Brown et al., 2015). Moreover, *FUB7* and *FUB9* also have an ambiguous role in FA biosynthesis, whereas the functions of *FUB10*, *FUB11* and *FUB12* are understood, being C6 transcription factor coding (*FUB10* and *FUB12*) and transporter-encoder (*FUB11*) respectively (Brown et al., 2015). The most crucial genes that produce FA include *FUB6*, *FUB8* and *FUB10* and hold the key to unlocking more information on the mycotoxin. *FUB10* regulates the other gene clusters and *FUB11* aids in the detoxification process of any FA that isn't utilized (Studt et al., 2016). The last gene in the cluster, *FUB12,* also serves to remove excess FA (Studt et al., 2016). Overall, gaining a deeper understanding of the *FUB* cluster and its implementations could eventually lead to developing strategies to limit FA exposure.

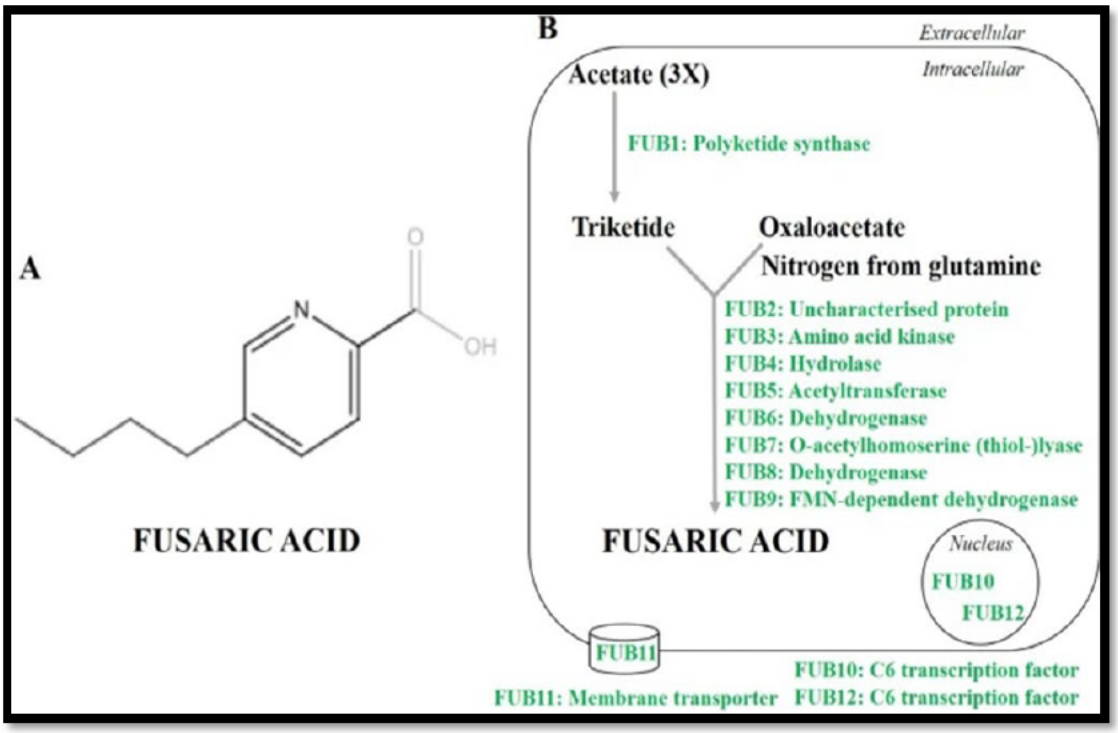

Figure 1.5: Biosynthesis of FA including the respective genes activated (Iqbal et al., 2024).

FA causes a host of disorders in animals and plants, yet the mechanism of action remains poorly understood. Pirayesh et al. (2015) showed that FA commonly causes wilt disease symptoms, such as the shrivelling of leaves or necrotic spots, in numerous plant species. Additional impacts that FA imposes include increased electrolyte leakage, suppression of respiration (Pavlovkin et al., 2004) and changes in membrane permeability (D'Alton & Etherton, 1984). In humans, the complications imposed by fusariosis depends on the immunocompetency and pathway of infection of the host. Keratitis and onychomycosis were seen as the most common infections among immunocompetent hosts. Peritonitis was another common infection seen among individuals who were undergoing continuous ambulatory peritoneal dialysis (Flynn et al., 1996). Sinusitis (Kurien et al., 1992), endophthalmitis (Gabriele & Hutchins, 1996), osteomyelitis (Bourguignon et al., 1976), pneumonia (Sandler et al., 1998), thrombophlebitis (Murray et al., 2003), and septic arthritis (Jakle et al., 1983) are also common infections seen in immunocompetent patients.

1.4 Fusaric acid toxicity in humans

FA has gathered mass attention recently due to its toxic effects on human health. Due to FA inhibiting dopamine β-hydroxylase, it has gained the ability to cause catastrophic effects on neurological and physiological tasks (Nagatsu et al., 1970).

When plants contaminated with FA are ingested by humans, the mycotoxin content begins to rise in body cells with disastrous consequences (Sobral et al., 2018). Abnormally high FA levels exert carcinogenic effects on many human systems, such as the kidney, brain, reproductive organs, liver and the immune system (Mamur et al., 2020). According to studies, FA has harmful effects on HepG2 cells, including post-translational alterations of P53 as well as damage to DNA, brought on by the inhibition of histone acetyltransferases and the activation of histone deacetylases (Ghazi et al., 2017). Additionally, this also caused cell proliferation and apoptosis to inadvertently increase (Ghazi et al., 2017).

To add to these consequences, FA also caused gastrointestinal; and dermal issues as well as problems with embryo development (Mézes, 2008). FA is also known for dysregulating mitochondrial bioenergetics in kidney and liver cells (Abdul et al., 2016; Mamur et al., 2020). FA's chelating ability causes unnecessary binding of critical trace metals which also causes cellular task impairment (Arumugam et al., 2021). The nervous system in humans is also greatly affected, since FA inhibits the enzyme dopamine β-hydroxylase (Reddy et al., 1996). It is also highly cytotoxic to fibroblast, colon and breast cancer cells (Fernandez-Pol et al. 1993). FA is also immunosuppressive, causing downregulation of mitogen-activated protein kinase (*MAPK*) and cytokine production (Dhani et al., 2017). It also presents genotoxic effects in human lymphocytes and cervical cancer cells (Mamur et al., 2020). Additionally, FA shows neurological defects such as dopamine and serotonin alteration in the brain, causing severe psychological disorders (Sack & Goodwin, 1974).

The pharmacological effects FA exerts are already being heavily researched in clinical trials, showing hope of modulating catecholaminergic activity for mood disorders and health conditions such as hypertension (Matta & Wooten, 1973).

1.5 Fusaric acids impact on the human brain

The brain constitutes 2% of an organism's total body mass, however it requires a substantial amount of consistent energy (Magistretti & Allaman, 2015). Despite having glucose as its main source of energy, the brain also efficiently makes use of neuronal substrates and blood-derived substrates (Magistretti & Allaman, 2015). The brain makes use of blood-derived substrates, which

ultimately gives FA a means of inducing neurotoxicity through its ability to weaken the integrity and transcend the blood-brain barrier (Behrens et al., 2015). FA uses various mechanisms to cause disruptions and damage, including oxidative stress induction, disruption of ion homeostasis, and interference with neurotransmitter systems (Ghazi et al., 2017).

Research regarding FA's neurotoxic effects is mainly based on *in vitro* and animal models with minimal research based on the impact FA has on human brain toxicity. It has shown neuroactivity, but its metabolic effects are hardly researched. From what literature exists, FA has exhibited the ability to induce apoptosis along with mitochondrial dysfunction within HepG2 cells (Abdul et al., 2016). There are also existing links to its ability to alter brain neurochemistry, whereby serotonin and tryptophan levels are raised, proving it can be a beneficial treatment for neurological diseases and hypertension (Terasawa & Kameyama, 1971).

FA possesses the ability to inhibit dopamine β-hydroxylase, causing neurochemical conversions (dopamine to norepinephrine) in the brain (Nagatsu et al., 1970). An important regulatory process in the brain, norepinephrine synthesis, is suppressed and serotonin is increased in the human brain after FA exposure (Nagatsu et al., 1970; Sack & Goodwin, 1974). As previously established, FA also causes psychological effects such as mood disorders and has been noted for cognitive disabilities as well (Sack & Goodwin, 1974)

FA exposure has also been recorded to have toxic consequences to mitochondria, ultimately leading to mitochondrial malfunctions and severe oxidative stress. Findings from Abdul et al. (2019) show that the bioenergetic functionality of mitochondria are disrupted under FA exposure, causing energy metabolism to shift from oxidative phosphorylation to glycolysis, ultimately causing a disruption in the cellular function of human neuronal cells. The disruption of AMP-activated protein kinase (*AMPK*)/*Akt* signalling in mice brain tissue by FA, confirmed by Dhani et al. (2020), indicates that FA has a crucial function in neurotoxicity.

1.6 m6A RNA methylation/demethylation

A total of 170 types of posttranscriptional RNA modifications are documented (Weiner & Schwartz, 2021). Of these, the N6-methyladenosine (m6A) modification is the most abundant eukaryotic RNA chemical modification, controlling RNA functionality and metabolic activity (Wiener & Schwartz, 2021). In mammals, modifications of m6A account for between 0.1% and 0.4% of the adenosine concentration in isolated RNA, and these adenosines make up 50% of all methylated ribonucleotides (Wei et al., 1975). The modification is highly important; controlling and regulating nucleation, RNA stability, RNA processing as well as splicing, which all play crucial roles in disorders such as cancer (Wang et al., 2020). Notably, the RNA m6A "writer"

METTL3, “reader” *YTH* domain families and “eraser” *FTO* (Figure 1.6) have been found to be hopeful targets for anticancer therapy due to their involvement in tumours.

The m6A modification is governed by two groups of enzymes with reversible capability, mainly methylases called ‘writers’ and demethylases called ‘erasers’. The ‘writers’ are enzymes that serve to initiate the installation of the m6A mark. *WTAP*, zinc finger CCCH-type containing 13 (*ZC3H13*), RNA-binding motif protein 15 (*RBM15*) and putative RNA-binding protein 15B (*RBM15B*), *METTL3*, methyltransferase-like 16 (*METTL16*), *METTL14* and vir-like m6A methyltransferase-associated protein (*VIRMA*) make up the "writer" complex (Zhang et al., 2021; Jiang et al., 2021). From these, the most important ‘writers’ of this complex are *WTAP*, *METTL3* and *METTL14* which catalyses the formation of m6A (Oerum et al., 2021).

A multicomponent methyltransferase complex made up of *METTL14*, *METTL3*, and *SAM* (S-adenosylmethionine) first starts the m6A methylation process (Bokar et al., 1994). The methyltransferase complex's catalytic component is *METTL3*, whereas *METTL14* increases the specificity of the substrate. From *SAM*, a methyl group is removed and relocated to the N6 position of RNA adenine bases (Shi et al., 2019; Liu et al., 2014). *METTL3* also enables RNA substrate binding; which is stabilized by *METTL14* and the nuclear localization of *METTL3-METTL14* complex is governed by *WTAP* (Liu et al., 2014; Shi et al., 2019). Additional enzymes acquainted with complex (*RMB15* etc.) all function to confer specificity to the ‘writer’ complex whereby specific RNA regions such as stop codons are targeted (Feng et al., 2023). *METTL14* and *METTL3* interact with each other to produce a stable heterodimer that improves catalytic efficacy during m6A deposition on nuclear RNAs (Wang et al., 2014; Liu et al., 2019). *WTAP* combines with *METTL3* and *METTL14* forming a protein complex. This protein complex causes adenosine residues (N6) to be methylated utilizing the *DRACH* motif (D – A, G, U; R – A, G; H – A, C, U) on *PI3K/Akt* transcripts (Deng et al., 2018). The enzymatic process is governed by *METTL3* and *METTL14*, while *WTAP* does not catalytically activate any enzymes but stabilizes the entire complex, anchoring it to mRNA processing sites (*PI3K/Akt*) (Wang et al., 2016). Upon deletion of the protein complex, the methyltransferase complex has a reduced ability to perform RNA-binding and embryonic differentiation (Ping et al., 2014).

The ‘erasers’ are also known as demethylases comprised of *FTO* along with *ALKBH5* function to separate m6A from their N-methyl groups (remove m6A modifications) (Oerum et al., 2021). These enzymes basically reverse the actions of the ‘writers’. *FTO*’s purpose is also to control RNA stability and translation (Meyer & Jaffrey, 2017). *ALKBH5* also functions to demethylate nuclear RNA which controls RNA fertility and exportation (Zheng et al., 2013). Literature that investigates the effect of FA on the brain is minimal, however findings by Ghazi et al. (2022) show that it induces differential expression of m6A regulatory genes. *METTL14* along with *METTL3*

expression profiles are increased, while simultaneously, *FTO* and *ALKBH5* expression profiles are decreased when exposed to FA (Ghazi et al., 2022). Furthermore, findings from Ghazi et al (2021) show that FA also downregulates p53 expression through m6A RNA methylation and promoter methylation alterations in HepG2 cells. This alteration in the balance between methyltransferases and demethylases shows that FA can influence m6A expression levels.

The m6A 'readers' serve to bridge interactions between the 'writers' and 'erasers'. The 'readers' bind m6A-modified RNA to mediate downstream effects, composed of enzymes *IGF2BPs, HNRNP, YTHDF1/2/3* and *YTHDC1/2* (Liao et al., 2018; Zhao et al., 2020). This is done by m6A 'readers' identifying and binding to transcripts of modified m6A, controlling a host of essential cellular procedures involving mRNA structure, stability and splicing (Xiao et al., 2016; Spitale et al., 2015). The function of *YTHDC2, YTHDF3* & *YTHDF1* include promoting translation of mRNA through ribosomal protein interaction (Meyer et al., 2015). In the cytoplasm, these proteins show preference in binding to the *RRm6ACH* consensus sequence of m6A-modified RNA (Wang et al., 2014). *YTHDF1* interacts with ribosomes and translation initiating factors to improve translation (Wang et al., 2015). *YTHDF2* destabilizes mRNA through the means of decaying and deadenylation of m6A modified mRNAs (Wang et al., 2014). *YTHDF3* facilitates the protein synthetic synergy between *YTHDF1* and *YTHDF2* in protein synthesis as well as regulates *YTHDF2*'s mRNA degradation (Shi et al., 2017). *YTHDC1* operates in the nucleus, serving to increase exon inclusion by regulating splicing factors, such as Serine/arginine-rich splicing factors (*SRSFs*), that bind to m6A-modified RNAs (Xiao et al., 2016). X-chromosome silencing is facilitated by *XIST* (X-inactive specific transcript) m6A methylation, which is mainly recognized by *YTHDC1* (Patil et al., 2016). YTHDC1 signals Nuclear RNA export factor (*NXF1*) and *SRSF3*, increasing exporting m6A-methylated mRNA exportation (Roundtree et al., 2017). *YTHDC2* picks up on these signals and enhances mRNA translation in the cytoplasm by binding to methylated sites, as well as regulating transcript decay through these markings (Hsu et al., 2017). *YTHDF2* initiates the breakdown of m6A transcripts by utilizing *CCR4-NOT* (Carbon Catabolite Repression - Negative On TATA-less) deadenylase (Du et al., 2016). *PI3K/Akt* pathway signalling is also dependent on *YTHDC2* due to its translation initiation factor and ribosome loading enhancement, which both reduce specific mRNA abundance (Zhang et al., 2023; Bian et al., 2021).

Dysregulation of the machinery in the m6A complex has been known to cause numerous neurological disorders and even cancer. Research compiled by Yang et al. (2018) indicates cancer formation was associated with *METTL3* and *FTO* overexpression, and these two enzymes contribute to tumour growth by stabilizing oncogenic transcripts. Similar findings were found by Chen et al. (2024) but for *YTHDF2*, where mutations in this enzyme caused disruption in mRNA decay pathways causing aberrant gene expression.

The m6A modification has garnered massive attention due to its influence on cell differentiation and immune responses (Wiedmer et al., 2019). Technological advancements have been made to understand the m6A landscape in greater detail, utilizing techniques such as crosslinking immunoprecipitation (CLIP) and m6A-seq (Shi et al., 2019). Further research into noncanonical m6A sites also expands possible functional repertoires and challenges past dogmas (Bao et al., 2023). Despite these insights, research into m6A is still relatively new and much is still to be discovered regarding the spatiotemporal regulation of m6A and its interactions with other RNA modifications.

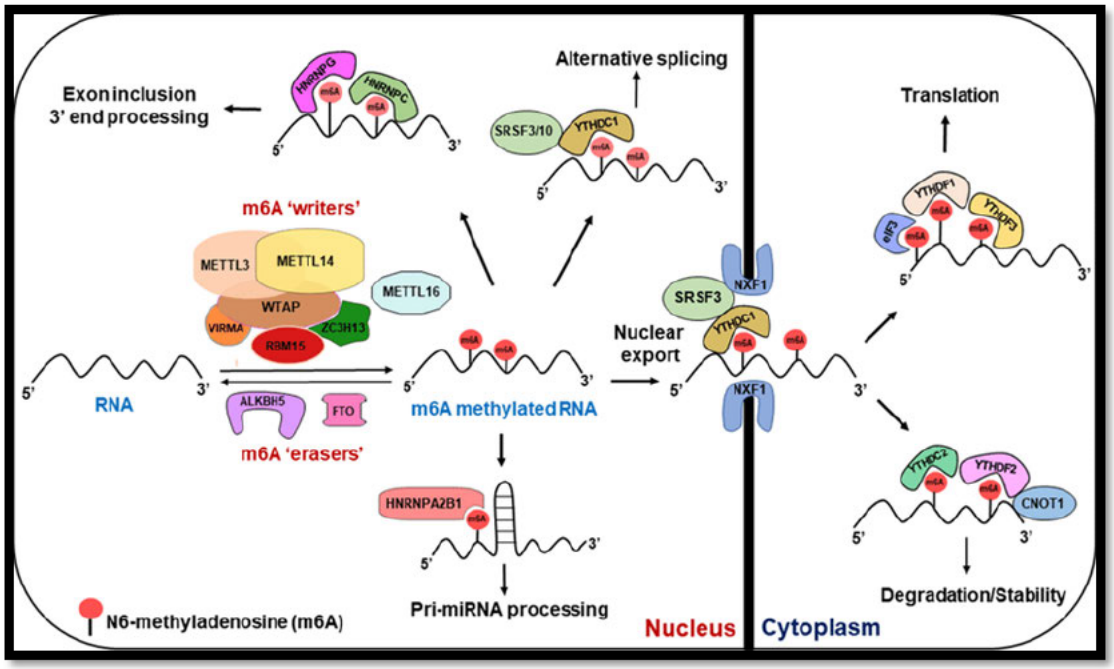

Figure 1.6: m6A RNA methylation and regulation with regard to the expression of specific genes involved (Karthiya & Khandelia, 2020).

1.7 The *PI3K/Akt* pathway

Among other neuronal pathways, the *PI3K/Akt* signalling pathway is a critically important intracellular cascade that regulates a host of essential cellular functions. Dysregulation in *Akt* function is linked with numerous diseases mainly cancer, neurodegeneration and metabolic disorders (Manning & Toker, 2017; Wang et al., 2017).

PI3K, a lipid kinase, and *P-AKT*, a serine/threonine kinase, function in the *PI3K/Akt* pathway as critical and essential components for survival. *PI3K* controls cell functions like survival, differentiation and proliferation making it a cornerstone of growth factor signalling pathways

(Krasilnikov, 2000). It is activated by G-protein-coupled receptors (*GPCRs*) or receptor tyrosine kinases (*RTK*s) after ligand binding (Vanhaesebroeck and Waterfield, 1999). The phosphorylation and activation of *PI3K* causes *PIP2* to phosphorylate into *PIP3* whereby *Akt* is recruited and activated by *PDK1* and *mTORC2* in the plasma membrane (Porta et al., 2014). Once activated, downstream signalling is initiated by Akt utilizing phosphorylating substrates (*mTOR*, forkhead box transcription factors (*FOXO*) etc.) to control cellular functions like survival and apoptosis (Huang et al., 2018). Phosphatase and tensin homolog (*PTEN*) ensures that *Akt* activation is tightly regulated, while also acting as a tumour suppressor that dephosphorylates *PIP3* to *PIP2* (LoPiccolo et al., 2008).

The *PI3K/Akt* pathway (Figure 1.7) seems to have significant influence in cancer by promoting tumorigenesis and therapy resistance. Hyperactivation of the pathways is frequently seen when there is a *PTEN* quantity loss, mutation of *PI3K* isoforms or atypical upstream receptor signal (Garcia-Echeverria & Sellers, 2008; Mayer & Arteaga, 2016). This is important to note since this hyperactivity initiates oncogenic procedures like angiogenesis and apoptosis evasion. Due to this aspect, the pathway has become a prominent target for cancer therapy and treatments, with multiple *PI3K* and *Akt* inhibitors undergoing clinical trials (Martini et al., 2014).

Latest research has emerged showing m6A alterations mediate a novel epitranscriptomic layer of control in the *PI3K/Akt* pathway. Cancer research is now showing significant backing that m6A has a critical role in *PI3K/Akt* regulation. Findings from Shi et al. (2019) show that *METTL3*-mediated m6A modifications enhance the translation and stability of oncogenic transcripts such as epidermal growth factor receptor (*EGFR*) and *MYC* proto-oncogene, BHLH transcription factor (*MYC*) causing an amplification in *Akt* signalling. When *METTL3* is downregulated, *Akt* activation is seemingly suppressed thereby, inhibiting tumour growth in gliomas, endometrial cancers and gastric carcinomas (Ji et al., 2020; Zhang et al., 2021).

Looking beyond cancer, both m6A modifications and the *PI3K/Akt* pathway have significant metabolic and neurological interplay. When looking at neuronal cells, *YTHDF1*, an m6A 'reader', regulates *Akt*-dependent pathways critical in supporting axonal plasticity and regeneration, which gives insight into possible therapeutic treatments for neurodegenerative diseases (Wiedmer et al., 2019).

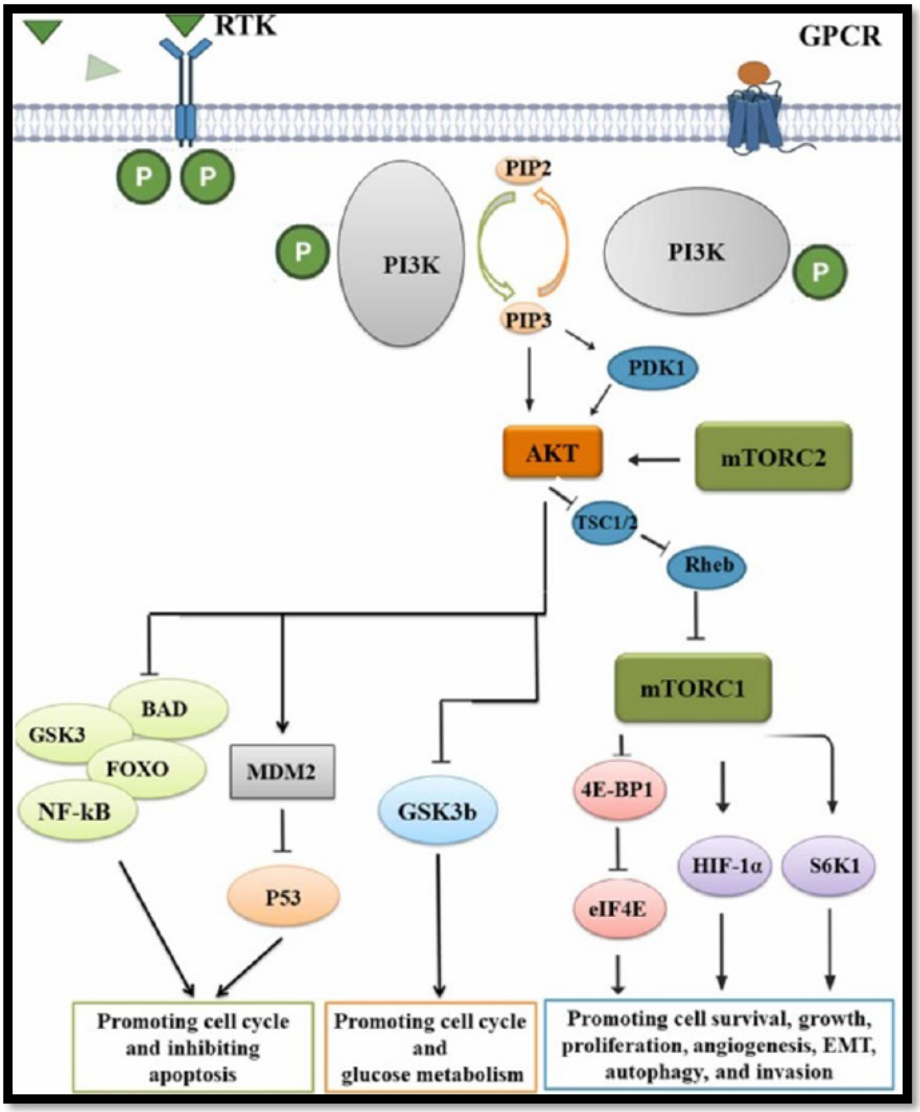

Figure 1.7: Components and the biochemical cascade of the *PI3K/Akt/mTOR* pathway (Karami et al., 2023).

1.8 BDNF and CREB's importance in the PI3K/Akt pathway

Cyclic AMP-response element-binding protein (*CREB*) along with Brain – derived neurotrophic factor (*BDNF*) are pivotal in maintaining neuronal survival, synaptic plasticity and cognitive function. With regards to the *PI3K/Akt* pathway, they govern a host of interplaying neurobiological roles mainly focused on cellular stress and injury (Fakhri et al., 2021). In collaboration with each other, these molecules orchestrate pathways essential for cellular homeostasis and neuroprotection, highlighting them as crucial subjects of neurodegenerative and psychiatric research (Amidfar et al., 2020).

BDNF is synthesized as pro-*BDNF* and processed into mature *BDNF*, which then interacts with its receptor tropomyosin receptor kinase B (*TrkB*) to mediate plasticity as well as neuronal survival (Angoa-Pérez et al., 2017; Ahmed et al., 2021). Downstream signaling pathways are activated when binding to TrkB, such as *PI3K/Akt* which are essential for neuronal functions including dendritic growth, synaptic strength and axonal repair (Huang & Reichardt, 2003).

Existing research shows that *BDNF* is indispensable for critical brain functions, such as memory and learning. Dysregulation of *BDNF* expression is linked to two of the most ravaging neurodegenerative disorders, Alzheimer's and Parkinson's disease. A balance between mature *BDNF* and pro-*BDNF* is essential for pathological as well as physiological conditions (Angoa-Pérez et al., 2017). When pro-*BDNF* binds to the p75NTR receptor, potentially promoting apoptosis, while mature *BDNF* interacts with the TrkB receptor, mediating neuronal survival and synaptic plasticity (Angoa-Pérez et al., 2017). *BDNF* modulates synaptic plasticity through activity-dependent release and local protein synthesis (Mizui et al., 2014). The Val66Met polymorphism in the *BDNF* gene affects pro-domain structure and function, potentially influencing vulnerability to neurological and psychiatric disorders (Arango-Lievano et al., 2015). Abnormal *BDNF* signaling has been implicated in various psychiatric and neurological disorders, and some psychotropic drugs are known to activate *BDNF* signaling (Angoa-Pérez et al., 2017).

CREB is a transcription factor that controls crucial cellular processes such survival, differentiation and proliferation in the nervous system (Wen et al., 2010). It's activated by phosphorylation at Serine 133 through the *PI3K/Akt* pathway, which then binds to the cAMP-response element (*CRE*) within the promoter regions of target genes, such as *BDNF*, initiating transcription (Figure 1.8) (Bonni et al., 1995; Andrisani, 1999). To initiate transcription, the co-activator *CREB*-binding protein (*CBP*) interacts with phosphorylated *CREB* (Andrisani, 1999). Fluctuations in *CREB* expression and activation are linked with cancer development (Xiao et al., 2010). Inhibition of *CREB* in cancer lines has shown promising results in reducing proliferation and inducing

apoptosis, which point it in the direction of being a potential target for cancer therapy (Xiao et al., 2010).

P-CREB is activated on *Ser133* via Akt phosphorylation and uses the *CRE*-dependent mechanism to increase cell survival (Du & Montminy, 1998). *BDNF* transcription and secretion are regulated by *CREB* creating a feedback loop where *BDNF* signalling via *TrkB* activates *PI3K/Akt* leading to *CREB* phosphorylation which amplifies neurotrophic support (Bathina & Das, 2015). In the hippocampus, this interaction facilitates dendritic spine remodelling and synaptic connectivity, essential for learning and memory (Jin et al., 2022).

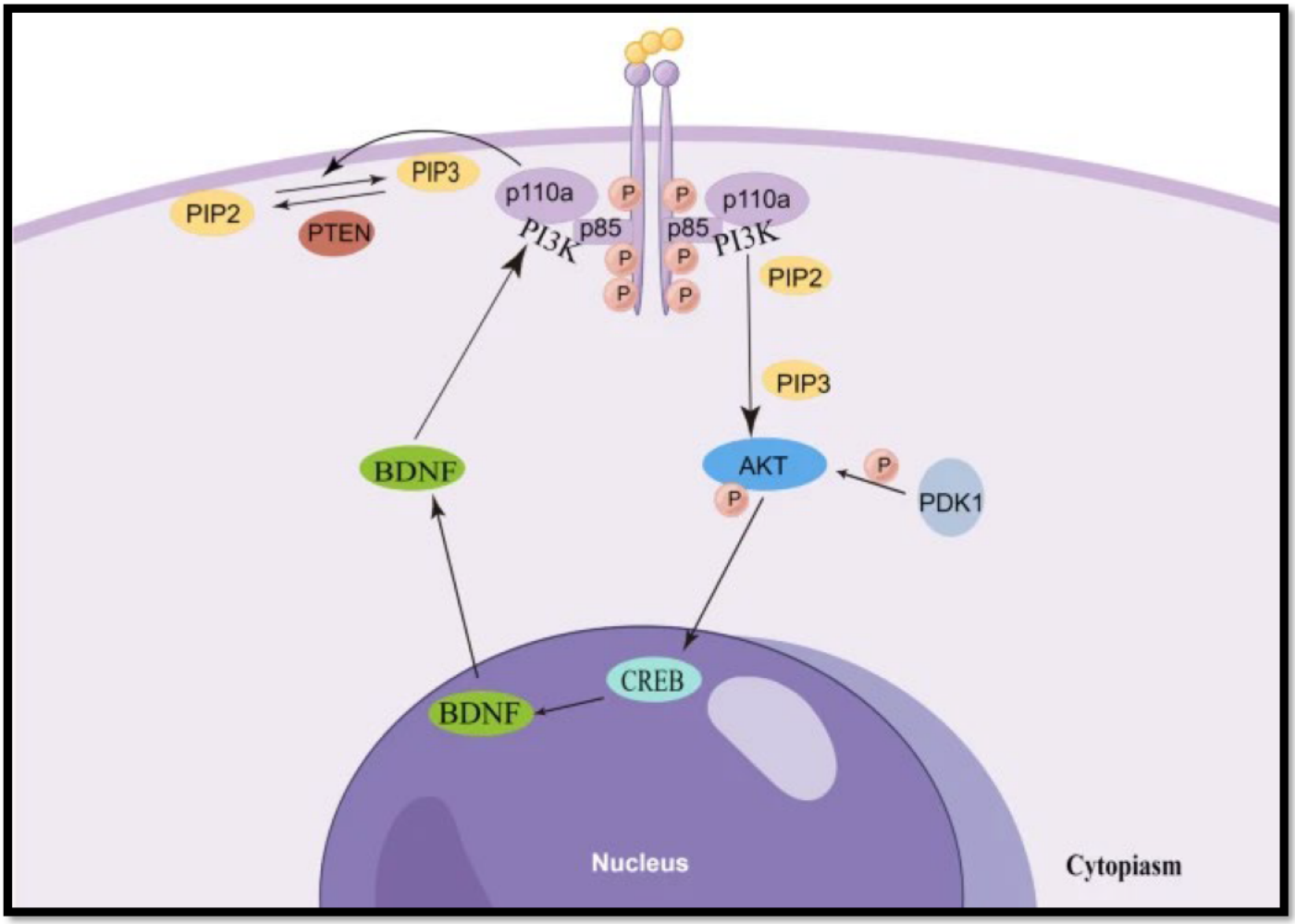

Figure 1.8: The intricate role of *BDNF* and *CREB* in the biochemical processes of the *PI3K/Akt* pathway (Li et al., 2023).

1.9 Rationale, Significance, Research Questions, Hypothesis, Aim and Objectives

Rationale

The *Fusarium* produced mycotoxin FA poses a significant threat to agricultural production worldwide impacting crop yield, quality of goods and food safety. Its presence in crops leads to extensive losses making it a critical concern for farmers and food safety experts (Bacon et al., 2006). Above the impact on the agricultural sector, when it is ingested by livestock or humans, it has severe and disastrous effects. FA has been shown to cause hepatotoxicity, nephrotoxicity, cardiotoxicity and genotoxicity and its effects on organs such as the liver, heart and kidneys have been thoroughly documented. However, relevant literature on FA impact in the brain is poorly researched and epigenetic mechanisms underlying its neurotoxicity remain incompletely understood. This study will give an understanding of the molecular and epigenetic mechanisms underlying FA-induced brain toxicity which will be crucial for developing effective preventative and therapeutic strategies.

Significance / Implications

Investigating the neurotoxic effects FA imposes on the U87MG brain cell line will provide valuable insights that will broaden knowledge on FA and neural health. Therapeutical cancer treatments can be developed by identifying potential vulnerabilities in cancer cells, since FA has been shown to be tumoricidal and have anti-cancer properties (Stack et al., 2003). FA could display selective effects on the U87MG cell line that could be further explored for new therapeutic agents. The epigenetic effects FA has on m6A RNA modifications will reveal a deeper understanding of neural toxicity, which is crucial since this RNA modification directly governs protein translation and RNA stability (Wang et al., 2020). The study will also highlight how cellular pathways are augmented by FA, which would potentially lead to cellular damage, apoptosis and mitochondrial dysregulation.

Proposed research questions for the study

1. Is FA cytotoxic to U87MG human glioblastoma cells?
2. Does FA affect the methylation and demethylation processes in U87MG human glioblastoma cells?
3. Does FA alter the global m6A RNA methylation levels in U87MG human glioblastoma cells?
4. Will FA cause changes in the *PI3K/Akt* signaling pathway and alter m6A gene expression profiles?

Hypothesis

1. FA presents cytotoxic effects to U87MG human glioblastoma cells.
2. FA alters global m6A RNA methylation as well as gene and protein expression in the m6A complex.
3. FA downregulates *PI3K/Akt* signaling in U87MG cells.

Aim

To investigate the effect of FA on global m6A RNA methylation levels and the *PI3K/Akt* pathway.

Objectives

- To determine the toxicity of different concentrations of FA in the U87MG cells.
- To determine the global levels of m6A RNA methylation in U87MG cells.
- To analyze the mRNA expression levels of m6A 'writers', 'readers' and 'erasers'.
- To analyze the mRNA and protein expression levels of *BDNF*, *CREB*.
- To analyze the protein expression levels of *PI3K* and *Akt*.

CHAPTER 2

MATERIALS AND METHODS

2.1. Materials

FA (F6513) was acquired from Sigma-Aldrich (St. Louis, MO, USA). The U87MG cell line was acquired from Separations Scientific (Johannesburg, SA). Cell culture consumables and reagents were acquired from Lonza Biotechnology (Basel, Switzerland). The primer sequences used for quantitative real-time polymerase chain reaction **(**qRT-PCR) were synthesized and acquired from Inqaba Biotechnical Industries (Pretoria, SA). Western blot equipment and reagents were acquired from Bio-Rad (Hercules, CA, USA). The m6A RNA methylation assay kit was acquired from Abcam (Cambridge, UK). Reagents not specifically mentioned were purchased from Merck (Darmstadt, Germany).

2.2 Cell Culture

2.2.1. Background on U87MG

The Uppsala 87 Malignant Glioma (U87MG) is an epithelium-based cell line. In 1966, it was initially collected from a female patient at Uppsala University who was 44 years old (Dolgin, 2016). The U87MG cell line is highly utilized in significant scientific and medical implications. It is a highly adaptable human cell line, found in the brain, having a 2n = 46 karyotype. They are a useful tool in research due to the relevance to human glioblastoma, which is an aggressive type of brain cancer. The Glioblastoma multiforme (GBM) has the highest prevalence of any malignant brain tumour line, showing close to 16 000 diagnoses yearly in the USA (Clark et al., 2010). Along with its high occurrence, it also has a disastrous survival rate of 29,6% making it a top contender for the deadliest type of cancer to acquire (CBTRUS, 2008). They have an adherent monolayer growth pattern and usually develop in clusters. The cell line is characterized by its extremely high migratory and proliferative capabilities, making them ideal candidates for studying tumor behavior and response to drugs (Verdugo et al., 2022). They also have the ability to mimic specific qualities of GBM pathophysiology such as gene expression alterations and apoptosis resistance (Verdugo et al., 2022). Therapeutic strategies (radiotherapy, chemotherapy etc.) for the disease are non-existent (Stupp et al., 2005). The cell line shows resistance to all current treatments due to

mutations in the PTEN tumour suppressing gene and aberrant EGFR signalling (Parsons et al., 2008), resulting in a survival time estimated between 12-15 months (Ushio et al., 2005), highlighting the importance of studying the U87MG in greater detail. Many studies have proven that the U87MG cell line is useful for studying neurotoxicity and the effects of drugs, chemicals, or other substances on brain cells. They can be employed to assess cellular responses such as cell viability, apoptosis, oxidative stress, and changes in signalling pathways that are relevant to neurotoxic effects. Literature from Martinkova et al. (2009) showed sensitivity and mechanisms of DNA adduct formation of the cell line (ellipticine). Another study by Heidarzadeh et al. (2019) analysed the inhibition effects of cytochalasin H on U87MG cells, finding a relationship between tumour regulatory gene expression and apoptotic pathways. Findings from Arcella et al. (2018) explored the aloe emodin effects on U87MG cells, revealing its inhibitory action on glioblastoma cell proliferation and tumour progression.

2.2.2 Cell culture

U87MG cells were cultivated from cryopreserved stores in 25cm^3 sterile cell culture flasks with complete culture media (CCM) [Dulbecco's modified eagle medium (DMEM) supplemented with 1% L-glutamine and 25 mM 4-(2-hydroxyethyl) piperazine-1-ethanesulfonic acid 10% fetal bovine serum (FBS) and 1% penicillin-streptomycin-fungizone]. The cell culture flasks were placed in a 5% carbon dioxide (CO_2) incubator at 37°C. Every two days the cells were rinsed with 0.1M phosphate-buffered saline (PBS) and the complete culture media (5ml) was reconstituted. As soon as approximately 90% confluency was reached, the cells were dislodged from the flask using 1 ml trypsin and sub-passaged for incubation (37°C, 5% CO_2) with FA. The trypan blue cell exclusion technique was used to count the cells.

2.3 Preparation of FA treatments

1 mg of FA was dissolved in 1 ml 0.1M PBS to produce a 1mg/ml FA stock solution. An inhibitory concentration of 50% (IC_{50}: 180 µg/ml) was determined from a 3-(4,5-dimethylthiazol-2-yl)-2-5-diphenyltetrazolium bromide (MTT) assay (Figure 3.1) and was used as the treatment condition in all following assays. All treatments were conducted over 24 hours (hrs) (37°C, 5% CO_2). An untreated control containing CCM only was included for comparison of results

2.4 MTT assay

2.4.1 Background

This assay was first conducted by Mosmann in 1983. It is a colorimetric assay that evaluates the viability and metabolic activity of a plethora of cell types after treatment with a test compound (Mossman, 1983). The MTT salt is a yellow tetrazole that converts into an insoluble purple formazan due to mitochondrial enzymes in viable cells (Kumar et al, 2018). An organic solvent is used to solubilize the insoluble formazan. The purple colour intensity, which is quantified by the absorbance measurement at 570nm, is proportional to the number of viable cells.

2.4.2 Assay Protocol

The MTT assay was conducted to determine the cytotoxic effects FA has in U87MG cells (Figure 2.1). Into a 96-well plate, U87MG (25,000 cells/well) were seeded in triplicate and incubated (37°C, 5% CO_2) overnight. This is a crucial step for cell proliferation along with cell adhesion to the wells. Thereafter, 12 serial dilutions of FA (0, 50, 100, 150, 200, 250, 300, 350, 400, 500, 600, 700 µg/ml) were prepared, and added in triplicate to the adhered cells on the 96-well plate. The plate was incubated (37°C, 5% CO_2) for 24 hrs. CCM (100 µl) and the MTT salt solution (20 µl, 5mg/ml) were added to each well and the plate was incubated (37°C, 5% CO_2, 4 hrs). Post incubation, the MTT salt solution and CCM was removed from all wells and dimethyl sulfoxide (DMSO) (100 µl) was added to each well and the plate was incubated (37°C, 5% CO_2, 1 hr). The purple formazan colour shift intensity was measured at 570/690nm using a spectrophotometer (SPECTROstar nano, BMG Labtech). The cell viability was computed using the absorbance measurements in the following equation:

cell viability (%) = $(\frac{Absorbance\ of\ sample}{Absorbance\ of\ control} x100)$

The half-maximal inhibitory concentration (IC_{50}) value was then determined for further assays.

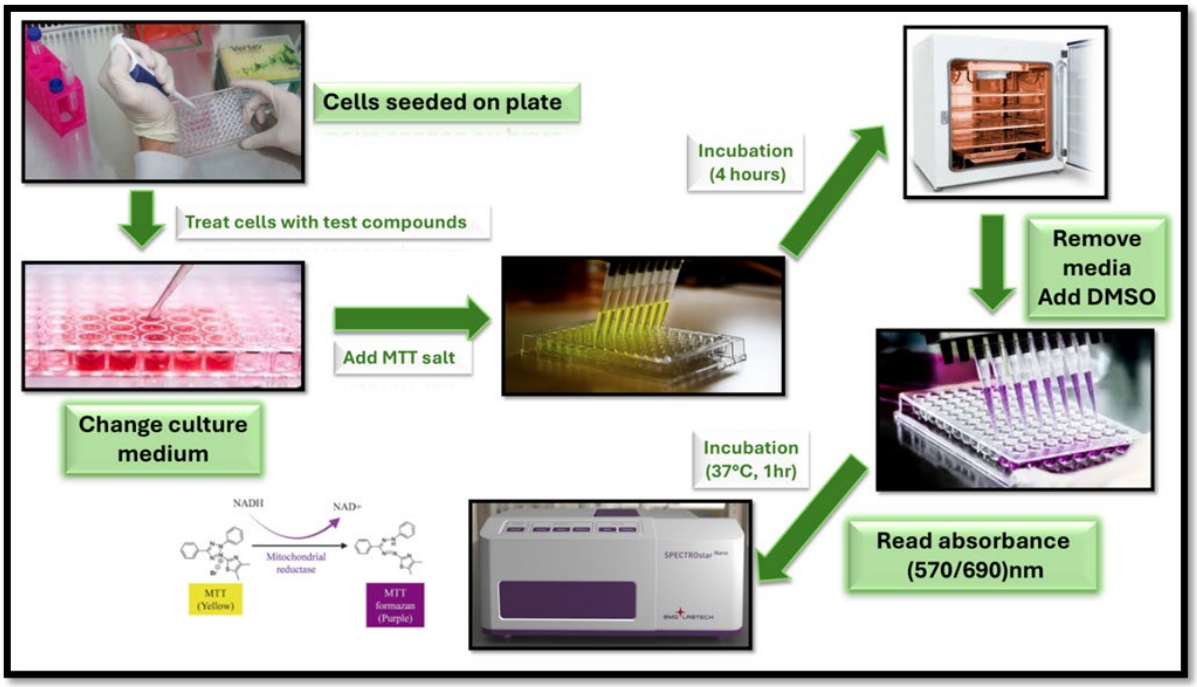

Figure 2.1: Overview of the MTT assay (Composed by author)

2.5 Enzyme-linked immunosorbent assay (ELISA)

2.5.1 Background

ELISA is a technique used for identifying and quantifying antibodies, antigens, hormones and proteins in biological samples. The assay was first introduced in 1971, thought to replace the radioimmunoassay as it was more efficient safer. It also had other advantages such as a higher scalability, specificity and sensitivity being able to detect analytes at the picogram level, thus making it useful in clinical assays with low biomarker quantities (Crowther, 2000). It is also compatible with high-throughput screening, showing its versatility ranging from pathogen identification to cytokine detection (Hayrapetyan et al., 2023).

A typical ELISA assay is constituted of 3 main steps; 1) coating 2) detection and 3) substrate addition. The coating step involves a microplate being coated with a specific antigen/antibody which causes the target molecule to bind through affinity interactions. An enzyme-conjugated secondary antibody attaches itself to the antigen-antibody complex as part of the detection stage, which will cause the detection sensitivity to be amplified. The last step involves a substrate for the enzyme being added, which produces a colorimetric change proportional to the analyte concentration (Engvall, 1980). The ELISA requires materials such as high-binding microplates

and optimized blocking agents that are essential for keeping the assay specificity and sensitivity high.

The m6A ELISA has a slightly different approach to the conventional ELISA, The RNA is bound to a plate and the capture (or primary) antibody is added before the detection (or secondary) antibody is added. The signal is then enhanced followed by the developer (to create the colour change) and a stop solution (to inhibit the reaction) before the plate is read.

2.5.2 Protocol

The m^6A RNA Methylation Quantification Kit (catalogue no. ab185912, Abcam) was used to quantify the m6A content of total RNA (Figure 2.2). The positive control standards (0.01–0.50 ng) and negative control that came with the kit were added to a strip well plate with standardized RNA samples (200 ng) and RNA binding solution (80 µl). Parafilm M was used to seal the plate and it was gently shaken for 2 minutes (min). This ensured thorough mixing of the RNA and the solution. The plate was incubated (37°C, 90 min). 1X wash buffer (150 µl) was used to wash each well three times. Each well had m6A capture antibody added to it (50 µl (1: 1,000), 1 hr) at room temperature (RT). 1X wash buffer (150 µl) was used to wash each well three times. Each well had the detection antibody added to it (50 µl (1: 2,000), 30 min, RT). 1X wash buffer (150 µl) was used to wash each well four times. Each well had the enhancer solution added to it (50 µl (1: 5,000), 30 min, RT). 1X wash buffer (150 µl) was used to wash each well five times. Each well had the developer solution added to it (100 µl, 10 min, RT). In the presence of m6A, the developer solution underwent a colour shift to blue. The enzymatic process was inhibited by adding a stop solution (100 µl). The absorbance level was recorded at a wavelength of 450nm using the SPECTROstar Nano microplate reader (BMG Labtech). A standard curve was created using the mean absorbances of the positive control standards, and the following formula was used to determine the percentage of m6A in total RNA:

$$\text{m6A (ng)} = (\text{sample optical density} - \text{negative control optical density}) \div (\text{slope})$$

$$\text{m6A (\%)} = (\text{m6A(ng)} \div \text{input RNA (ng)}) \times 100\%$$

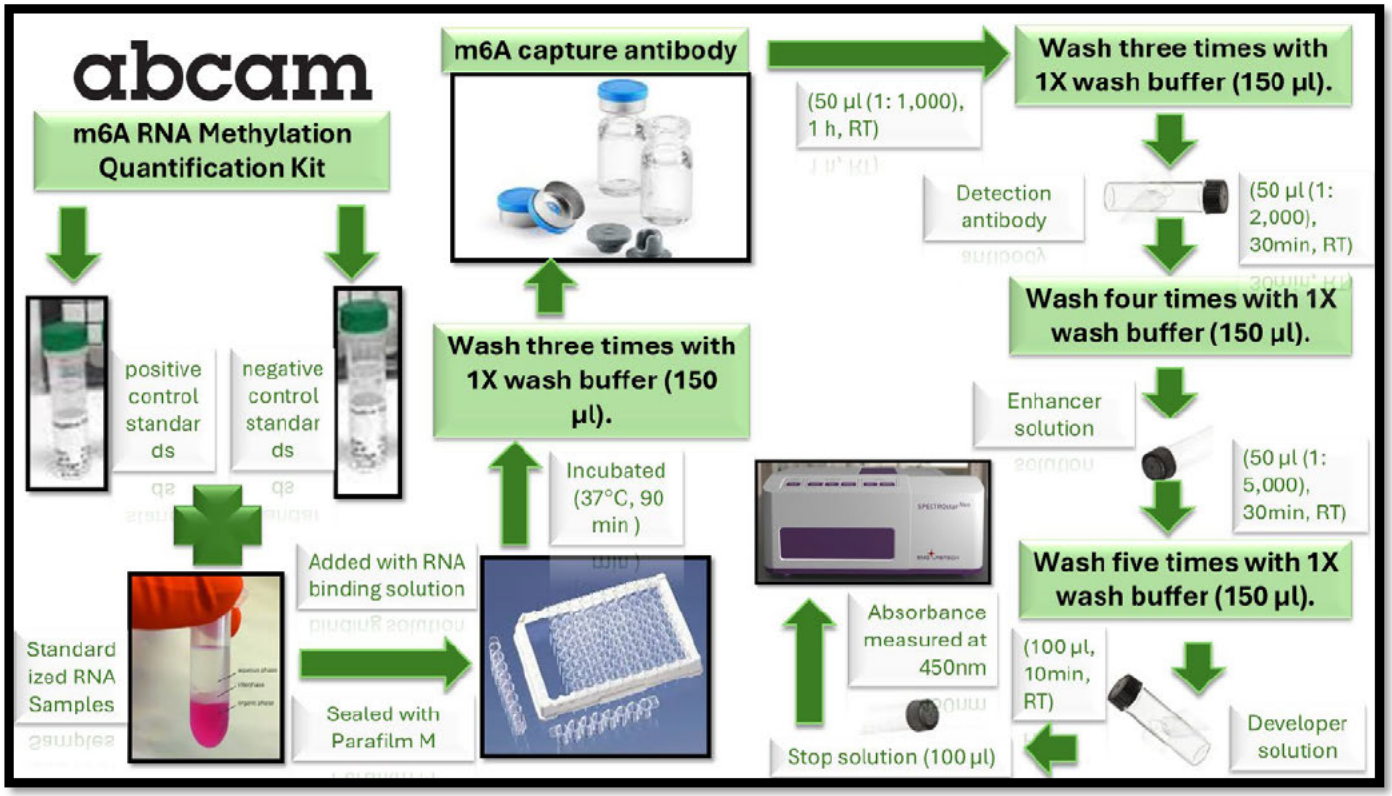

Figure 2.2: Overview of the ELISA assay (Composed by author)

2.6 qRT-PCR

2.6.1 Background

qRT-PCR is an accurate and precise method for evaluating gene expression. This method was built on the concepts of the original polymerase chain reaction (PCR) that Mullis created in 1983 (Mullis et al., 1986). The benefits qRT-PCR has over traditional PCR is in the real-time data collection, whereby fluorescent probes/dyes are introduced that allow amplified DNA to be quantified faster and more precisely without post-PCR processing (Heid et al., 1996).

There are seven core steps involved in the qRT-PCR. Using reverse transcriptase, the extracted RNA is reverse transcribed to create complementary DNA (cDNA). This is a critical step since PCR amplification is only compatible with DNA. The cDNA is then amplified with specific primers that target genes of interest along with a fluorescent reporter. The purpose of the reporter is to fluoresce in the presence of target DNA amplification, which allows for a linear measurement of the PCR product in real-time (Schmittgen & Livak, 2008). The last step involves quantifying the gene expression relative to the reference gene called the cycle threshold (Ct) value. The Ct value indicates the number of cycles at which the fluorescence exceeds a predetermined threshold (Schmittgen & Livak, 2008).

The reporter fluoresces as the target DNA is amplified, allowing for continuous, quantitative measurement of the PCR product in real-time. Finally, gene expression in relation to a reference gene or sample is measured using the Ct value, which is the cycle number at which fluorescence exceeds a predetermined threshold (Schmittgen & Livak, 2008). SYBR green binds to double-stranded DNA in addition to ensuring real-time monitoring (Kubista et al., 2006). Measuring the fluorescence in a thermal cycler allows for high-throughput quantification.

2.6.2 RNA Extraction

Control and FA-treated U87MG cells were used for total RNA extraction (Figure 2.3). The $25cm^3$ sterile cell culture flasks had their treatments removed and were washed three times with PBS. Trizol (500 µl) and PBS (500 µl) were added to each flask and mixed thoroughly. The flasks were incubated (5 min, RT). The cells were mechanically removed with a cell scraper and the cell solution was pipetted into appropriately labelled Eppendorf tubes. The samples were centrifuged (12,000 xg, 4°C, 15 min), isopropanol (500 µl) was added to the aqueous supernatant and incubated (-80°C, 24hrs). The samples were centrifuged (12,000 xg, 4°C, 20 min) and the supernatants were removed. The RNA pellets were washed in 75% ethanol (500 µl), centrifuged (7,400 xg, 4°C, 15 min), air dried (30 min, RT) and resuspended in nuclease-free water (15 µl). The Nanodrop2000 spectrophotometer (Thermo-Fisher Scientific, SA) was used to determine the purity and concentration of the RNA. For all further assays, samples having A260/A280 ratios between 1.9 and 2.1 were regarded as pure.

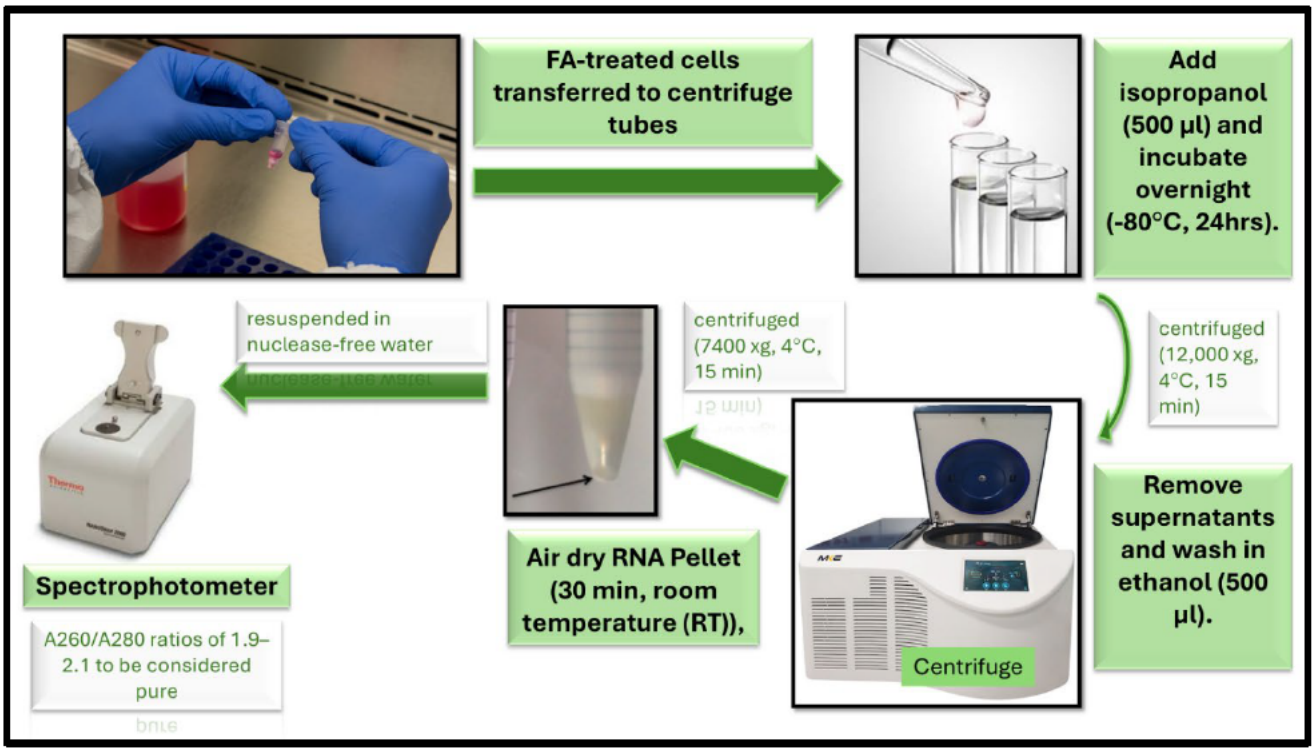

Figure 2.3: Overview of RNA isolation protocol (Composed by author)

2.6.3 cDNA Protocol

cDNA was synthesized using the Maxima H Minus First Strand cDNA Synthesis Kit (catalogue no. K1652, Thermo-Fisher Scientific), as per the manufacturers protocol. Master mix (14µl) and template RNA (500 ng/µl;1µl) were added into micro-centrifuge tubes and incubated (65°C, 5 min) in a thermo-cycler (Thermo-Fisher Scientific). The micro-centrifuge tubes were placed on ice (5 min). Another master mix was prepared [5x RT Buffer (4µl), Maxima H Minus enzyme mix (1µl)]. 5µl of the master mix was added to all samples and mixed gently (2 min). The micro-centrifuge tubes were then incubated (25°C, 10 min), followed by a second incubation (50°C, 15 min) and finally a third incubation to terminate the reaction (85°C, 5 min) in a thermo-cycler (Thermo-Fisher Scientific). Nuclease-free water (60µl) was added to the micro-centrifuge tubes and stored (-80°C)

2.6.4 qRT-PCR Protocol

The mRNA expression levels of *METTL3, WTAP, METTL14, YTHDF1, YTHDF2, YTHDF3, YTHDC1, YTHDC2, ALKBH5, FTO, BDNF* and *CREB* were determined using the qRT-PCR assay (Figure 2.4). The PowerUp™ SYBR™ Green Master Mix (catalogue no. A25742, Thermo-Fisher

Scientific) and the QuantStudio™ 3 Real-Time PCR System (Thermo-Fisher Scientific) were used to perform the assay. The conditions for the thermocycler were:

- initial denaturation (95°C, 8 min)
- 40 cycles of denaturation (95°C, 15 s); annealing (Table 1, 40 s); extension (72°C, 30 s)

To normalize mRNA expression, GAPDH was used as the endogenous control. The relative change in mRNA expression was determined using the comparative threshold cycle ($2^{-\Delta\Delta Ct}$) approach (Livak & Schmittgen, 2001).

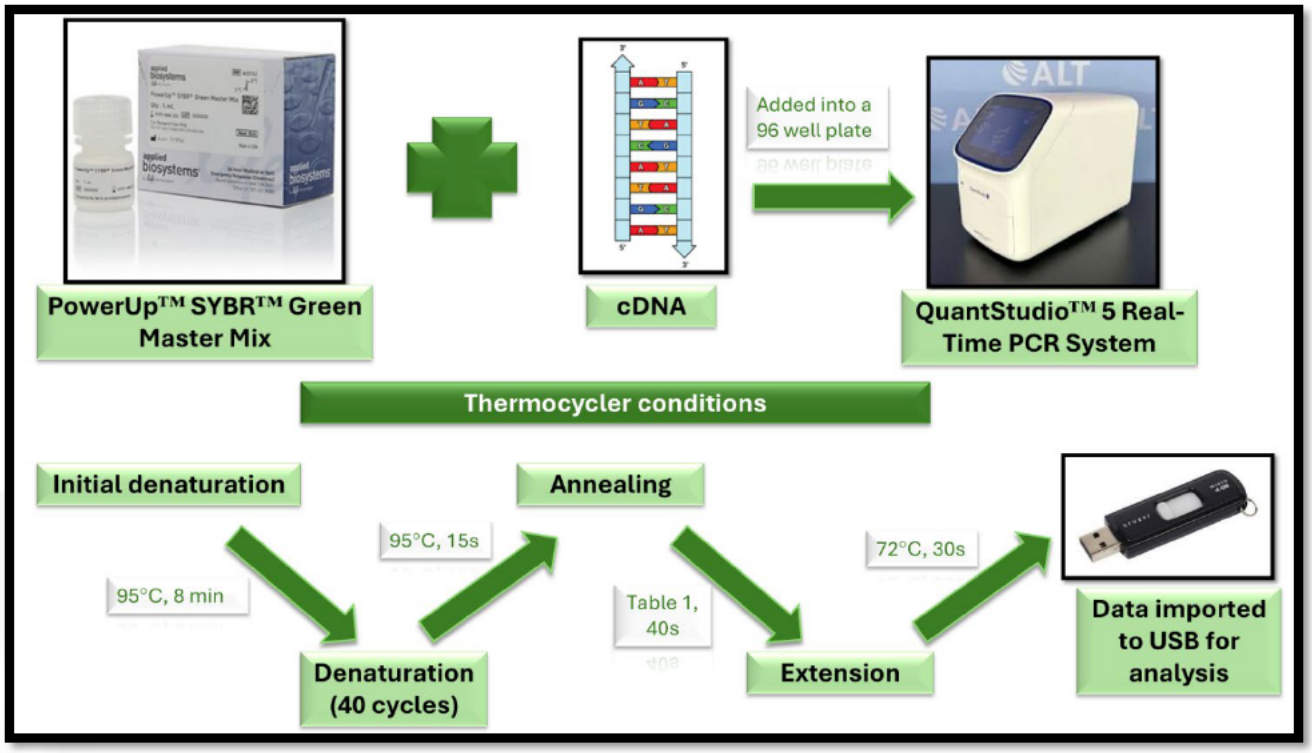

Figure 2.4: Overview of the qPCR protocol (Composed by author)

Table 1. The primer sequences utilized for qRT-PCR.

Gene	Accession number	Primer Sequence	Annealing Temperature (°C)
METTL3	NM_019721	F: TTGTCTCCAACCTTCCGTAGT R: CCAGATCAGAGAGGTGGTGGTGTAG	56°C
METTL14	NM_201638	F: GAACACAGAGCTTAAATCCCCA R: TGTCAGCTAAACCTACATCCCTG	56°C
YTHDF1	NM_173761	F: ACCTGTCCAGCTATTACCCG R: TGGTGAGGTATGGAATCGGAG	60°C
YTHDF2	NM_ 145393	F: CCTTAGGTGGAGCCATGATTG R: TCTGTGCTACCCAACTTCAGT	56°C
YTHDF3	NM_172677	F: TCAGAGTAACAGCTATCCACCA R: GGTTGTCAGATATGGCATAGGCT	56°C
FTO	NM_011936	F: ACTTGGCTCCCTTATCTGACC R: TGTGCAGTGTGAGAAAGGCTT	56°C
WTAP	NM_175394	F: CTTCCCAAGAAGGTTCGATTGA R: TCAGACTCTCTTAGGCCAGTTAC	56°C
YTHDC1	NM_177680	F: AACTGGTTTCTAAGCCACTGAGC R: GGAGGCACTACTTGATAGACGA	60°C
YTHDC2	NM_001163013	F: CAAAACATGCTGTTAGGAGCCT R: CCACTTGTCTTGCTCATTTCCC	60°C
ALKBH5	NM_172943	F: ATCCTCAGGAAGACAAGATTAG R: TTCTCTTCCTTGTCCATCTC	60°C
CREB	NM_001301.5	F: AGCAGCTCATGCAACATCATC R: AGTCCTTACAGGAAGACTGAACT	60°C
BDNF	NM_170732.6	F: GGCTTGACATCATTGGCTGAC R: CATTGGGCCGAACTTTCTGGT	60 °C
GAPDH	NM_001289726	F: TCCACCACCCTGTTGCTGTA R: ACCACAGTCCATGCCATCAC	Same as the gene of interest

F: forward; R: reverse

2.7 Western Blot Assay

2.7.1 Introduction

The Western blotting technique was first developed by Towbin et al. (1979) for detecting and quantifying specific proteins within samples. It is a worldwide standard in molecular biology, protein research and immunology due to its adaptability and specificity in protein quantification (Towbin et al., 1979).

The assay has four major steps involved: protein separation, protein transfer, protein blocking and protein detection. Using a technique known as sodium dodecyl sulphate-polyacrylamide gel electrophoresis (SDS-PAGE), proteins are first separated according to their size. Adding Laemmli buffer and boiling (100°C) denatures proteins and leaves behind a negative charge that facilitates separation. This is done by applying a voltage that negatively charges proteins, causing them to move downwards towards the positively charged electrode in the gel matrix (Mahmood & Yang, 2012). Therefore, heavier proteins migrate slower while lighter proteins migrate faster.

From the gel, proteins from within are moved to a nitrocellulose membrane which facilitates stable antibody binding (Towbin et al., 1979). The blocking process utilizes a solution like non-fat milk or Bovine Serum Albumin (BSA) that prevents nonspecific antibody binding and increases specificity. The protein detection phase involves incubating the membrane with a primary antibody that is target protein specific, after which an enzyme-conjugated secondary antibody is added for detection by chemiluminescence (Mahmood & Yang, 2012).

The materials used (blocking agents and nitrocellulose membranes) are essential for maximizing protein binding efficiency as well as reducing the background noise, which boosts the reliability of the assay. The western blotting technique has a host of advantages, including high specificity for target proteins as well as simultaneous size estimation, providing a deeper look into protein alterations (Kurien & Scofield, 2006). It is also a valuable method in disease detection with specific protein biomarkers.

2.7.2 Protein Isolation

The Cytobuster™ Protein Extraction Reagent (catalogue no. 71009-4, Novagen, Bloemfontein, SA) was utilized to extract total protein from the U87MG cells. The CytoBuster™ Protein Extraction Reagent is a detergent-based solution that simplifies the process of protein isolation from mammalian cells. This is achieved by ensuring rapid lysis under mild conditions, ensuring

no damage to the proteins. CytoBuster™ was engineered to solubilize nuclear and cytoplasmic proteins.

When CytoBuster™ is added to cell cultures, the cells are lysed by membrane disruption, yet the protein structure and their functionality are retained. When the cells compartmentalization is degraded, several phosphatases and proteases that damage cellular proteins are released. Phosphatase and protease inhibitors added to the lysis reagent serve to prevent the degradation of proteins during this step. Endogenous proteolytic and phospholytic enzymes are rendered inactive by these inhibitors.

2.7.2.1 Protocol

FA was added to U87MG cells for 24 hr treatments. The flasks had their supernatants removed and the cells were washed with 0.1M PBS three times. CytoBuster™ reagent (200µl) (Novagen, catalogue no. 71009) supplemented with protease inhibitors (Roche, catalogue no. 05892791001) and phosphatase inhibitors (Roche, catalogue no. 04906837001) was then added to each flask and placed on ice (30 min). This prevents the denaturation of the proteins. A cell scraper was used to further lyse the cells and the lysates were transferred into 1.5ml micro-centrifuge tubes. The tubes were then centrifuged (12 000xg, 10 min, 4°C). The crude protein was aspirated into new 1.5 ml microcentrifuge tubes and stored (-80°C) to be quantified and standardized. The pellets contained cellular debris and were discarded.

2.8 Bicinchoninic Acid (BCA) Assay

2.8.1 Background

Smith et al. (1985) were the first to create the Bicinchoninic Acid assay. It is largely accepted as being the most successful method for protein quantification. The assay replaced the Lowry assay since it provided a greater stability and sensitivity in detecting protein concentrations (Smith et al., 1985). The assay incorporates two pivotal reactions (Figure 2.5), the first being cupric (Cu^{2+}) ions undergoing reduction to form cuprous (Cu^{1+}) ions by protein samples while subjugated to an alkaline environment surrounded by bicinchoninic acid (Walker, 1996). The reaction is facilitated by positively charged amino acids (histidine and lysine) and negatively charged amino acids (aspartic and glutamic acids). Two molecules of BCA selectively bind to reduced Cu ions (Walker, 2009). Secondly, the absorbance of the solution complex is directionally proportional to the protein

concentration and is measured at 562 nm (Walker, 1996). The quantity of protein present is also measured by the intensity of the purple colour shift and represents the number of peptide bonds in the reaction (Walker, 1996). The protein samples are mixed with the BCA reagent and incubated (37°C). This assay is highly compatible due to its versatility with many detergents and reducing agents, making it exceptionally useful for cell and tissue lysates where these components are needed (Wiechelman et al., 1988). Advantages of the BCA assay include its high compatibility and sensitivity which are core essentials of high-throughput research (Noble & Bailey, 2009).

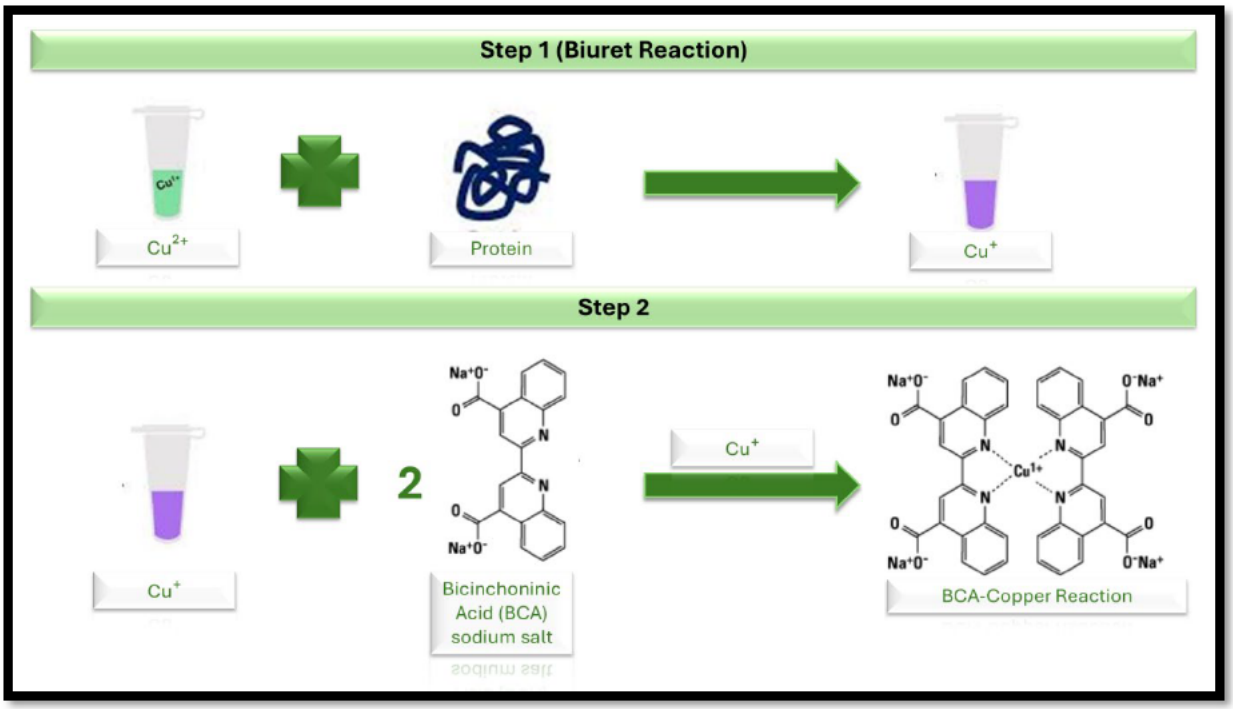

Figure 2.5: Overview of the BCA assay (Composed by author)

2.8.2 Protocol

Bovine serum albumin (BSA) standards of different concentrations [0, 0.2, 0.4, 0.6, 0.8 and 1mg/ml] were composed in distilled water in 1.5ml micro-centrifuge tubes. Each standard (25µl) was run in triplicate and each protein sample (25µl) was run in duplicate. The samples were loaded into a 96-well microtiter plate and a working solution was added (200µl) [made up of 4µl copper sulphate ($CuSO_4$) and 198µl BCA] to each well and the plate was incubated (37°C, 30 min). A SPECTROstar Nano microplate reader (BMG Labtech) was used to measure the absorbance at 562nm. Using the absorbances of the BSA standards, a standard curve was created (Appendix B).

2.8.3 Quantification and Standardization of proteins

CytoBuster™ reagent (200µl) (Novagen, catalogue no. 71009) was utilized to standardize (1.5mg/ml) the relevant proteins (Figure 2.6). The protein samples were prepared in Laemmli buffer [0.5M Tris-HCl (pH 6.8), 5% β-mercaptoethanol, glycerol, 1% bromophenol blue, 10% sodium dodecyl sulphate (SDS), distilled water (dH_2O)] and boiled (100°C, 5 min). The Laemmli buffer and its constituents have unique purposes. The glycerol makes the samples denser, making them descend into the SDS-PAGE gel wells easier (Mahmood and Yang, 2012). Tris-HCl regulates pH levels and serves as a buffer. SDS creates a negative charge and denatures proteins to their linear form. The proteins separate according to their distinct sizes as a result of the negative charge (Mahmood and Yang, 2012). Protein denaturation is brought on by the β-mercaptoethanol breaking disulphide bonds and bromophenol blue stains the samples so they can be tracked through the gel as they migrate during electrophoresis. After boiling, the samples were allowed to cool down to room temperature and stored (-20°C).

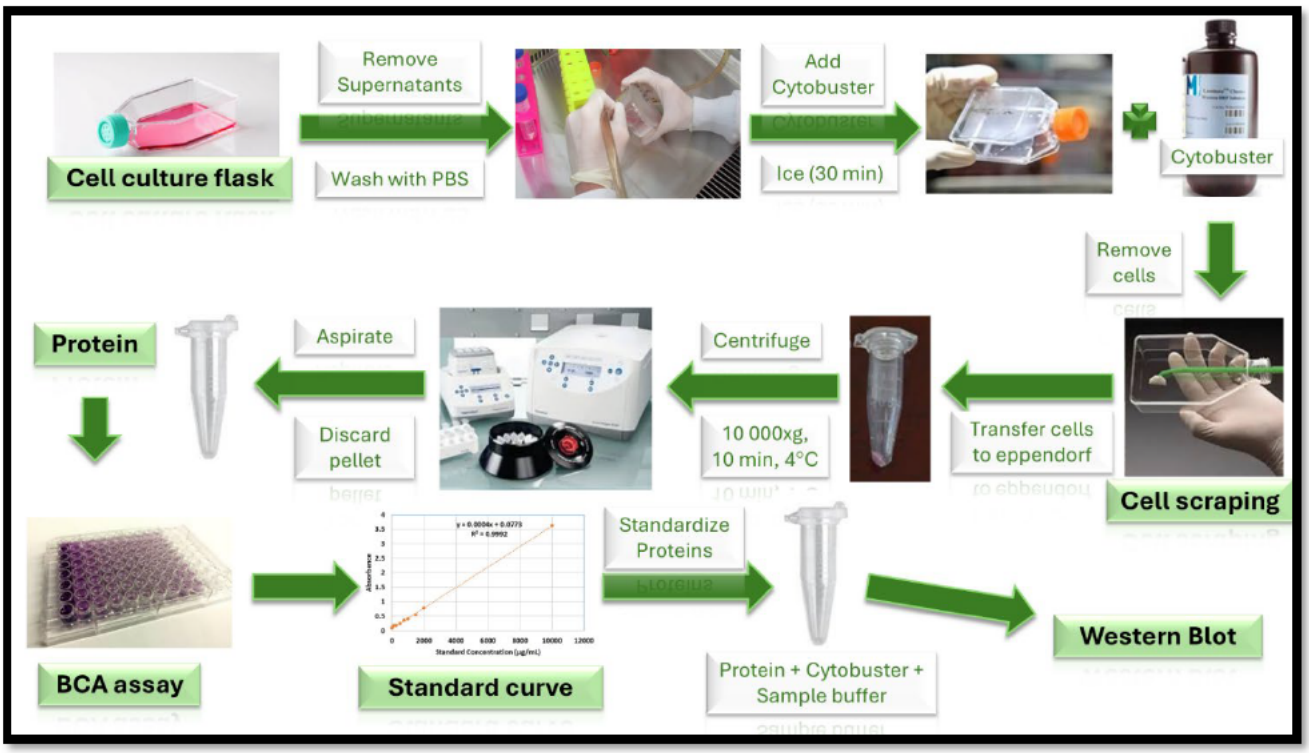

Figure 2.6: Visual representation of the protein standardization and quantification method (Composed by author)

2.9 Gel preparation for SDS – PAGE

2.9.1 Introduction

The gel preparation for SDS-PAGE is a crucial step in Western blotting (Figure 2.7). Two gel layers are prepared, being the stacking and resolving gel. The resolving gel has higher acrylamide concentrations and provides a medium for protein separation. This is done with small pores that sort proteins based on size. Above it, the stacking gel, with a lower acrylamide concentration, compresses protein samples into a narrow band for sharper resolution and separation by the resolving gel (Walker, 2009). The advantages of SDS-PAGE include its high-resolution separation and compatibility with downstream applications (Mahmood & Yang, 2012)

2.9.1.1 Protocol

The Mini-PROTEAN Tetra Cell casting stand (Bio-Rad) was used to prepare the SDS-PAGE gels (Figure 2.7). A 10% resolving gel [1.5M Tris-HCl (pH 8.8), 10% ammonium persulphate solution (APS), 10% SDS, bis-acrylamide, Tetramethylethylenediamine (TEMED) and dH2O] was composed and polymerized (1 hr). A 4% stacking gel [0.5M Tris-HCl (pH 6.8), bis-acrylamide, 10% APS, TEMED, 10% SDS and dH2O,] was composed and placed on top of the resolving gel (Figure 2.8). A 1cm plastic comb was inserted in between both glass plates to ensure proper well formation for loading samples. The gel was left to set (40 min).

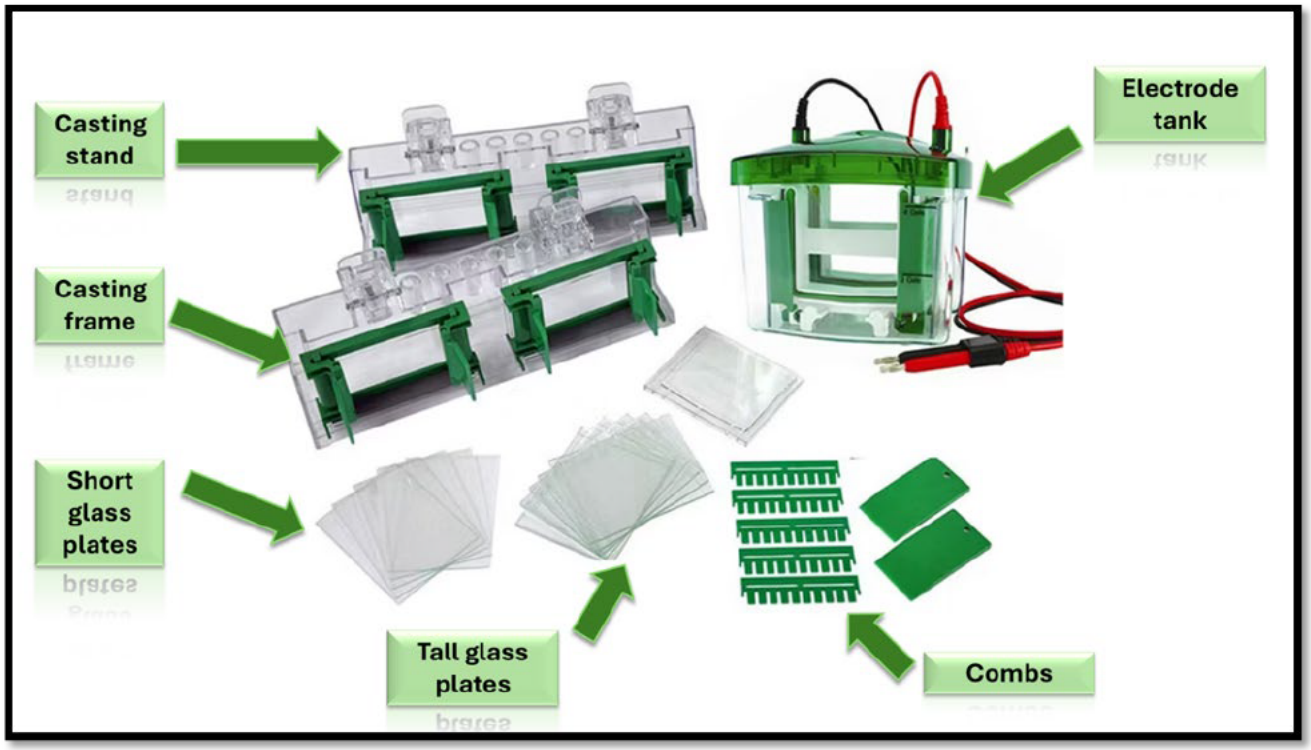

Figure 2.7: Different apparatus used to prepare for SDS-PAGE gels (Composed by author)

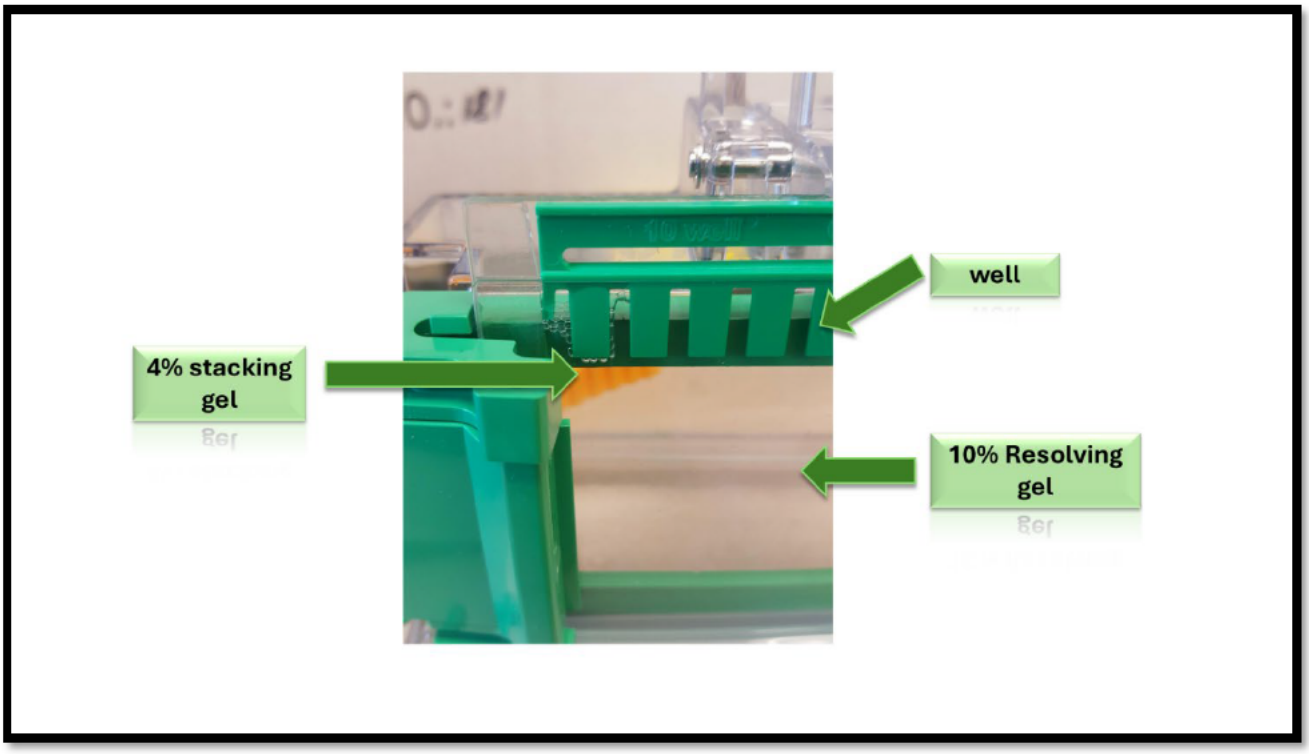

Figure 2.8: Different SDS-PAGE gel layers (Composed by author)

2.9.1.2 SDS PAGE procedure

The assembly starts by placing the gel cassettes into the electrode assembly which is then placed into the electrode tank (Mini- PROTEAN Tetra Cell System, Bio-Rad) (Figure 2.9). Molecular weight marker (5µl) (Precision Plus Protein All Blue Standards, catalogue no. #161 0373, Bio-Rad) and protein samples (25µl) are loaded into each well. The electrode tank was filled with running buffer [0.1% SDS, 25mM Tris-HCl and 192mM glycine] and the loaded samples were electrophoresed (150 volts (V), 1hr) using a compact power supply (Bio-Rad).

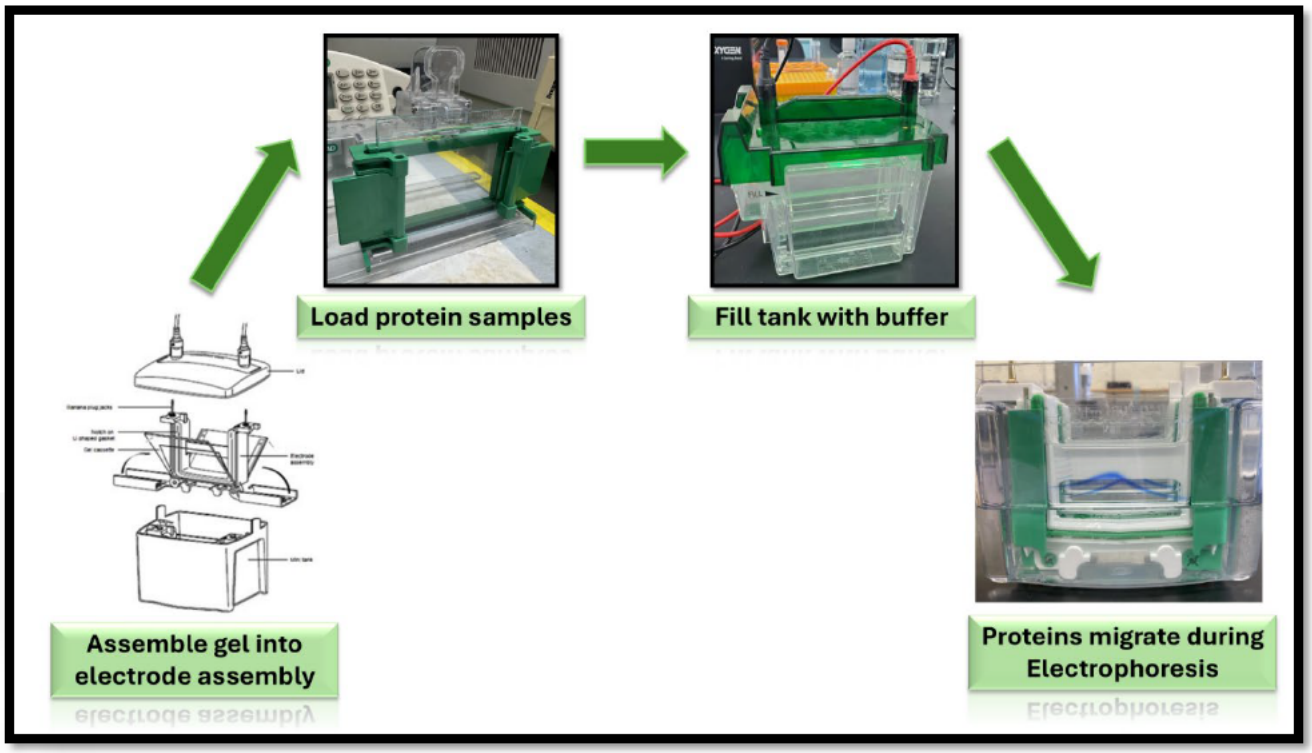

Figure 2.9: SDS-PAGE protocol overview (Composed by author)

2.9.1.3 Protein transfer

Post electrophoresis, the proteins were transferred onto a nitrocellulose membrane (Figure 2.10). The electrophoresed gels were removed from the glass plates. The gels, nitrocellulose membranes and two fibre pads were equilibrated for 10 min in transfer buffer [pH 8.3, 192mM glycine, 20% methanol, 25mM Tris]. A gel sandwich was built between the two electrodes in the transfer device, consisting of a nitrocellulose membrane and gel sandwiched between two fibre pads. Using the Bio-Rad Trans-Blot Turbo Transfer System (30 min, 20V), separated proteins were electro-transferred to the nitrocellulose membrane.

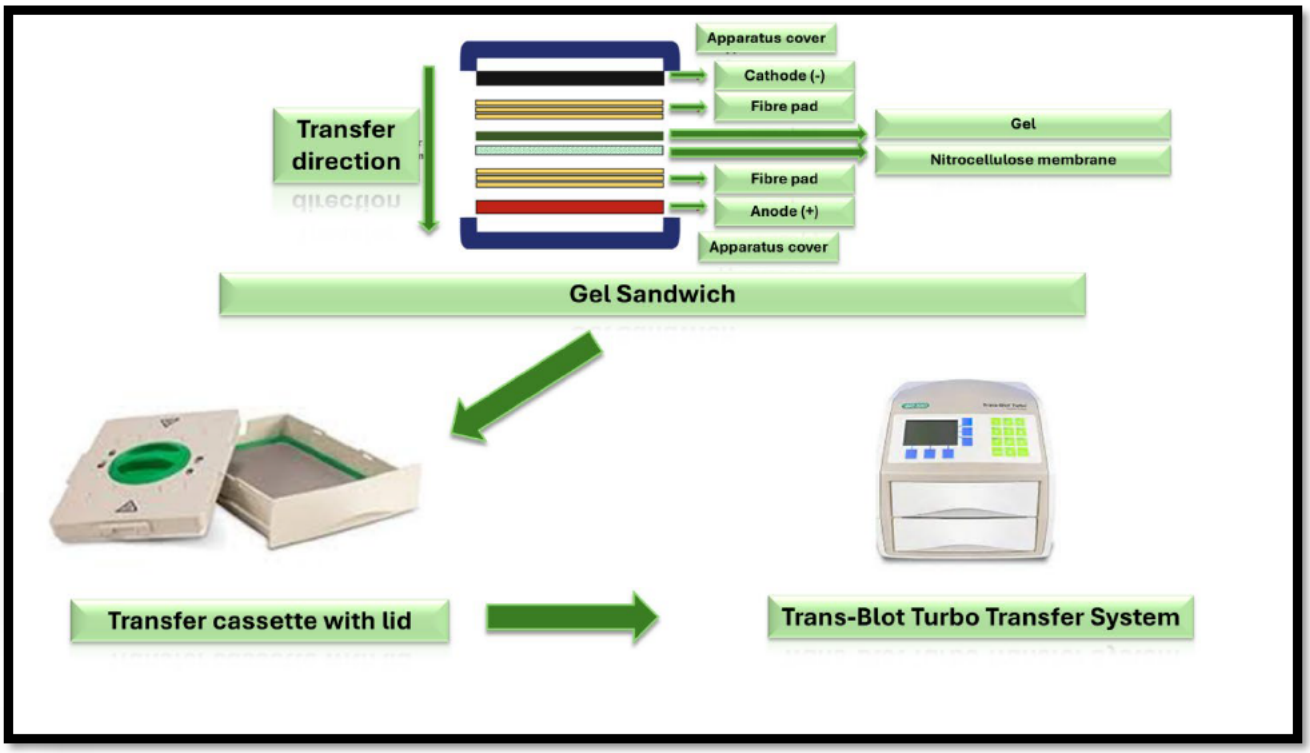

Figure 2.10: Overview of protein transfer to membrane (Composed by author)

2.9.1.4 Blocking and antibody incubation

The nitrocellulose membranes were blocked (1hr, RT) in 5ml blocking buffer (5% BSA) in Tris buffered saline with 0.05% Tween 20 (TTBS) [pH 7.5, 3mM potassium chloride (KCl), 25mM Tris-HCl, 150mM NaCl and dH_2O,]. During the blocking process, the membranes were placed in a container and put on a shaker. This step was done to reduce the chance of the proteins undergoing non-specific binding. The specific primary antibody (Table 1) was added to the membranes (1 hr, RT) and left on the shaker. The membranes were placed into the fridge (4°C) overnight. The target protein is selective in its binding properties to the primary antibody. After incubation the membranes were equilibrated (30 min, RT) and washed five times with TTBS (10 min each, RT). This step ensures any primary antibody that did not bind is removed. Membranes were incubated with horse-radish peroxidase (HRP)-conjugated secondary antibodies (2 hrs, RT) with gentle shaking. The dilutions for the secondary antibodies were 1:10 000 in 5%. The membranes were then washed with TTBS five times (10 min each, RT) to remove any secondary antibody that did not bind.

Table 2: Antibody dilutions for Western blot

Target protein	Primary Antibody host	Secondary Antibody	Dilution	Company	Catalogue no.
BDNF	Rabbit	Anti-Rabbit IgG, HRP-linked	1: 1000	Cell Signaling Technology	47808S
p-AKT	Rabbit	Anti-Rabbit IgG, HRP-linked	1: 1000	Cell Signaling Technology	9272S
PI3K	Mouse	Anti-Mouse IgG, HRP-linked	1: 500	Proteintech	PTE67071-1-IG
p-CREB (S133)	Rabbit	Anti-Rabbit IgG, HRP-linked	1: 1000	Cell Signaling Technology	9191L

2.9.1.5 Imaging

The Clarity™ Western ECL Substrate Kit (catalogue no. #170-5060, Bio-Rad) was used for the antigen- antibody complex. The kit includes enhanced luminol solution and a hydrogen peroxide substrate. The signal was detected using the iBright™ CL1500 Imaging System (Thermo-Fisher Scientific). The HRP-conjugated secondary antibody undergoes a reaction with the hydrogen peroxide (H_2O_2) substrate, forming oxygen radicals (Figure 2.11). Following a reaction with these oxygen radicals, luminol degrades into aminophthalic acid. Following a reaction with enhancer molecules, the aminophthalic acid glows and reveals the protein bands.

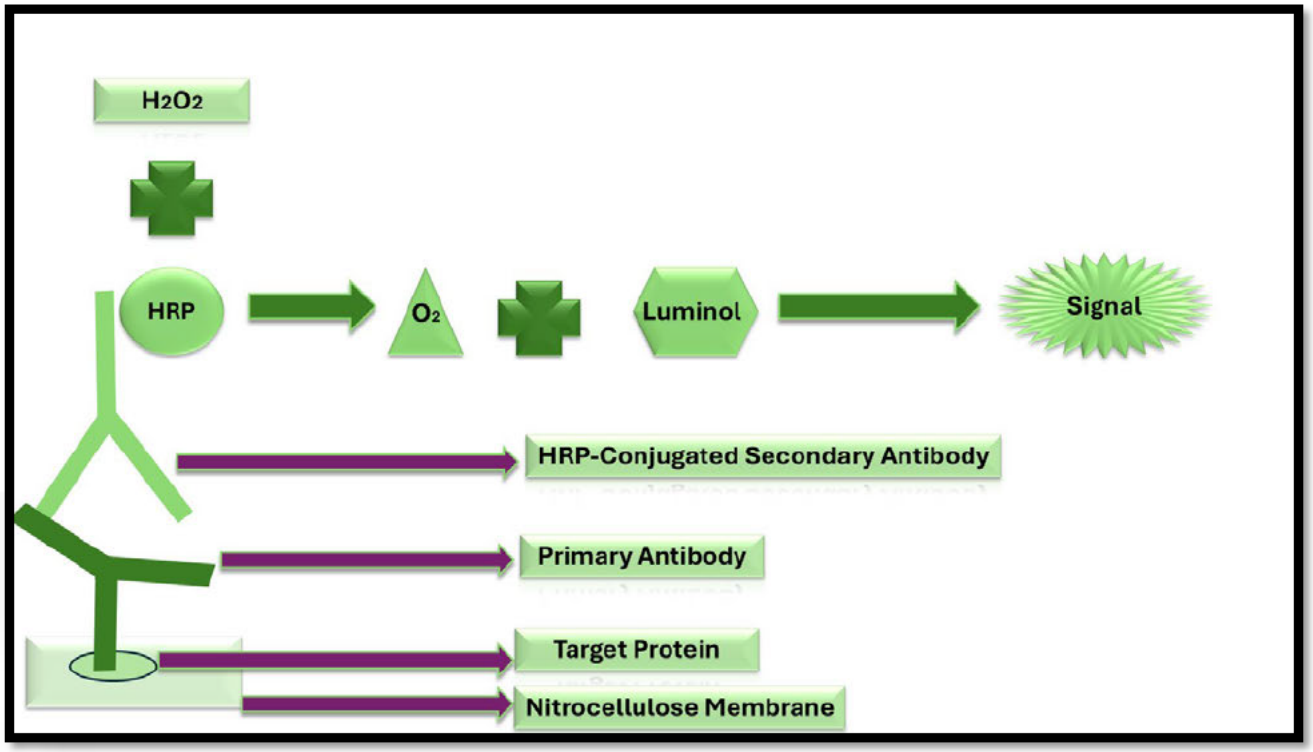

Figure 2.11: Overview of the antigen-antibody binding and detection principle (Composed by author)

2.9.1.6 Quenching and normalization

Post detection, the membranes were quenched in 5ml H_2O_2 (30 min, 37°C) and washed with TTBS (10 min, RT) once. The housekeeping protein anti-β-actin (catalogue no. A3854, Sigma-Aldrich, 1:5 000 dilution in 5% BSA) was then used to probe the membranes after they had been blocked in 5% BSA in TTBS (1 hr, RT). This precaution was done to normalize protein expression to account for discrepancies in loading. Protein expression was analyzed using the Invitrogen™ iBright™ Analysis Software (Thermo-Fisher Scientific). Fold-change and relative band density (RBD) were used to illustrate the results. To normalize protein expression, the RBD of the protein of interest was divided by the RBD of β-actin. To calculate the fold-change in comparison to the control, the normalized protein expression of the treatment was divided by the normalized protein expression of the control.

3.1 Statistical analysis

GraphPad Prism version 5.0 (GraphPad Software Inc., California) and Microsoft Excel (Office, 2024) were used to perform all statistical analyses. The unpaired t-test with Welch's Correction was used for all assays. All results were represented as the mean ± standard deviation (SD) unless

otherwise stated. A value of $p<0.05$ was considered statistically significant. A minimum of four technical replicates was used for each experiment and each experiment was performed three independent times.

CHAPTER 3

RESULTS

3.1 The MTT assay

FA was cytotoxic to U87MG cells

This assay was utilized to determine the metabolic activity and cell viability of U87MG cells after 24-hrs treatment with FA. The cell viability in each sample was determined using the absorbance measurements. As FA concentration increased the cell viability decreased, indicating that FA altered the metabolic activity of U87MG cells and was cytotoxic (Figure 3.1). The IC_{50} value of FA was determined to be 180 µg/ml.

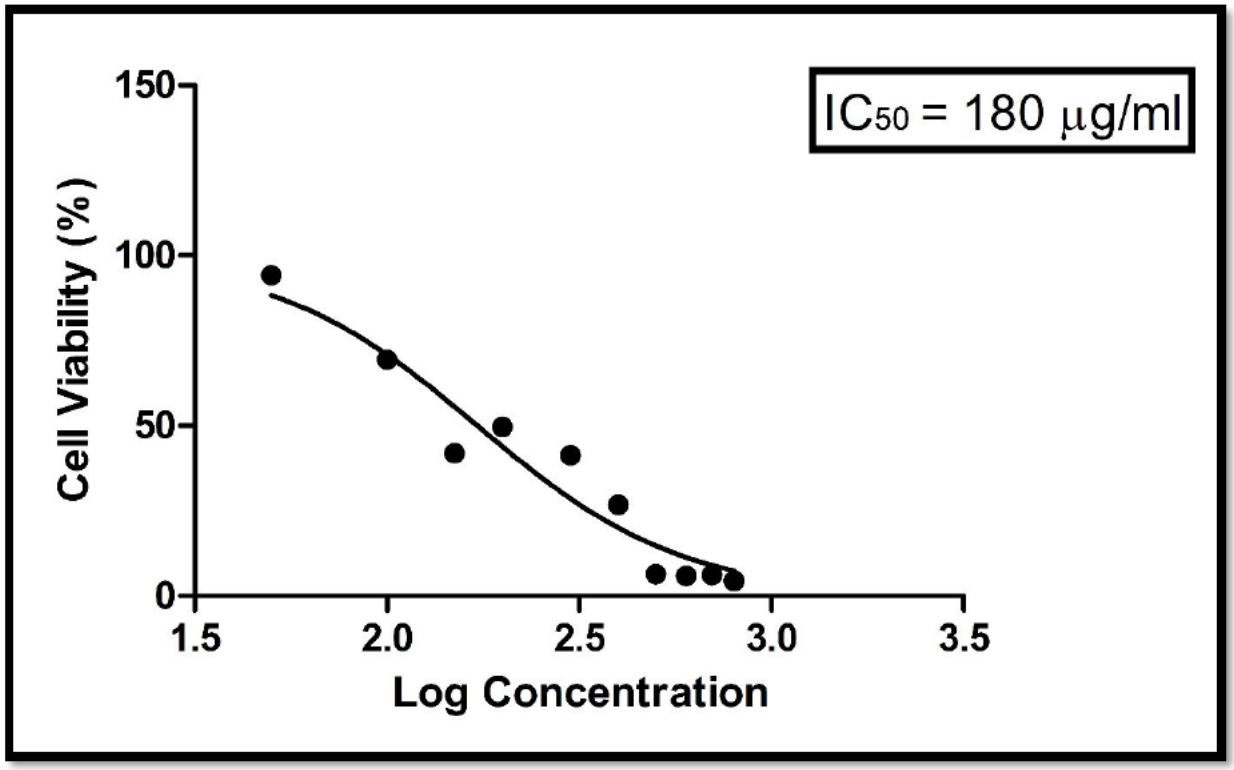

Figure 3.1: The IC_{50} of FA on the cell viability of U87MG cells. X-axis represents the log-transformed concentration of FA, while the y-axis shows cell viability (%). As the FA concentration increased, the cell viability of the U87MG cells decreased, showing an inverse relationship.

3.2 ELISA

This assay was conducted for the purpose of identifying and quantifying the global m6A content in the U87MG cells after FA exposure for 24 hrs (Figure 3.2).

Global m6A RNA methylation increased in U87MG cells due to FA exposure

The results (Figure 3.2) depict elevated global m6A levels in relation to the control due to FA exposure by (2.1059-fold; $p = 0.0150$)

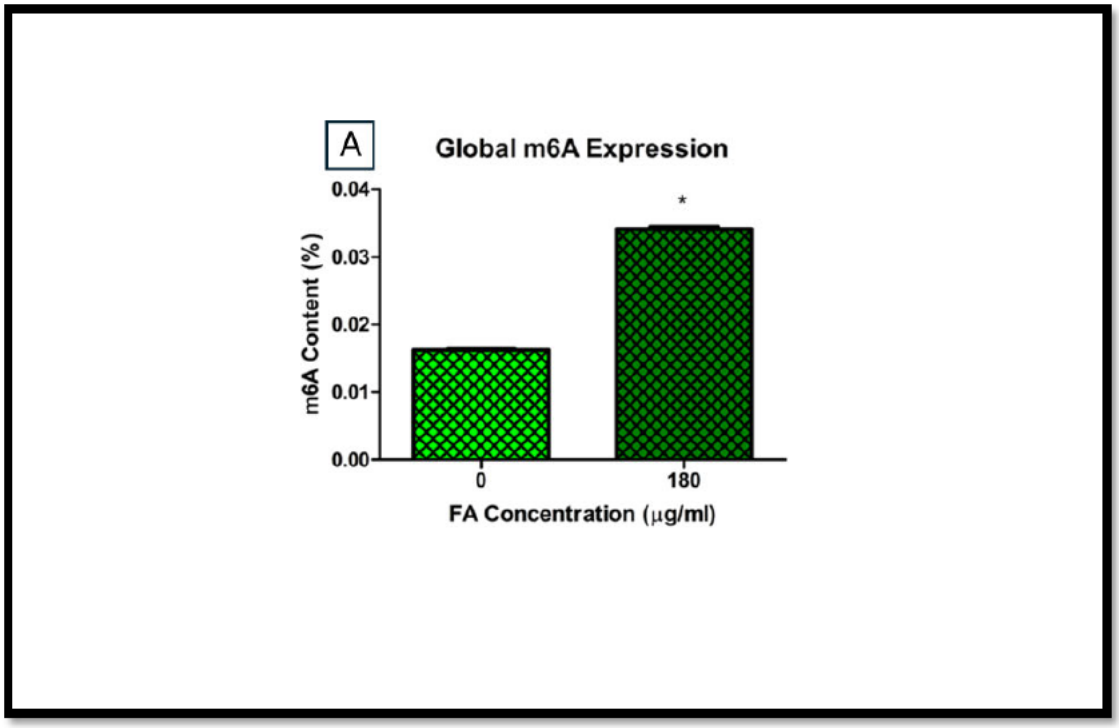

Figure 3.2: FA's impact on global m6A RNA methylation in FA-treated U87MG cells. Results displayed are the mean ± SD (n = 4). Statistical significance was evaluated using the unpaired t-test with Welch's correction, $*p < 0.05$. Global m6A RNA methylation levels increased.

3.3 The qRT-PCR assay

This assay was used to quantify mRNA expression levels of m6A writers (*METTL3/14* and *WTAP*) readers (*YTHDF 1/2/3* and *YTHDC1/2*), erasers (*FTO* and *ALKBH5), BDNF* and *CREB*. The results are presented as relative fold-change (rfc) which is calculated as treatment divided by control (control = 1-fold).

3.3.1 m6A 'writers'

FA exposure downregulated 'writers' mRNA expression

FA significantly decreased the mRNA expression of *METTL3* (Figure 3.3A; 0.2605-fold; p = 0.0007). FA significantly decreased the mRNA expression of *METTL14* (Figure 3.3B; 0.4137-fold; p = 0.0068). FA significantly decreased the mRNA expression of *WTAP* (Figure 3.3C; 0.2740-fold; p = 0.0004). FA demonstrated a significant downregulation of key m6A writer genes.

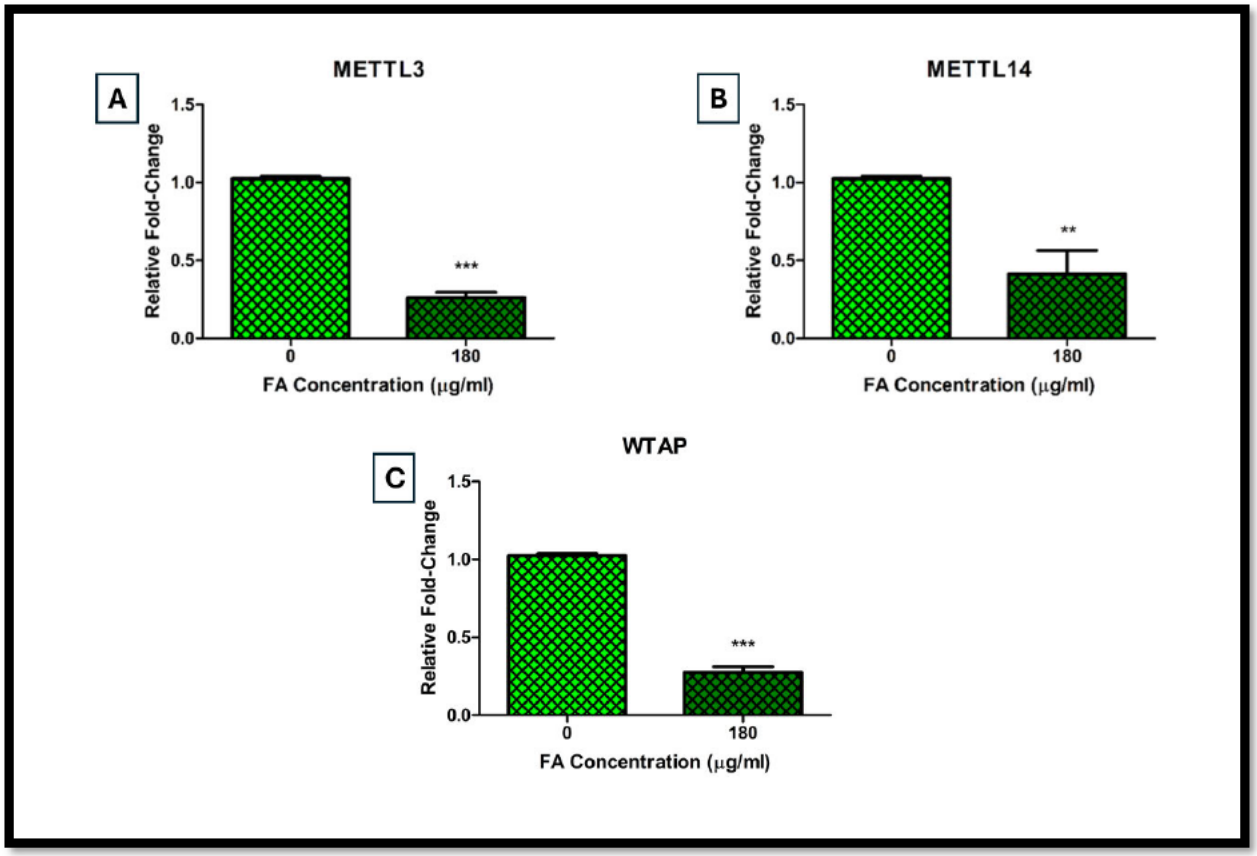

Figure 3.3: mRNA expression of m6A 'writers' after treatment with FA in U87MG cells. Results displayed are the mean ± SD (n = 4). Statistical significance was evaluated using the unpaired t-test with Welch's correction, $^{**}p < 0.01$, $^{***}p < 0.001$. *METTL3*, *METTL14* and *WTAP* mRNA expression decreased after FA treatment.

3.3.2 m6A erasers

FA exposure downregulated m6A erasers ALKBH5 and FTO

FA significantly decreased the mRNA expression of *FTO* (Figure 3.4A; 0.4534-fold; $p = 0.0039$). FA significantly decreased the mRNA expression of *ALKBH5* (Figure 3.4B; 0.0066-fold; $p = 0.0004$)

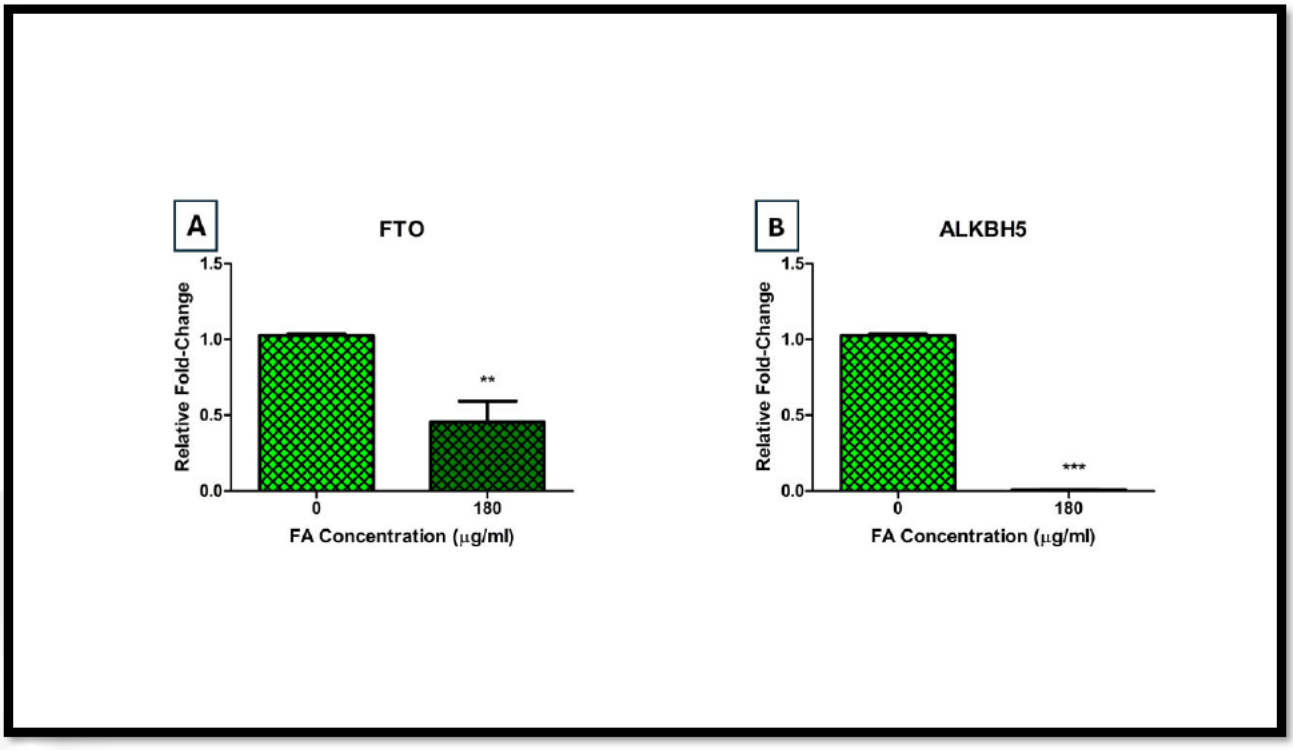

Figure 3.4: mRNA expression of m6A 'erasers' after treatment with FA in U87MG cells. Results displayed are the mean ± SD (n = 4). Statistical significance was evaluated using the unpaired t-test with Welch's correction, $^{**}p < 0.01$, $^{***}p < 0.001$. *FTO* and *ALKBH5* mRNA expression decreased after FA treatment.

3.3.3. m6A readers

FA exposure down-regulated 'readers' mRNA expression

The mRNA expression of *YTHDF1* (Figure 3.5A; 0.7170-fold; $p = 0.0793$) was non-significant ($p > 0.05$). FA significantly decreased the mRNA expression of *YTHDF2* (Figure 3.5B; 0.6269-fold; $p = 0.0224$). The mRNA expression of *YTHDF3* (Figure 3.5C; 1.335-fold; $p = 0.0647$) was non-significant ($p > 0.05$). FA significantly decreased the mRNA expression of *YTHDC1* (Figure 3.5D; 0.9867-fold; $p = 0.0008$). FA significantly decreased the mRNA expression of *YTHDC2* (Figure 3.5E; 0.0570-fold; $p = 0.0003$). FA demonstrated a significant downregulation of 'readers' *YTHDF1/2* and *YTHDC1/2* while upregulating *YTHDF3*.

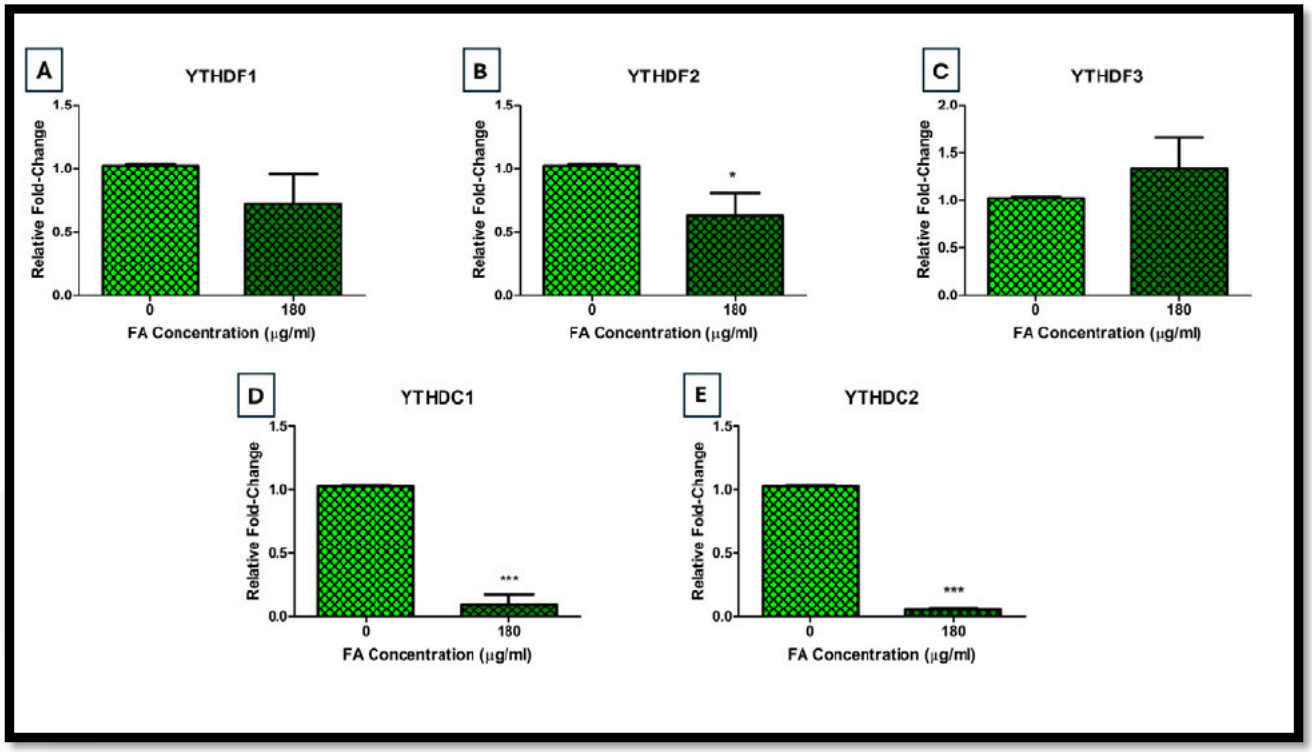

Figure 3.5: mRNA expression of m6A 'readers' after treatment with FA in U87MG cells. Results displayed are the mean ± SD (n = 4). Statistical significance was evaluated using the unpaired t-test with Welch's correction, $*p < 0.05$, $***p < 0.001$. *YTHDF1/2* and *YTHDC1/2* mRNA expression increased; however, *YTHDF3* mRNA expression decreased after FA treatment.

3.3.4 *BDNF* and *CREB* expression

FA exposure downregulated CREB and BDNF

FA significantly decreased the mRNA expression of *BDNF* (Figure 3.6A; 0.0106-fold; $p = 0.0006$). FA significantly decreased the mRNA expression of *CREB* (Figure 3.5B; 0.9172-fold; $p = 0.0003$).

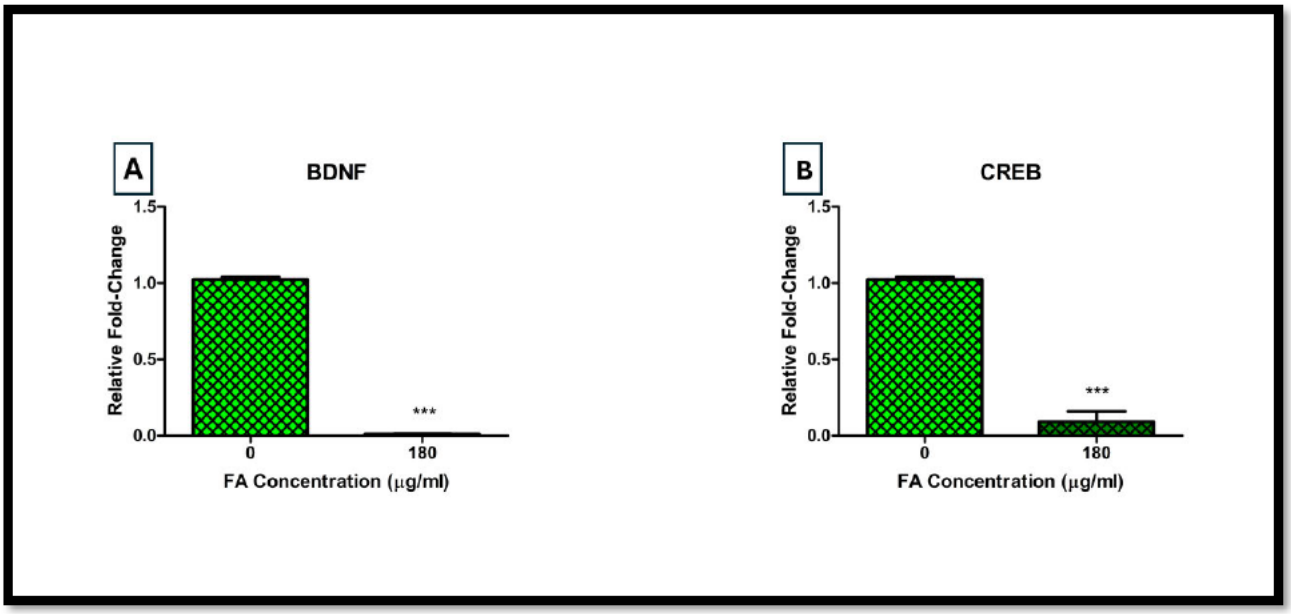

Figure 3.6: mRNA expression of *CREB* and *BDNF* after treatment with FA in U87MG cells. Results displayed are the mean ± SD (n = 4). Statistical significance was evaluated using the unpaired t-test with Welch's correction, ***$p < 0.001$. *CREB* and *BDNF* mRNA expression decreased after FA treatment.

3.4 Western Blot

This assay was utilized to quantify protein expressions of *BDNF*, *P-CREB*, phosphorylated protein kinase B (*P-Akt*) and *PI3K* in FA treated and control U87MG cells for 24 hrs. The results are represented as fold-change compared to the control (control = 1-fold).

BDNF expression is upregulated due to FA exposure

BDNF is triggered to respond to increased neuronal activity, brain injury as well as stress. FA significantly increased the protein expression level of *BDNF* by (Figure 3.7; 1.205-fold; p = 0.0173).

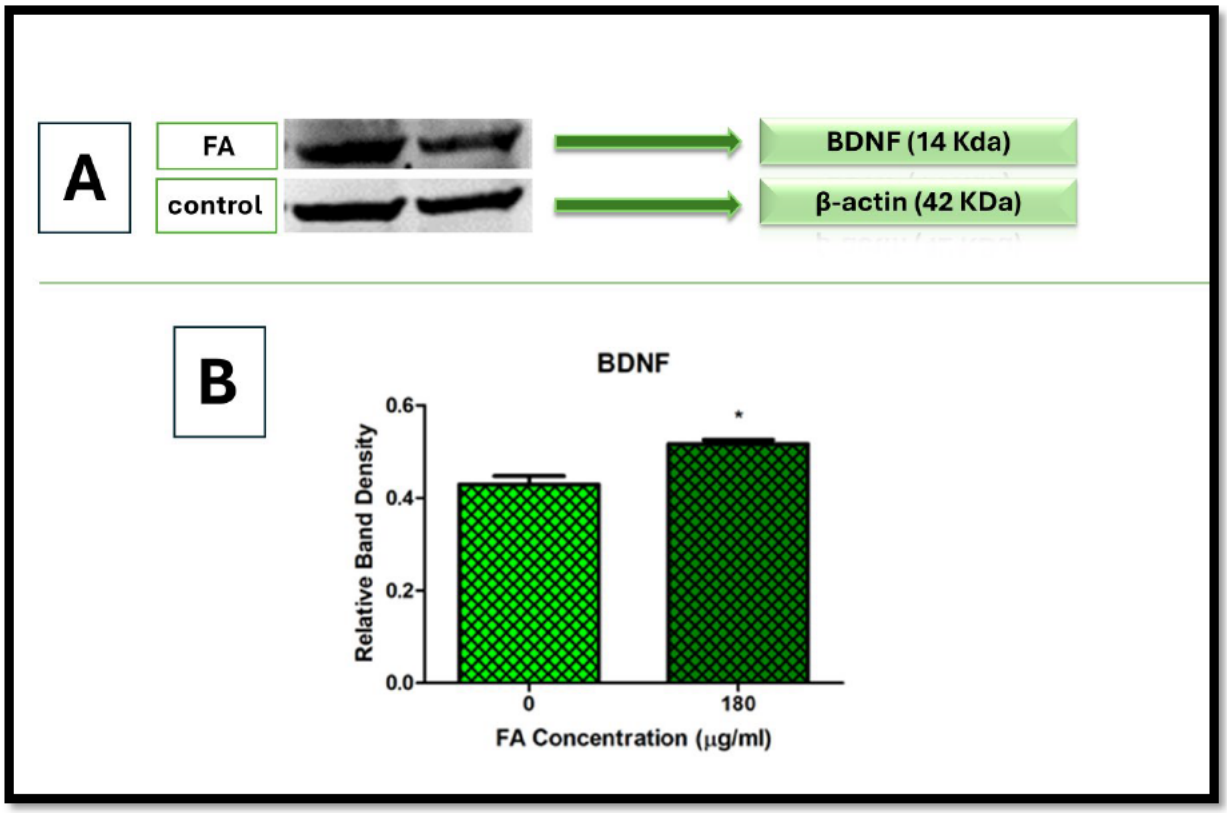

Figure 3.7: Protein expression levels of *BDNF* after FA exposure for 24 hrs. (A) represents the Western blot images and (B) represents the Relative Band Density. Statistical significance was evaluated using the unpaired t-test with Welch's correction, *$p < 0.05$. *BDNF* protein expression levels increased after FA exposure

P-CREB expression is upregulated due to FA exposure

P-CREB is activated in response to increased neurotransmitters, neurotrophins and cytokines. FA significantly increased the protein expression levels of *P-CREB* (Figure 3.8; 1.5537-fold; p = 0.0002)

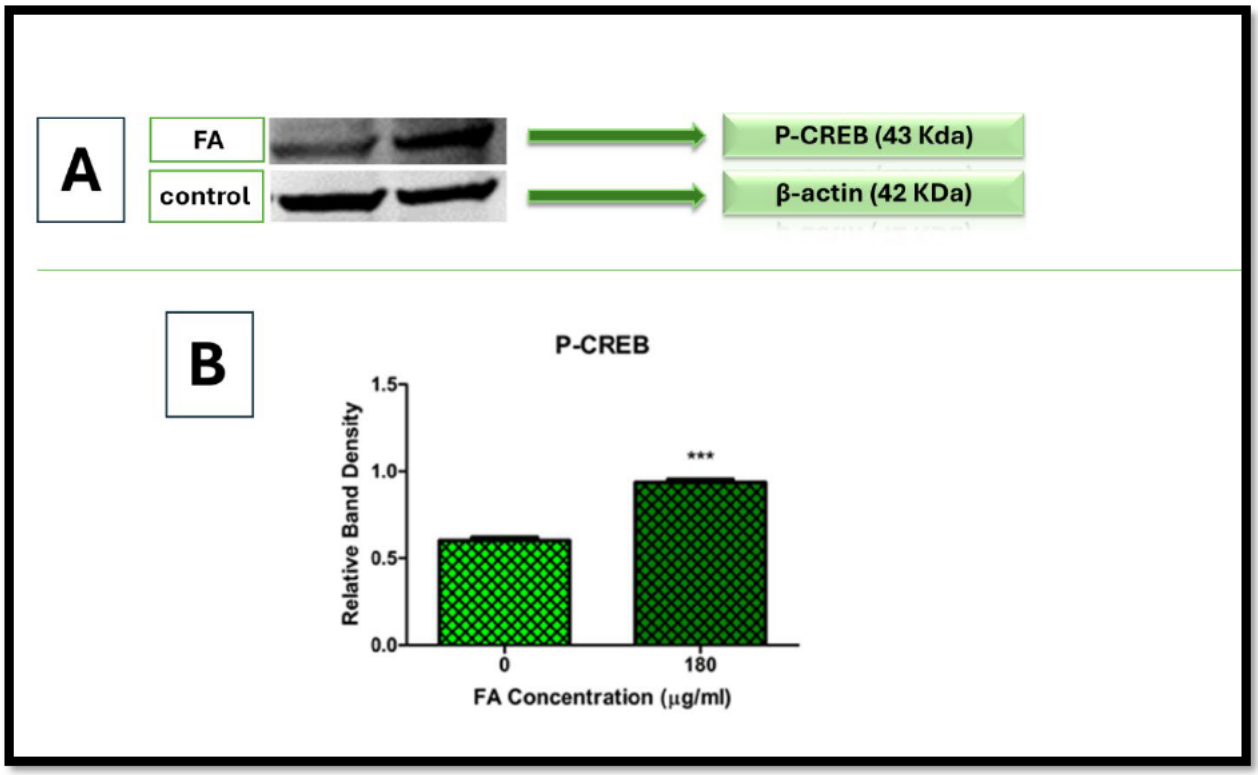

Figure 3.8: Protein expression levels of *P-CREB* after FA exposure for 24 hours. (A) represents the Western blot images and (B) represents the Relative Band Density. Statistical significance was evaluated using the unpaired t-test with Welch's correction, ***$p < 0.001$. *P-CREB* protein expression levels increased after FA exposure

PI3K expression is downregulated due to FA exposure

PI3K is activated as a feedback mechanism to growth factors, cytokines and hormone fluctuations. FA significantly decreased the protein expression levels of *PI3K* (Figure 3.9; 0.8411-fold; p = 0.0346)

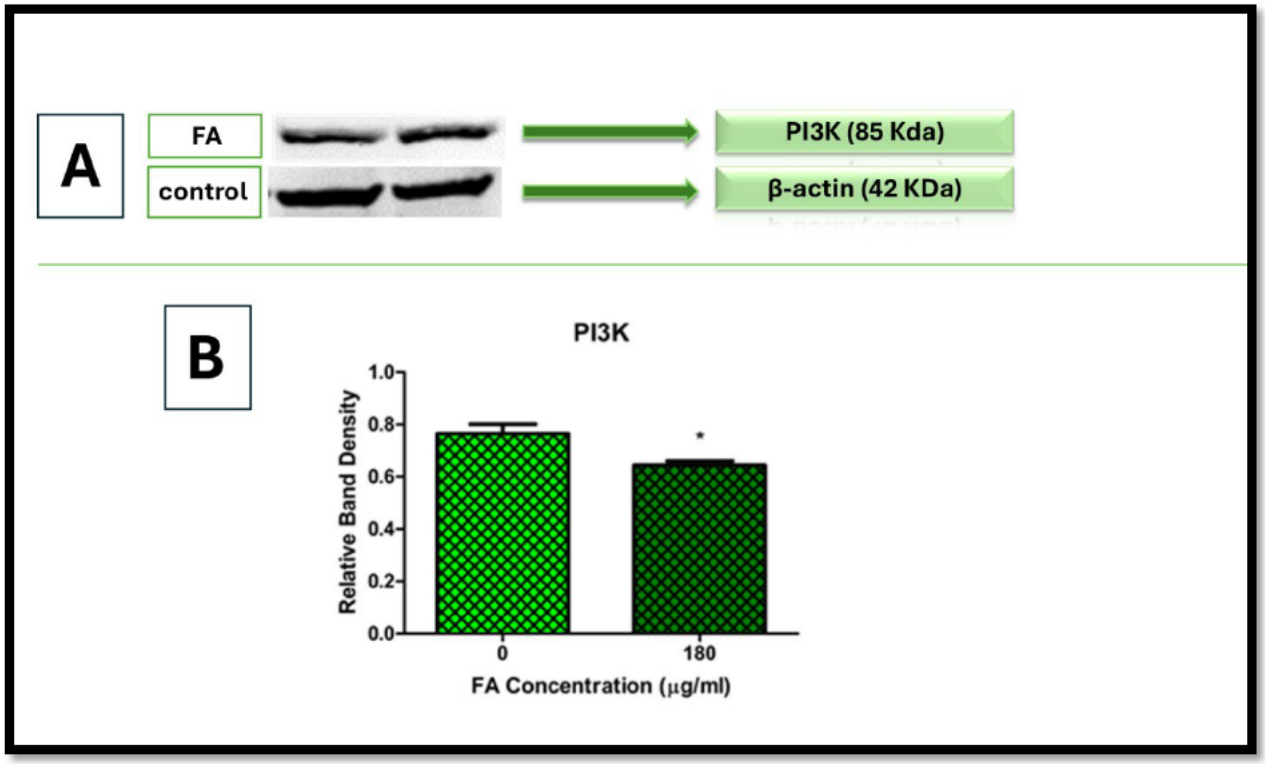

Figure 3.9: Protein expression levels of *PI3K* after FA exposure for 24 hrs. (A) represents the Western blot images and (B) represents the Relative Band Density. Statistical significance was evaluated using the unpaired t-test with Welch's correction, *$p < 0.05$. PI3K protein expression levels decreased after FA exposure.

P-Akt expression is downregulated due to FA exposure

P-Akt is activated as a trigger mechanism to mitogens, adhesion to monitor cell growth and apoptosis resistance. FA significantly decreased *P-Akt* expression by (Figure 3.10; 0.8274-fold; $p = 0.0493$).

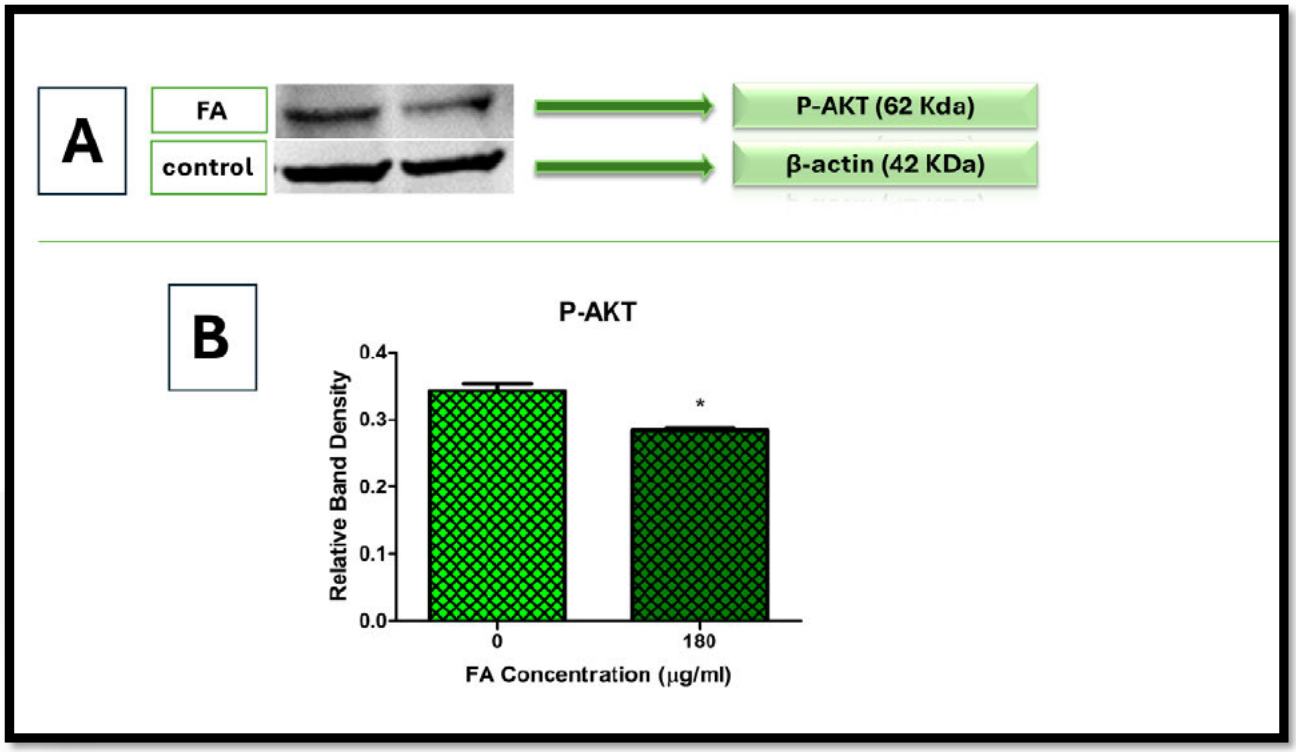

Figure 3.10: Protein expression levels of *P-Akt* after FA exposure for 24 hrs. (A) represents the Western blot images and (B) represents the Relative Band Density. Statistical significance was evaluated using the unpaired t-test with Welch's correction, $*p < 0.05$. *P-Akt* protein expression levels decreased after FA exposure

CHAPTER 4

DISCUSSION

The Fusarium produced mycotoxin FA is well-known for frequently contaminating large scale agricultural commodities such as maize, wheat and barley (Bacon et al., 1996). Once a plant becomes infected, it presents an unprecedented health risk to animals and humans.

FA expresses severe toxicity in animals (Bacon et al., 1995; Fairchild et al., 2005; Voss et al., 1999), bacteria (Ruiz et al., 2015; Bacon et al., 2006) as well as plants (Pirayesh et al., 2015; Diniz and Oliveira, 2009; Pavlovkin et al., 2004). However, the core of FA's cellular toxicity is still yet to be understood. Through the analysis of the m6A complex, global m6A RNA methylation levels, key brain markers as well as the *PI3K*/*Akt* pathway, this study aimed to determine the impact of FA in the brain.

This study found that cell viability decreased due to FA exposure (Figure 3.1). FA is known for exhibiting potent cytotoxic as well as antiproliferative effects on multiple cancer cell lines, not only U87MG. Findings by Fernandez-Pol et al. (1993) found that FA decreases cell viability in a time/dose-dependent manner in human adenocarcinoma cells. More recent studies show the same trend in decreased cell viability due to FA exposure, such as Seçme et al. (2023) in pancreatic cancer cells, Mamur et al. (2018) in human cervix carcinoma cells and Gulbay et al. (2023) in Ishikawa endometrial cancer cells. This study found an IC_{50} value of 180 µg/ml (Figure 3.1) in U87MG cells after FA exposure. There has been no definitive IC_{50} value for FA, and it's seen to vary across cell lines. Mamur et al. (2018) and Seçme et al. (2023) found IC_{50} values ranging between 134.83 µg/ml -200 µg/ml, which still aligns to findings in this study showing cell viability decreases due to FA exposure.

The most well-known alteration of all eukaryotic mRNAs is m6A methylation (Wei et al., 1975). Global m6A RNA methylation reflects the holistic activity of the 'writers', 'readers' and 'erasers'. When the m6A RNA methylation modification is dysregulated, diseases such as cancer, neurodegeneration and diabetes occur (Yang et al., 2019). Recent studies have developed a substantial amount of evidence that proves mycotoxins influence the m6A RNA methylation functionality in animal models along with cell lines (Ghazi et al., 2021; Hu & Lin, 2020; Arumugam et al., 2021). Findings from Wu et al. (2021) show that aflatoxin M1 and aflatoxin B1 downregulated global m6A methylation levels in bovine mammary epithelial (BME) cells. Other findings from Wu et al. (2020) found global m6A RNA methylation was upregulated due to aflatoxin B1, causing dysregulated hepatic function and cellular toxicity. Findings by Ghazi et al.

(2021) found that p53 RNA m6A levels were downregulated in HepG2 cells due to FA exposure and this was associated with altered p53 expression levels.

This study found the global level of m6A RNA methylation was significantly upregulated in brain U87MG cells (Figure 3.2). This could have resulted from the increased 'writer' activity, albeit the decrease in m6A 'writer' expression (Figure 3.3). Fluctuations in global m6A levels could result from dysregulated cellular stress responses (Chen et al., 2021). The increase in global m6A RNA methylation levels could also be directly caused by the downregulation of *FTO* and *ALKBH5* mRNA expression (Figure 3.4). Findings from Yang et al. (2021) had similar results, showing a downregulation in *FTO* expression in diabetes models increased global m6A levels, altering metabolic gene expression. Further support comes from Ye et al. (2021) showing an enhanced *METTL3* activity (hypoxia) upregulated global m6A levels to prioritize translation of stress-response genes.

FA is known to induce oxidative stress and disrupt cellular homeostasis. Findings from Ghazi et al. (2021) explain that oxidative stress has been implicated in altering the expression and activity of m6A methylation enzymes, such as *METTL14* and *METTL3*. Increased oxidative stress can promote the expression of m6A 'writers' (Chen et al., 2022). This would lead to a global elevation of methylation levels, even in the presence of downregulated mRNA expression of these enzymes. The cellular stress caused by the exposure to FA could have also caused the cells to significantly increase the m6A modification to prioritize specific transcription of genes. An increase in m6A content in neurons caused by oxidative stress stabilize neuroprotective transcripts (Diao et al., 2020). Findings from Arumugam et al. (2021) also found global m6A RNA methylation to be upregulated, however this was due to oxidative stress induced by fumonisin B1. *YTHDF3* may also enhance translation of key transcripts despite transcriptional downregulation, which aligns with the increased *BDNF* and *CREB* protein levels observed. Similar findings by Anders et al. (2018) support this claim showing *YTHDF3* selectively enhanced survival pathway mRNA translation of m6A modifications under stress.

Furthermore, increased m6A modification could result in the promotion of *BDNF* that could support alternative signalling that bypasses *PI3K*/*Akt*. *PI3K/Akt* pathway regulators will be altered due to the increase in m6A modification, causing signalling disruptions and pathway inhibition. Similar findings by Zhao et al. (2020) show that increased global m6A levels (gastrointestinal cancers) enhanced RNA stability, causing activation of survival pathways where *PI3K*/*Akt* signalling was reduced.

The increase in m6A levels will target transcripts for decay such as *PI3K* and *Akt*. The increase in *YTHDF2* binding to m6A-modified *PI3K* and *Akt* will hasten their degradation, causing the pathway to be suppressed. This is confirmed by Ai et al. (2023) showing that lead neurotoxicity

caused *METTL3*-induced m6A methylation to destabilize related mRNA's and caused inhibition of the *PI3K*/*Akt* pathway. While *PI3K*/*Akt* was suppressed, *BDNF* and *CREB* were stabilized and enhanced to increase cell survival of alternative pathways. A study by Lan et al. (2019) also found that dysregulated m6A methylation may enhance pro-apoptotic transcripts or destabilize pro-survival factors, aligning with the observed downregulation of *PI3K* and *P-Akt* proteins.

To gain a deeper understanding into the upregulation of global m6A expression levels, the 'writers', 'readers' and 'erasers' were examined in excessive detail. The 'writers' *METTL14*, *WTAP* and *METTL3* are responsible for catalysing m6A RNA methylation (Oerum et al., 2021). FA downregulated mRNA expression for all three 'writers' (Figure 3.3) in the brain. This could result in decreased m6A methylation capacity and have tumour suppressive characteristics. This agrees with findings from Wu et al. (2019) which investigated m6A methylation in breast cancer, showing that a downregulation of *WTAP* and *METTL14* decreased m6A RNA methylation, resulting in potential tumour growth suppression. FA is known to confer oxidative stress, which disrupts cellular redox balance and damages critical transcriptional machinery. Oxidative stress can suppress the transcription of *METTL3*, *METTL14* and *WTAP*, leading to reduced methyltransferase activity (Arumugam et al., 2021). Support for these findings come from Wu et al. (2020) which show significant downregulation in *METTL3* due to mycotoxin exposure (*DON*) in IPEC-J2 cells. In contrast, Zhou et al. (2019) observed *METTL3* upregulation and *FTO* downregulation in cisplatin treated kidney cells which interestingly also increased global m6A levels. Findings from Soni et al. (2018) also support these results, showing *METTL3* upregulation and *FTO* downregulation due to aflatoxin B1. This may seem paradoxical but reflects a critical point: *FTO*'s role as an eraser often outweighs the contribution of *METTL3* in determining m6A levels. When *FTO* is suppressed, the removal of existing m6A marks is hindered, allowing methylation to accumulate even if *METTL3* levels are reduced.

FA's capacity for metal ion sequestering makes it a powerful chelator of divalent cations (Rani et al., 2009; Fernandez-Pol et al., 1993). Its capability to remove essential metal ions may be how FA exerts its toxicity (Stack et al., 2003). Zinc is a naturally occurring metal essential for cell survival. Zinc finger CCCH domain-containing protein 13 (*ZC3H13*) interacts with *WTAP* to promote the function of the m6A writer complex (Yang et al., 2018). Disruption of this interaction by zinc chelation could destabilize *WTAP*, impairing the assembly and enzymatic activity of the *METTL3-METTL14-WTAP* writer complex. FA's chelating ability has been documented to remove metal ions, such as zinc, from cellular processes (Ekwomadu et al, 2021). The loss of zinc may impair the structural integrity of *WTAP* and its interaction with *METTL3* and *METTL14*, disrupting the localization and assembly of the writer complex.

The ‘erasers’, also known as demethylases, restore unmodified cytosine and play pivotal roles in tumorigenesis and cellular stress regulation (Zhao et al., 2021; Chen et al., 2023). FA downregulated mRNA expression of both ‘erasers’ (Figure 3.4) in the brain. This could result from FA-induced cellular stress, which prioritizes RNA stability over dynamic turnover. This is supported by Krejčí et al. (2023) showing that *ALKBH5* downregulation was involved with RNA turnover modulation and cell protection in mice. The ‘erasers’ purpose is to remove methyl groups from m6A- modified RNAs to revert them to their original structure. However, due to FA-induced cellular stress, these enzymes are downregulated to conserve energy and reduce transcription for protection. This is supported by findings from Adjibade et al. (2024) highlighting *ALKBH5* and *FTO* suppression caused RNA demethylation and mRNA stability disruptions, which overall impacted the cellular stress responses. *FTO* suppression directly impacts mRNA methylation in oncogenic pathways such as *PI3K/Akt* and *MYC* (Yang et al., 2024). The downregulation of *ALKBH5* is seen to affect RNA splicing and reduce mRNA stability. This is supported by Shen et al. (2022) showing that suppressed *ALKBH5* reduced mRNA stability of specific transcripts involved in lung cancer, causing detrimental downstream effects on angiogenesis. The *PI3K/Akt* pathway will also experience severe downstream effects, since both *FTO* and *ALKBH5* modulate its transcripts.

FTO as well as *ALKBH5* are both Fe^{2+}- and 2-oxoglutarate (2-OG)-dependent dioxygenases (Lai et al., 2024; Gerken et al., 2007). The Fe^{2+} ion is crucial for the catalytic activity of *ALKBH5* and *FTO* enzymes, enabling them to demethylate m6A-modified RNAs through distinct mechanisms (Toh et al., 2020). The chelation of iron by FA could disrupt *FTO’*s active site and impair its demethylase activity, causing an increase in global m6A RNA methylation levels, which is coherent with the study’s findings. *ALKBH5*’s function can also be impaired by the chelation of iron, inhibiting its ability to demethylate m6A-modified RNA’s. Therefore, FA’s ability to sequester Fe^{2+} may have inhibited the enzymatic activity of *ALKBH5* and *FTO* thereby effectively removing their essential cofactors as well as promoting m6A accumulation due to reduced demethylase activity.

The m6A ‘readers’ serve to bridge interactions between the ‘writers’ and ‘erasers’. The readers confer downstream effects of the m6A complex by reading and binding to methylation sites (Allis & Jenuwein, 2016). FA downregulated ‘readers’ *YTHDF2*, *YTHDC1/2* (Figure 3.3). The downregulation of *YTHDF2* and *YTHDC1/2* indicate a coordinated reduction in m6A reader activity that will likely reduce all functionality of the involved ‘readers’, including RNA stability, splicing and translation. Downregulation of ‘readers’ *YTHDF1/2* due to FA exposure could increase mRNA degradation or prevent global translation, which aligns with the *PI3K/Akt* pathway. These findings align with Zhong et al. (2019) which showed *YTHDF2* downregulation due to stress (hypoxia) reduced *EGFR* mRNA degradation in HepG2 cells. Even though

considered insignificant in this study, an upregulation in *YTHDF3* could be due to it compensating for the stress conditions (FA) by maintaining translation of specific m6A-modified mRNAs critical for cell-stress response. Under toxic conditions, its seen to adapt uniquely compared to *YTHDF1/2*. This is supported by Anders et al. (2018) showing a maintained *YTHDF3* expression under oxidative stress, but a downregulation in *YTHDF1/2*. Literature by Shi et al. (2017) concluded with results very similar to Anders et al. (2018), showing *YTHDF3* overexpression counteracted *YTHDF1/2* reductions resulting in enhanced translation of selective transcripts. Zou et al. (2023) also found *YTHDF3* to sustain the activity of stress-influenced cells by stabilizing transcripts when *YTHDF1/2* were downregulated. Findings from Ghazi et al. (2021) showed downregulation of *YTHDF1/2/3*, *YTHDC2* as well as global m6A levels in HepG2 cells, which contradict the findings from this study. This is also coherent with Ghazi et al. (2022), showing downregulation of *YTHDF2/3* and *YTHDC2* in C57BL/6 mice. This difference could be due to the experimental models used, treatment concentration of FA as well as the stress responses induced by FA. In HepG2 cells and C57BL/6 mice, FA exposure may lead to a systemic suppression of m6A readers including *YTHDF2/3* and *YTHDC2*, potentially as part of a broader transcriptional repression linked to oxidative stress and epigenetic dysregulation. This study investigated U87MG cells indicating selective upregulation of *YTHDF3* alongside downregulation of *YTHDF1/2, YTHDC1/2*, hinting towards a compensatory mechanism to counteract FA-induced neurotoxicity.

YTHDC1/2 downregulation due to FA treatment could limit the export and translation of specific survival-related transcripts. Transcripts affected include *MYC* causing imbalanced oncogenic activity (Shen et al., 2022), *XIST* causing accelerated regulatory functions (Chen et al., 2023) and *PIK3CA* (phosphatidylinositol-4,5-bisphosphate 3-kinase catalytic subunit alpha) causing diminished stability and translation in *PIK3CA* mRNA, compromising *PI3K/Akt* signalling (Wu et al., 2024). Similar findings were found by Anders et al. (2018) showing that downregulation of *YTHDC1/2* caused suppressed RNA metabolism under stress by facilitating mRNA triaging.

P-CREB and *BDNF* are critical components of the *PI3K/Akt* pathway. *P-CREB* is linked to a host of brain functions, such as neuronal development, memory processing, cell stress survival and synaptic plasticity (Finkbeiner, 2000). The study found that FA induced reduced mRNA expression levels (Figure 3.6) yet increased protein expression levels (Figure 3.7 and 3.8) of *BDNF* and *P-CREB* in the brain. The downregulation of mRNA levels may be due to transcriptional repression or RNA degradation caused by FA. This could indicate a protective mechanism in which *BDNF* and *P-CREB* fight against overstimulation of survival pathways under stress, causing augmented signalling and energy depletion. Similar findings by Sen (2019) show that stress (endoplasmic

reticulum) downregulates *CREB*, which subsequently represses *BDNF* transcription to conserve energy.

Therefore, the increased protein levels seen for *BDNF* and *P-CREB* could be due to cellular compensation mechanisms that stabilize or enhance translation and phosphorylation of existing transcripts under FA-induced stress to increase survival. A research paper by Zhang et al. (2013) found very similar results showing increased protein expression levels of *P-CREB* and *BDNF* despite reduced mRNA expression due to nobiletin-induced cellular stress, indicating stress adaptation by *PI3K/Akt* activation. Another study by Li et al. (2015) found *BDNF* transcription was suppressed under stress while *CREB* phosphorylation (CREB activation) increased to ensure neuroprotective signalling. FA induced downregulation of *BDNF* transcription alongside increased *P-CREB* protein levels represents a cellular adaptation to support neuroprotection in the study.

P-Akt and *PI3K* function in the *PI3K/Akt* pathway as critical and essential components for survival. FA exposure caused reduced protein expression levels of *PI3K* and *P-Akt* (Figure 3.9 and Figure 3.10) in the brain. The downregulation for *P-Akt* and *PI3K* may be due to transcriptional suppression of upstream activators (e.g. *RKT*) due to FA. Downstream effects could be reduced *P-Akt* activation and dysregulated lipid phosphorylation (Liu et al., 2015). The membrane localization of *PI3K* and its *PIP3* production can also be upset which will reduce the amount of *Akt* phosphorylated. This agrees with findings from Sun et al. (2011), showing stress (oxidative damage) caused a downregulation of *PI3K* and *P-Akt* activity, causing cell apoptosis. *PTEN* activity could also be increased and could diminish *PI3K* signalling and *P-Akt* levels, since *PTEN* negatively regulates the *PI3K/Akt* pathway (Georgescu, 2010). This is supported by findings from Zhao et al. (2014) which demonstrated neuroinflammatory stress downregulated *P-Akt* activity through increased *PTEN* signalling, which caused impaired neuronal survival and memory in rat hippocampal neurons. Another study by Lu et al. (2018) confirmed that oxidative stress from a spinal cord injury significantly reduced *P-Akt* and *PI3K* expression levels, impairing cellular repair mechanisms.

In summary, the study explored the impact of FA on global m6A RNA methylation and associated molecular pathways (Figure 4.1), highlighting significant disruptions to the m6A RNA methylation machinery and key signalling proteins in U87MG cells. These findings will set the foundation for more in-depth research to deduce the effect FA has on molecular mechanisms associated with m6A RNA methylation and their influence on overall cellular functions and disastrous health defects.

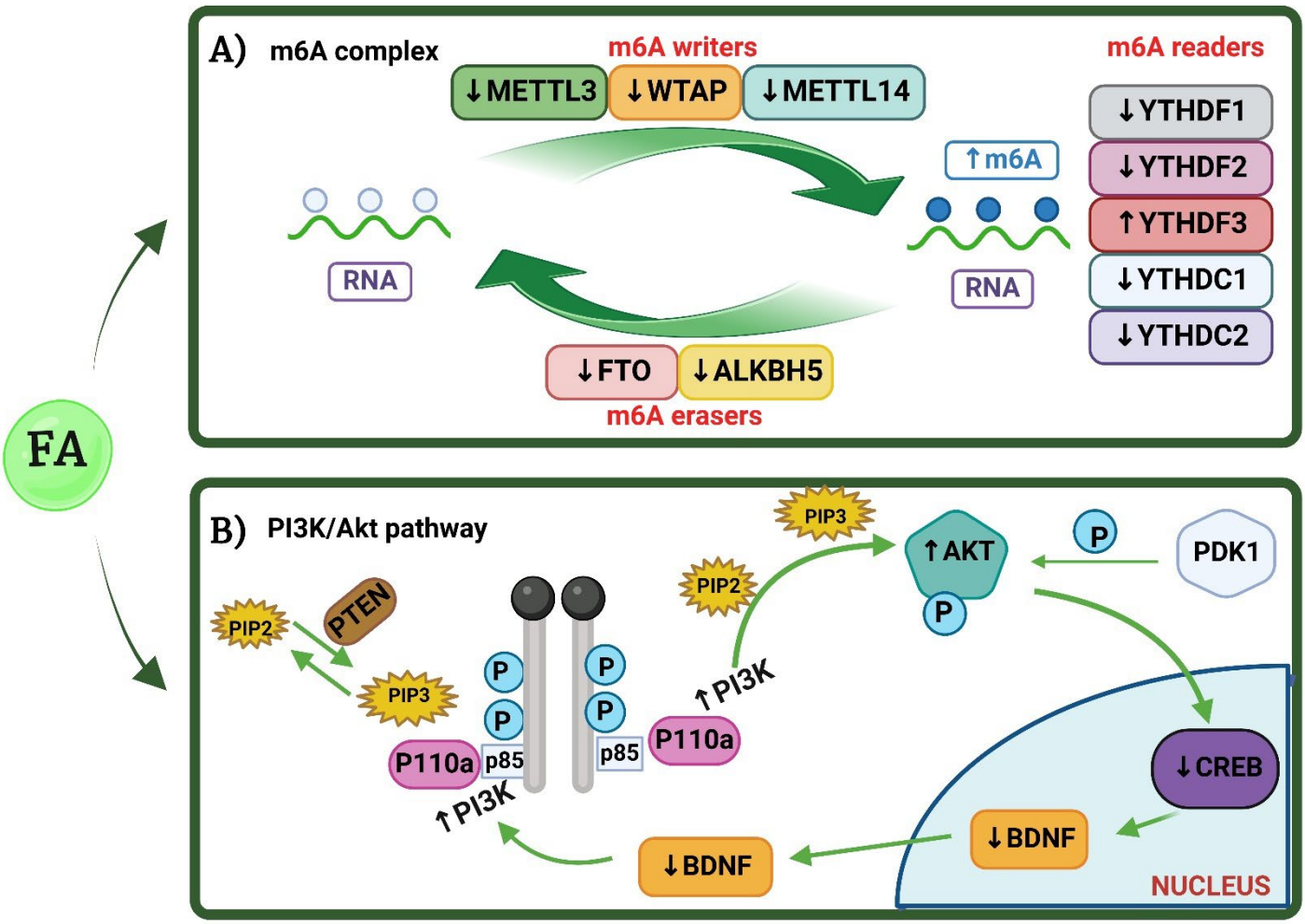

Figure 4.1: Mechanism of FA induced toxicity in A) m6A complex and B) *PI3K/Akt* pathway. FA caused disrupted regulation in m6A 'writers', 'readers' and 'erasers' and showed an upregulation in m6A RNA expression. *BDNF* and *CREB* were downregulated along with *PI3K* and *Akt* upregulation due to FA exposure (Composed by author using Biorender).

CHAPTER 5

CONCLUSION

Mycotoxins are a massive and highly prevalent problem in the agricultural sector, causing disastrous losses to the economy and severe health and safety concerns to both animals and humans (Bennett & Klich, 2003; Yiannikouris & Jouany, 2002). These toxins result in a plethora of disorders in animals and humans ranging from acute poisoning, immunosuppression and cancer (Alberts et al., 2016). Various mitigation strategies have been brought about including biological controls, regulatory practices and detoxification but their efficacy remains context-specific (Sheik-Abdul, 2019).

Despite extensive research on mycotoxins FA remains poorly researched. New research shows FA's potential in worsening oxidative stress, mitochondrial dysfunction and altering biochemical signalling pathways (Abdul et al., 2016; Arumugam et al., 2021). FA has been shown extensively to be toxic in animals (Dowd, 1988; Voss et al., 1999), bacteria (Ruiz et al., 2015; Bacon et al., 2006) as well as plants (Rani et al., 2009; Pavlovkin et al., 2004); however, its biochemical mechanisms at which it exerts its toxic effects remain to be discovered. This is an important aspect of research as it allows for a deeper understanding of the potential dangers FA can have on human and animal health. The study being conducted in Africa has a high relevance in aiding other developing countries that suffer from mycotoxin contamination.

This study brings forth a novel potential mechanism for brain toxicity induced by FA. The observed increase in global m6A RNA methylation, despite downregulation of 'writers' and 'erasers' underscores a complex interplay of compensatory mechanisms resulting from FA exposure. FA's ability to chelate essential metal ions, such as zinc and iron, likely destabilizes the m6A 'writer' and 'eraser' complexes impairing their enzymatic activities and transcriptional regulation. Furthermore, the differential expression of m6A 'readers', particularly the upregulation of *YTHDF3* amidst the downregulation of *YTHDF1*/*2* and *YTHDC1/2*, suggests selective stabilization of survival-related transcripts to counteract FA-induced neurotoxicity. At the protein level, FA exposure resulted in the upregulation of *BDNF* and *P-CREB* which indicates a compensatory mechanism aimed at preserving neuroprotective signalling despite transcriptional repression. However, the downregulation of *PI3K* and *P-Akt* indicates a suppression of growth and survival pathways which are potentially linked to oxidative stress and energy conservation under toxic stress. All three study hypotheses are in full agreement with the results, which implies FA is cytotoxic to the brain.

The study was limited by a lack of protein expression as well as a lack of activity data for m6A regulators and readers. Another limitation was that the study did not directly examine the m6A levels of mRNA transcripts, which should be explored further in future studies. Other aspects to be examined in future studies include examining how FA affects DNA methylation, histone modification and non-coding RNA expression in U87MG cells as well as an *in vivo* brain model. Other stress responses such as cellular apoptosis, inflammation and oxidative stress should be evaluated to determine the effects FA has on the brain.

REFERENCES

ABDUL, N. S., NAGIAH, S. & CHUTURGOON, A. A. 2016. Fusaric acid induces mitochondrial stress in human hepatocellular carcinoma (HepG2) cells. *Toxicon,* 119**,** 336-344.

ABDUL, N. S., NAGIAH, S. & CHUTURGOON, A. A. 2019. The neglected foodborne mycotoxin Fusaric acid induces bioenergetic adaptations by switching energy metabolism from mitochondrial processes to glycolysis in a human liver (HepG2) cell line. *Toxicology letters*, 318, 74-85.

ADJIBADE, P., DI-MARCO, S., GALLOUZI, I. E. & MAZROUI, R. 2024. The RNA demethylases ALKBH5 and FTO regulate translation of the ATF4 mRNA in sorafenib-treated hepatocarcinoma cells. *Biomolecules*, 14, 932.

AHMED, S., KWATRA, M., GAWALI, B., PANDA, S. R. & NAIDU V. G. M. 2021. Potential role of TrkB agonist in neuronal survival by promoting CREB/BDNF and PI3K/Akt signaling in vitro and in vivo model of 3-nitropropionic acid (3-NP)-induced neuronal death. *Apoptosis*, 26, 52-70.

AI, S., LI, D., GU, X., XU, Y., WANG, Y., WANG, H. L. & CHEN, X. 2023. Profile of N6-methyladenosine of Pb-exposed neurons presents epitranscriptomic alterations in PI3K-AKT pathway-associated genes. *Food and Chemical Toxicology*, 178, 113821.

ALBERTS, J. F., VAN ZYL, W. H. & GELDERBLOM, W. C. A. 2016. Biologically Based Methods for Control of Fumonisin-Producing *Fusarium* Species and Reduction of the Fumonisins. *Frontiers in Microbiol*ogy, 7, 548.

ALLIS, C. & JENUWEIN, T. 2016. The molecular hallmarks of epigenetic control. *Nature Reviews Genet*ics 17, 487-500.

AMIDFAR, M., DE OLIVEIRA, J., KUCHARSKA, E., BUDNI, J. & KIM, Y. K. 2020. The role of CREB and BDNF in neurobiology and treatment of Alzheimer's disease. *Life Sciences*, 257, 118020.

ANDERS, M., CHELYSHEVA, I., GOEBEL, I., TRENKNER, T., ZHOU, J., MAO, Y., VERZINI, S., QIAN, S. B. & IGNATOVA. 2018. Dynamic m6A methylation facilitates

mRNA triaging to stress granules. *Life Science Alliance*, 1, e201800113.

ANDRISANI, O. M. 1999. CREB – mediated transcriptional control. *Critical reviews in eukaryotic gene expression*, 9, 19-32.

ANGOA – PÉREZ, M., ANNEKEN, J. H. & KUHN, D. 2017. The Role of Brain-Derived Neurotrophic Factor in the Pathophysiology of Psychiatric and Neurological Disorders. *Journal of Psychiatry and Psychiatric Disorders*, 1, 252–269.

ARANGO-LIEVANO, M., ANASTASIA, A. & JEANNETEAU, F. 2015. ProBDNF biology and emerging roles in the CNS: the unexpected journey of proneurotrophins, Corpus ID: 210954865

ARCELLA, A., OLIVA, M. A., STAFFIERI, S., SANCHEZ, M., MADONNA, M., RIOZZI, B., ESPOSITO, V., GIANGASPERO, F. & FRATI, L. 2018. Effects of aloe emodin on U87MG glioblastoma cell growth: In vitro and in vivo study. *Environmental Toxicology*, 33, 1160-1167.

ARUMUGAM, T., GHAZI, T., ABDUL, N. S. & CHUTURGOON, A. A. 2021. A review on the oxidative effects of the fusariotoxins: fumonisins B1 and fusaric acid. *Toxicology*, 19, 181-190.

ARUMUGAM, T., GHAZI, T., CHUTURGOON, A. A. 2021. Fumonisin B1 alters global m6A RNA methylation and epigenetically regulates Keap1-Nrf2 signaling in human hepatoma (HepG2) cells. *Archives of Toxicology*, 95, 1367-1378.

BACON, C., PORTER, J., NORRED, W. & LESLIE, J. 1996. Production of fusaric acid by Fusarium species. *Applied and Environmental Microbiology,* 62**,** 4039-4043.

BACON, C. W., HINTON, D. M. & HINTON, A. JR. 2006. Growth-inhibiting effects of concentrations of fusaric acid on the growth of *Bacillus mojavensis* and other biocontrol *Bacillus* species. *Journal of Applied Microbiol*ogy, 100, 185-194.

BACON, C. W., PORTER, J. K. & NORRED, W. P. 1995. Toxic interaction of fumonisin B1 and fusaric acid measured by injection into fertile chicken egg. *Mycopathologia*, 129, 29-35.

BAO, X., ZHANG, Y., LI, H., TENG, Y., MA, L., CHEN, Z., LUO, X., JIAN, Z. ZHAO, A., REN, J. & ZUO, Z. 2023. RM2Target: a comprehensive database for targets of writers, erasers and readers of RNA modifications. *Nucleic Acids Research*, 51, 269-279.

BATHINA, S. & DAS, U. N. 2015. Brain-derived neurotrophic factor and its clinical implications. *Archives of Medical Science*, 11, 164-1178.

BEHRENS, M., HÜWEL, S. GALLA, H. J. & HUMPF H. U. 2015. Blood-Brain Barrier Effects of the Fusarium Mycotoxins Deoxynivalenol, 3 Acetyldeoxynivalenol, and Moniliformin and Their Transfer to the Brain. *PLoS ONE*, 10, e0143640.

BENNETT, J. W. & KLICH, M. 2003. Mycotoxins. *Clinical Microbiology Reviews*, 16, 497-516.

BERTHILLER, F., SULYOK, M., KRSKA, R., SCHUHMACHER, R. 2007. Chromatographic methods for the simultaneous determination of mycotoxins and their conjugates in cereals. *International Journal of Food Microbiology*, 119, 33–37.

BHATNAGAR, D., PAYNE, G. A., CLEVELAND, T. E. & ROBENS, J. F. 2004. Mycotoxins: current issues in USA. *Wageningen Academic Publishers*, 10, 17-47.

BIAN, S., NI, W., ZHU, M., SONG, Q., ZHANG, J., NI, R. & ZHENG, W. 2020. Identification and Validation of the N6-Methyladenosine RNA Methylation Regulator YTHDF1 as a Novel Prognostic Marker and Potential Target for Hepatocellular Carcinoma. *Frontiers in Molecular Biosciences,* 7, 604766.

BIANCHINI, A. & STRATTON, J. E. 2019. Spoilage of Plant Products: Cereals and Cereal Flours. *Reference module in Food Science*, Corpus ID: 201199488.

BINDER, E. M. 2007. Managing the risk of mycotoxins in modern feed production. *Animal Feed Science and Technology*, 133, 149-166.

BOCHNER, B. R., HUANG, H. C., SCHIEVEN, G. L. & AMES, B. N. 1980. Positive selection for loss of tetracycline resistance. *Journal of Bacteriology,* 143**,** 926-933.

BOKAR, J. A., RATH-SHAMBAUGH, M. E., LUDWICZAK, R., NARAYAN, P. & ROTTMAN, F. 1994. Characterization and partial purification of mRNA N6-adenosine methyltransferase from HeLa cell nuclei. Internal mRNA methylation requires a

multisubunit complex. *Journal of Biological Chemistry*, 269, 17697-17704.

BONNI, A., GINTY, D., DUDEK, H & GREENBERG, M. 1995. Serine 133-Phosphorylated CREB Induces Transcription via a Cooperative Mechanism That May Confer Specificity to Neurotrophin Signals. *Molecular and Cellular Neuroscience*, 6, 168–183.

BOTTALICO, A. & PERRONE, G. 2002. Toxigenic fusarium species and mycotoxins associated with head blight in small-grain cereals in Europe. *European Journal of Plant Pathology*, 108, 611-624.

BOUARAB, K. 2009. *Molecular plant-microbe interactions, edited by Kamal Bouarab, Normand Brisson, Fouad Daayf*, edition 1, 319-335.

BOURGUIGNON, R. L., WALSH, A. F., FLYNN, J. C., BARO, C. & SPINOS, E. 1976. Fusarium species osteomyelitis. Case report. *Journal of Bone and Joint Surgery of America*. 58, 722-723.

BROWN, D. W., BUTCHKO, R. A., BUSMAN, M. & PROCTOR, R. H. 2012. Identification of gene clusters associated with fusaric acid, fusarin, and perithecial pigment production in Fusarium verticillioides. *Fungal Genetics and Biol*ogy, 49, 521-532.

BROWN, D. W., LEE, S. H., KIM, L. H., RYU, J. G., LEE, S., SEO, Y., KIM, Y. H., BUSMAN, M., YUN, S. H., PROCTOR, R. H. & LEE, T. 2015. Identification of a 12-gene fusaric acid biosynthetic gene cluster in *Fusarium* species through comparative and functional genomics. *Molecular Plant Microbe Interactions*, 28, 319–332.

BURGESS, L. W. 1981. General ecology of the fusaria. *Fusarium*: diseases, biology, and taxonomy. *Pennsylvania State University Press*, 225-235.

CBTRUS. 2008. Statistical Report: Primary Brain Tumors in the United States Statistical Report, 2000–2004 (Years of Data Collected). CBTRUS.

CHEN, D., GU, X., NURZAT, Y., XU, L., LI, X., WU, L., JIAO, H., GAO, P., ZHU, X., YAN, D., LI, S. & XUE, C. 2024. Writers, readers, and erasers RNA modifications and drug resistance in cancer. *Molecular Cancer*, 23, 178.

CHEN, D. H., ZHANG, J. G., WU, C. X. & LI, Q. 2021. Non-Coding RNA m6A Modification in Cancer: Mechanisms and Therapeutic Targets. *Frontiers in Cellular & Developmental Biology*, 9, 778582.

CHEN, L., GAO, Y., XU, S., YUAN, J., WANG, M., LI, T. & GONG, J. 2023. N6-methyladenosine reader YTHDF family in biological processes: Structures, roles, and mechanisms. *Frontiers in Immunology,* 14, 1162607.

CHEN, Y., ZHOU, Z., CHEN, Y. & CHEN, D. 2024. Reading the m^6A-encoded epitranscriptomic information in development and diseases. *Cell & Bioscience* 14, 124.

CHEN, Z., CHEN, X., JI, Y., ZHANG, L., WANG, W., SHEN, Y. & SUN, H. 2022. A narrative review of the role of m6A in oxidative stress and inflammation. *Biotarget*, 5.

CHEN, Z., LUO, Q., WANG, M. & CHEN, B. 2016. A rapid method with UPLC for the determination of fusaric acid in fusarium strains and commercial food and feed products. *Indian Journal of Microbiology*, 57, 68–74.

CLARK, M. J., HOMER, N., O'CONNOR, B. D., CHEN, Z., ESKIN, A., LEE, H., MERRIMAN, B., NELSON, S. F. 2010. U87MG Decoded: The Genomic Sequence of a Cytogenetically Aberrant Human Cancer Cell Line. *PLOS Genetics*, 14, 5.

CROWTHER, J. R. 2000. The ELISA Guidebook. *Methods in Molecular Biology*, 149: III-IV, 1-413.

D'ALTON, A. & ETHERTON, B. 1984. Effects of fusaric acid on tomato root hair membrane potentials and ATP levels. *Plant Physiology,* 74**,** 39-42.

DENG, X., SU, R., WENG, H., HUANG, H., LI, Z. & CHEN, J. 2018. RNA N^6-methyladenosine modification in cancers: current status and perspectives. *Cell Research*, 28, 507 – 517.

DEVNARAIN, N., TILOKE, C., NAGIAH, S. & CHUTURGOON, A. A. 2017. Fusaric acid induces oxidative stress and apoptosis in human cancerous oesophageal SNO cells. *Toxicon*, 126, 4-11.

DE VRIES, J.W., TRUCKSESS, M. W. & JACKSON, L.S. 2002. Mycotoxins and Food Safety.

Kluwer Academic/Plenum Publishers, New York, NY, USA.

DHANI, S., GHAZI, T., NAGIAH, S., BAIJNATH, S., SINGH, S. D., CHUTURGOON, A. A. 2020. Fusaric acid alters Akt and ampk signalling in c57bl/6 mice brain tissue. *Food and Chemical Toxicology*, 138, 111252.

DHANI, S., NAGIAH, S. & NAIDOO, D. B. & CHUTURGOON, A. A. 2017. Fusaric acid immunotoxicity and MAPK activation in normal peripheral blood mononuclear cells and Thp-1 cells. *Scientific Reports*, 7, 3051-3060.

DIAO, M. Y., ZHU, Y., YANG, J., XI, S. S., WEN, X., GU, Q. & HU, W. 2020. Hypothermia protects neurons against ischemia/reperfusion-induced pyroptosis via m6A-mediated activation of PTEN and the PI3K/Akt/GSK-3β signaling pathway. *Brain Research Bulletin*, 159, 25-31.

DINIZ, S. & OLIVEIRA, R. 2009. Effects of fusaric acid on Zea mays L. seedlings. *Phyton-International Journal of Experimental Botany*, 78, 155-160.

DOLGIN, E. 2016. Venerable brain-cancer cell line faces identity crisis. *Nature*, 537, 149-150.

DOWD, P. F. 1988. Toxicological and biochemical interactions of the fungal metabolites fusaric acid and kojic acid with xenobiotics in Heliothis zea (F.) and Spodoptera frugiperda (JE Smith). *Pesticide Biochemistry and Physiology*, 32, 123-134.

DU, H., ZHAO, Y., HE, J., ZHANG, Y., XI, H., LIU, M., MA, J. & WU, L. 2016. YTHDF2 destabilizes m6A-containing RNA through direct recruitment of the CCR4-NOT deadenylase complex. *Nature Communications*, 7, 12626.

DU, K. & MONTMINY, M. 1998. CREB is a regulatory target for the protein kinase Akt/PKB. *Journal of Biological Chemistry*, 273, 32377-32379.

EKWOMADU, T. I., AKINOLA, S. A. & MWANZA, M. 2021. Fusarium Mycotoxins, Their Metabolites (Free, Emerging, and Masked), Food Safety Concerns, and Health Impacts. *International Journal of Environmental Research and Public Health*, 18, 11741.

EL-SAYED, R. A., JEBUR, A. B., KANG, W. & EL-DEMERDASH, F. M. 2022. An overview on

the major mycotoxins in food products: characteristics, toxicity, and analysis. *Journal of Future Foods*, 2, 91-102.

ELVERS, K. T., LEEMING, K., MOORE, C. P. & LAPPIN-SCOTT, H. M. 1998. Bacterial-fungal biofilms in flowing water photo-processing tanks. *Journal of Applied Microbiol*ogy, 84, 607-618.

ENGVALL, E. 1980. Enzyme immunoassay ELISA and EMIT. *Methods in Enzymology*, 70, 419–439.

FAIRCHILD, A. S., GRIMES, J. L., PORTER, J. K., CROOM JR, W. J., DANIEL, L. R. & HAGLER JR, W. M. 2005. Effects of diacetoxyscirpenol and fusaric acid on poults: Individual and combined effects of dietary diacetoxyscirpenol and fusaric acid on turkey poult performance. *International Journal of Poultry Science*, 4, 350-355.

FAKHRI, S., IRANPANAH, A., GRAYANDI, M. M., MORADI, S. Z., RANIBARI, M., MAJNOONI, M. B., ECHEVERRIA, J., QI, Y., WANG, M., LIAO, P., FARZAEI, M. H. & XIAO, J. 2021. Natural products attenuate PI3K/Akt/mTOR signaling pathway: A promising strategy in regulating neurodegeneration. *Phytomedicine*, 91, 153664.

FENG, H., YUAN, X., WU, S., YUAN, Y., CUI, L., LIN, D., PENG, X., LIU, X. & WANG, F. 2023. Effects of writers, erasers and readers within miRNA-related m6A modification in cancers. *Cell Proliferation*, 56, e13340.

FERNANDEZ-POL, J., BONO, V. H. & JOHNSON, G. S. 1977. Control of growth by picolinic acid: differential response of normal and transformed cells. *Proceedings of the National Academy of Sciences,* 74**,** 2889-2893.

FERNANDEZ-POL, J. A., KLOS, D. J. & HAMILTON, P. D. 1993. Cytotoxic activity of fusaric acid on human adenocarcinoma cells in tissue culture. *Anticancer Research,* 13**,** 57-64.

FINKBEINER, S. 2000. CREB Couples Neurotrophin Signals to Survival Messages. *Neuron*, 1, 11- 14.

FLYNN, J. T., MEISLICH, D., KAISER, B. A., POLINSKY, M. S. & BALUARTE, H. J. 1996.

Fusarium peritonitis in a child on peritoneal dialysis: case report and review of the literature. *Peritoneal Dialysis International*, 16, 52-57.

GABRIELE, P. & HUTCHINS, R. K. 1996. *Fusarium* endophthalmitis in an intravenous drug user. *American Journal of Ophthamol*ogy, 122, 119-121.

GARCIA-ECHEVERRIA, C. & SELLERS, W. R. 2008. Drug discovery approaches targeting the PI3K/Akt pathway in cancer. *Oncogene*, 27, 5511-5526.

GERKEN, T., GIRARD, C. A., TUNG, Y. C., WEBBY, C. J., SAUDEK, V., HEWITSON, K. S., YEO, G. S., MCDONOUGH, M. A., CUNLIFFE, S., MCNEILL, L. A., GALVANOVSKIS, J., RORSMAN, P., ROBINS, P., PRIEUR, X., COLL, A. P., MA, M., JOVANOVIC, Z., FAROOQI, I. S., SEDGWICK, B., BARROSO, I., LINDAHL, T., PONTING, C. P., ASHCROFT, F. M., O'RAHILLY, S. & SCHOFIELD, C. J. 2007. The obesity-associated FTO gene encodes a 2-oxoglutarate-dependent nucleic acid demethylase. *Science*, 318, 1469-1472.

GEORGESCU, M. M. 2010. PTEN Tumor Suppressor Network in PI3K-Akt Pathway Control. *Genes & Cancer*, 112, 1170-1177.

GHAZI, T., NAGIAH, S., CHUTURGOON, A. A. 2021. Fusaric acid decreases p53 expression by altering promoter methylation and m6A RNA methylation in human hepatocellular carcinoma (HepG2) cells. *Epigenetics*, 16, 79–91

GHAZI, T., NAGIAH, S. & CHUTURGOON, A. A. 2022. Fusaric acid induces hepatic global m6A RNA methylation and differential expression of m6A regulatory genes *in vivo* - a pilot study. *Epigenetics,* 17, 695-703.

GHAZI, T., NAGIAH, S., TILOKE, C., ABDUL, N. S. & CHUTURGOON, A. A. 2017. Fusaric acid induces DNA damage and post-translational modifications of p53 in human hepatocellular carcinoma (HepG2) cells. *Journal of Cellular Biochemistry*, 118, 3866–3874.

GRANT, R., COGGAN, S. & SMYTHE, G. 2009. The physiological action of picolinic acid in the human brain. *International Journal of Tryptophan Research,* 2**,** 71-79.

GULBAY, G., SECME, M., MUTLU, D. 2023. Fusaric acid inhibits cell proliferation and downregulates expressions of toll-like receptors pathway genes in Ishikawa endometrial cancer cells. *European Reviews for Medical and Pharmacological Sciences*, 27, 7431-7436.

HASSAN, Z. U., THANI, R. A., BALMAS, V., MIGHELI, Q., JAOUA, S. 2019. Prevalence of Fusarium fungi and their toxins in marketed feed. *Food Control*, 104, 224-230.

HAYRAPETYAN, H., TRAN, T., TELLEZ-CORRALES, E. & MADIRAJU, C. 2023. Enzyme-Linked Immunosorbent Assay: Types and Applications. *Methods in Molecular Biology*, 2612, 1-17.

HEID, C. A., STEVENS, J., LIVAK, K. J. & WILLIAMS P. M. 1996. Real-time quantitative PCR. *Genome Research*, 6, 986-994.

HEIDARZADEH, S., MOTALLEB, G. & ZORRIEHZAHRA, M. J. 2019. Evaluation of Tumor Regulatory Genes and Apoptotic Pathways in The Cytotoxic Effect of Cytochalasin H on Malignant Human Glioma Cell Line (U87MG). *Cell Journal*, 21, 62-69.

HSU, P. J., ZHU, H., MA, Y., GUO, X., SHI, Y., LIU, M., QI, Z., SHI, H., WANG, J., CHENG, Y., LUO, G., DAI, Q., LIU, M., GUO, X., SHA, J., SHEN, B. & HE, C. 2017. Ythdc2 is an N(6)-methyladenosine binding protein that regulates mammalian spermatogenesis. *Cellular Research*, 27, 1115-1127.

HU, J. & LIN, Y. 2020. Fusarium infection alters the m6A-modifiedtranscript landscape in the cornea. *Experimental Eye Research*, 200, 108216.

HUANG, E. J. & REICHARDT, L. F. 2003. Trk receptors: roles in neuronal signal transduction. *Annual review of biochemistry*, 72, 609–642.

HUANG, X., LIU, G., GUO, J. & SU, Z. 2018. The PI3K/Akt pathway in obesity and type 2 diabetes. *International Journal of Biological Sciences*, 14, 1483-1496.

IQBAL, N., CZÉKUS, Z., ÖRDÖG, A. & POÓR, P. 2024. Fusaric acid-evoked oxidative stress affects plant defence system by inducing biochemical changes at subcellular level. *Plant Cell Reports*, 43, 2.

JAKLE, C., LEEK, J. C., OLSON, D. A. & ROBBINS, D. L. 1983. Septic arthritis due to *Fusarium solani. The Journal of Rheumatology* 10, 151-153.

JAYNE, T. & SÁNCHEZ, A. 2021. Agricultural productivity must improve in sub-Saharan Africa. *Science*, 372, 1045-1047.

JI, J. W., ZHANG, Y. D., LAI, Y. J. & HUANG, C. G. 2020. Mettl3 regulates the proliferation, migration and invasion of glioma cells by inhibiting PI3K/Akt signaling pathway. *European Review for Medical and Pharmacological Sciences*, 24, 3818-3828.

JIANG, X., LIU, B., NIE, Z., DUAN, L., XIONG, Q. & JIN, Z. 2021. The role of m6A modification in the biological functions and diseases. *Signal Transduction Target Therapy*, 6, 74.

JIAO, J., ZHOU, B., ZHU, X., GAO, Z. & LIANG, Y. 2013. Fusaric acid induction of programmed cell death modulated through nitric oxide signalling in tobacco suspension cells. *Planta*, 238, 727-737.

JIN, T., ZHANG, Y., BOTCHWAY, B. O. A., ZHANG, J., FAN, R., ZHANG, Y. & XUEHONG, L. 2022. Curcumin can improve Parkinson's disease via activating BDNF/PI3k/Akt signaling pathways, *Food and Chemical Toxicology*, 164, 113091.

KARAMIN, F. M., AKHAVAN, M. R., AFIFI, N. LOGHMANI, S., TAMIMI, P., FAZELI, A., MOUSAVIAN, S. A., FALSAFI, M. M., BARATI, G. 2023. PI3K/AKT/mTOR signaling pathway modulation by circular RNAs in breast cancer progression. *Pathology - Research and Practice*, 241, 338-344.

KARTHIYA, R. & KHANDELIA, P. 2020. m6A RNA Methylation: Ramifications for Gene Expression and Human Health. *Molecular Biotechnology*, 62, 90–105.

KEBEDE, H., LIU, X., JIN, J., XING, F. 2020. Current status of major mycotoxins contamination in food and feed in Africa. *Food Control*, 110, 106975.

KRASILNIKOV, M. 2000. Phosphatidylinositol-3 kinase dependent pathways: the role in control of cell growth, survival, and malignant transformation. *Biochemistry*, 65, 59-67.

KREJČÍ, J., ARCIDIACONO, O. A., ČEGAN, R., RADASZKIEWICZ, K., PACHERNÍK, J., PIRK, J., PEŠL, M., FILA, P. & BÁRTOVÁ, E. 2023. Cell Differentiation and Aging Lead To Up-Regulation of FTO, While the ALKBH5 Protein Level Was Stable During Aging but Up-Regulated During in vitro-Induced Cardiomyogenesis. *Physiological Research*, 72, 425-444.

KUBISTA, M., ANDRADE, J. M., BENGTSSON, M., FOROOTAN, A., JONÁK, J., LIND, K., SINDELKA, R., SJÖBACK, R., SJÖGREEN, B., STRÖMBOM, L., STÅHLBERG, A. & ZORIC, N. 2006. The real-time polymerase chain reaction. *Molecular Aspects of Medicine*, 27, 95-125.

KUIPER-GOODMAN, T. 2004. Risk assessment and risk management of mycotoxins in food. *Mycotoxins in Food, Detection and Control*, 15, 3-31.

KUMAR, P., NAGARAJAN, A. G. & UCHIL, P. D. 2018. Analysis of Cell Viability by the MTT Assay. *Cold Spring Harbor Protocols,* 2018.

KURIEN, B. T., & SCOFIELD, R. H. 2006. Western blotting. *Methods,* 38, 283–293.

KURIEN, M., ANANDI, V., RAMAN, R & BRAHMADATHAN, K. N. 1992. Maxillary sinus fusariosis in immunocompetent hosts. *Journal of Laryngology and Otology*, 106, 733-736.

LAI, G. Q., LI, Y., ZHU, H., ZHANG, T., GAO, J., ZHOU, H., YANG, C. G. 2024. A covalent compound selectively inhibits RNA demethylase ALKBH5 rather than FTO. *RSC Chemical Biology*, 5, 335-343.

LAN, Q., LIU, P. Y., HAASE, J., BELL, J. L., HÜTTELMAIER, S., LIU, T. 2019. The Critical Role of RNA m^6A Methylation in Cancer. *Cancer Research*, 79, 1285-1292.

LEE, H. J., RYU, D. 2017. Worldwide occurrence of mycotoxins in cereals and cereal-derived food products: Public health perspectives of their Co-occurrence. *Journal of Agriculture and Food Chemistry*, 65, 7034-7051.

LI, J., PEI, Y., ZHOU, R., TANG, Z., YANG, Y. 2021. Regulation of RNA N(6)-methyladenosine modification and its emerging roles in skeletal muscle development. *International Journal*

*of Biological Sci*ence, 17, 1682–1692.

LI, S., LU, C., KANG, L., LI, Q., CHEN, H., ZHANG, H., TANG, Z., LIN, Y., BAI, M. & XIONG, P. 2023. Study on correlations of BDNF, PI3K, AKT and CREB levels with depressive emotion and impulsive behaviors in drug-naïve patients with first-episode schizophrenia. *BMC Psychiatry* 23, 225.

LI, W., HE, Q. Z., WU, C. Q., PAN, X. Y., WANG, J., TAN, Y., SHAN, X. Y. & ZENG, H. C. 2015. PFOS Disturbs BDNF-ERK-CREB Signalling in Association with Increased MicroRNA-22 in SH-SY5Y Cells, *Biomedical Research International*, 302653.

LIAO, S., SUN, H. & XU, C. 2018. YTH domain: a family of N(6)-methyladenosine (m6A) readers. *Genomics Proteomics and Bioinformatics*, 16, 99–107.

LIM, W., MAYER, B., & PAWSON, T. 2014. Cell Signaling (1st ed.). *Garland Science.*

LIU, H., BEGIK, O., LUCAS, M. C., RAMIREZ, J. M., MASON, C. E., WIENER, D., SCHWARTZ, S., MATTICK, J. S., SMITH, M. A. & NOVOA, E. M. 2019. Accurate detection of m^6A RNA modifications in native RNA sequences. *Nature Communications*, 10, 4079.

LIU, J., SUN, L., ZHANG, J., GUO, J., CHEN, L., QI, D. & ZHANG, N. 2016. Aflatoxin B1, zearalenone and deoxynivalenol in feed ingredients and complete feed from central China. *Food Additives & Contaminants: Part B*, 9, 91-97.

LIU, J., YUE, Y., HAN, D., WANG, X., FU, Y., ZHANG, L., JIA, G., YU, M., LU, Z., DENG, X., DAI, Q., CHEN, W. & HE, C. 2014. A METTL3-METTL14 complex mediates mammalian nuclear RNA N6-adenosine methylation. *Nature Chemical Biology*, 2014, 10, 93–95.

LIU, S., DAI, H., ORFALI, R. S., LIN, W., LIU, Z. & PROKSCH, P. 2016. New Fusaric acid derivatives from the endophytic fungus *Fusarium oxysporum* and their phytotoxicity to barley leaves. *Journal of Agricultural and Food Chem*istry, 64, 3127-3132.

LIU, Z., ZHU, G., GETZENBERG, R. H. & VELTRI, R. W. 2015. The Upregulation of PI3K/Akt and MAP Kinase Pathways is Associated with Resistance of Microtubule-Targeting Drugs

in Prostate Cancer. *Journal of Cellular Biochemistry*, 116, 1341-1349.

LIVAK, K. J. & SCHMITTGEN, T. D. 2001. Analysis of relative gene expression data using real-time quantitative PCR and the 2(-delta delta C(T)} method. *Methods*, 25, 402-408.

LOPICCOLO, J., BLUMENTHAL, G. M., BERNSTEIN, W. B. & DENNIS, P. A. 2008. Targeting the PI3K/Akt/mTOR pathway: effective combinations and clinical considerations. *Drug Resistance Updates*, 11, 32-50.

LU, H., ZHANG, L. H., YANG, L., & TANG, P. F. 2018. The PI3K/Akt/FOXO3a pathway regulates regeneration following spinal cord injury in adult rats through TNF-α and p27kip1 expression. *International Journal of Molecular Medicine*, 41, 2832-2838.

MAGISTRETTI, P. J., & ALLAMAN, I. 2015. A cellular perspective on brain energy metabolism and functional imaging. *Neuron*, 86, 883-901.

MAHMOOD, T. & YANG, P. C. 2012. Western blot: technique, theory, and trouble shooting. *North American Journal of Medical Sciences*, 4, 429-434.

MAMUR, S., ÜNAL, F., YILMAZ, S., ERIKEL, E. & YÜZBAŞIOĞLU, D. 2020. Evaluation of the cytotoxic and genotoxic effects of mycotoxin fusaric acid. *Drug and Chemical Toxicology*, 43, 149–157.

MAMUR, S., YUZBASIOGLU, D., YILMAZ, S., ERIKEL, E. & UNAL, F. 2018. Assessment of cytotoxic and genotoxic effects of enniatin-A *in vitro*. *Food Additives & Contaminants: Part A*, *35*(8), 1633–1644.

MANNING, B. D. & TOKER, A. 2017. AKT/PKB signaling: Navigating the network. *Cell*, 169, 381-405.

MARTINI, M., DE SANTIS, M. C., BRACCINI, L., GULLUNI, F. & HIRSCH E. 2014. PI3K/Akt signaling pathway and cancer. *Annals of Medicine*, 46, 372-383.

MARTINKOVA, E., DONTENWILL, M., FREI, E. & STIBOROVA, M. 2009. Cytotoxicity of and DNA adduct formation by ellipticine in human U87MG glioblastoma cancer cells. *Neuroendocrinology Letters*, 1, 60-66.

MATTA, R. J. & WOOTEN, G. F. 1973. Pharmacology of fusaric acid in man. *Clinical Pharmacology & Therapeutics*, 14, 541-546.

MAY, H. D., WU, Q. & BLAKE, C. K. 2000. Effects of the Fusarium spp. mycotoxins fusaric acid and deoxynivalenol on the growth of Ruminococcus albus and Methanobrevibacter ruminantium. *Canadian Journal of Microbiology,* 46**,** 692-699.

MAYER, I. A., & ARTEAGA, C. L. 2016. The PI3K/Akt pathway as a target for cancer treatment. *Annual Review of Medicine*, 67, 11-28.

MEYER, K. D. & JAFFREY, S. R. 2017. Rethinking m6A Readers, Writers, and Erasers. *Annual Review of Cell and Developmental Biology,* 33, 319-342.

MEYER, K. D., PATIL, D. P., ZHOU, ZINOVIEV, J., SKABKIN, M. A., ELEMENTO, O., PESTOVA, T. V., QIAN, S. B. & JAFFREY, S. R. 2015. 5' UTR m6A promotes cap-independent translation. *Cell*, 163, 999–1010.

MÉZES, M. 2008. Mycotoxins and other contaminants in rabbit feeds. In: *Proc 9th World Rabbit Congr*ess, 491–506.

MILEĆEVIĆ, D. R., SKRINJAR, M. & BALTIĆ, T. 2010. Real and perceived risks for mycotoxin contamination in foods and feeds: Challenges for food safety control. *Toxins*, 4, 572-592.

MILLER, D. 1995. Fungi and mycotoxins in grain: implications for stored product research. *Journal of Stored Products Research*, 31, 1-6.

MIRICESCU, D., TOTAN, A., STANESCU-SPINU, I. I., BADOIU, S. C., STEFANI, C. & GREABU, M. 2021. PI3K/AKT/mTOR Signaling Pathway in Breast Cancer: From Molecular Landscape to Clinical Aspects. *International Journal of Molecular Sciences*, 22, 173.

MIRZA, O. M., BANC, R., COZMA-PERUŢ, A., LORENA, F., DOINA, M., MAŇES, J. & LOGHIN, F. 2015. Occurrence of *Fusarium* Mycotoxins in Wheat from Europe – A Review. *Acta Universitatis Cibiniensis Series E: FOOD TECHNOLOGY*, 19, 35-60.

MIZUI, T., TANIMA, Y., KOMATSU, H., KUMANOGOH, H. & KOJIMA, M. 2014. The Biological Actions and Mechanisms of Brain-Derived Neurotrophic Factor in Healthy and Disordered Brains. *Neuroscience and Medicine*, 2014, 183 – 195.

MOSMANN, T. 1983. Rapid colorimetric assay for cellular growth and survival: Application to proliferation and cytotoxicity assays. *Journal of Immunological Methods*, 65, 55-63.

MULLIS, K. & FALOONA, F. 1986. Specific synthesis of DNA in vitro via a polymerase-catalyzed chain reaction. *Methods in Enzymology*, 155, 335-350.

MURRAY, C. K., BECKIUS, M. L. & MCALLISTER, K. 2003. Fusarium proliferatum superficial suppurative thrombophlebitis. *Military Medicine*, 168, 426-427.

MURTHY, T. N. K., GIRISH, C. K., GOWDA, M. R. M. & RAMESH, K. R. 2005. Mycotoxins in feed and feed ingredients: A survey in India. *The Journal of Bombay Veterinary College*, 13, 94-95.

NAGATSU, T., HIDAKA, H., KUZUYA, H., TAKEYA, K., UMEZAWA, H. 1970. Inhibition of dopamine β-hydroxylase by fusaric acid (5-butylpicolinic acid) in vitro and in vivo. *Biochemical Pharmacology*, 19, 35-44.

NIEHAUS, E. M., VON BARGEN, K. W., ESPINO, J. J., PFANNMULLER, A., HUMPF, H. U. & TUDZYNSKI, B. 2014. Characterization of the fusaric acid gene cluster in Fusarium fujikuroi. *Applied Microbiology and Biotechnology,* 98, 1749-1762.

NELSON, P. E., DIGNANI, M. C. & ANAISSIE, E. J. 1994. Taxonomy, biology, and clinical aspects of *Fusarium* species. *Clinical Microbiology Rev*iews, 7, 479-504.

NOBLE, J. E., & BAILEY, M. J. A. 2009. Quantitation of protein. *Methods in Enzymology*, 463, 73–95.

OERUM, S., MEYNIER, V., CATALA, M. & TISNE, C. 2021. A comprehensive review of m6A/m6Am RNA methyltransferase structures. *Nucleic Acids Research*, 49, 7239–7255.

PALUMBO, J. D., O'KEEFFE T. S. & ABBAS, H. K. 2008. Microbial interactions with mycotoxigenic fungi and mycotoxins. *Toxin reviews*, 27, 261-285.

PARSONS, D. W., JONES, S., ZHANG, X., LIN, J. C., LEARY, R. J., ANGENENDT, P., MANKOO, P., CARTER, H., SIU, I. M., GALLIA, G. L., OLIVI, A., MCLENDON, R., RASHEED, B. A., KEIR, S., NIKOLSKAYA, T., NIKOLSKY, Y., BUSAM, D. A., TEKLEAB, H., DIAZ, L. A., JR., HARTIGAN, J., SMITH, D. R., STRAUSBERG, R. L., MARIE, S. K., SHINJO, S. M., YAN, H., RIGGINS, G. J., BIGNER, D. D., KARCHIN, R., PAPADOPOULOS, N., PARMIGIANI, G., VOGELSTEIN, B., VELCULESCU, V. E., & KINZLER, K. W. 2008. An Integrated Genomic Analysis of Human Glioblastoma Multiforme. *Science*, 321, 1807-1812.

PATIL, D. P., CHEN, C. K., PICKERING, B. F., CHOW, A., JACKSON, C., GUTTMAN, M. & JAFFREY, S. R. 2016. M6A RNA methylation promotes XIST-mediated transcriptional repression. *Nature*, 537, 369-373.

PAVLOVKIN, J., MISTRIK, I. & PROKOP, M. 2004. Some aspects of the phytotoxic action of fusaric acid on primary Ricinus roots. *Plant Soil and Environment,* 50**,** 397-401.

PENG, Y., WANG, Y., ZHOU, C., MEI, W. & ZENG, C. 2022. PI3K/AKT/mTOR pathway and its role in cancer therapeutics: are we making headway? *Frontiers in Oncol*ogy, 12, 819128.

PERAICA, M., RADIC, B., LUCIC, A. & PAVLOVIC, M. 1999. Toxic effects of mycotoxins in humans. *Bulletin of the World Health Organization,* 77**,** 754-766.

PING, X. L., SUN, B. F., WANG, L., XIAO, W., YANG, X., WANG, W. J., ADHIKARI, S., SHI, Y., LV, Y., CHEN, Y. S., ZHAO, X., LI, A., YANG, Y., DAHAL, U., LOU, X. M., LIU, X., HUANG, J., YUAN, W. P., ZHU, X. F., CHENG, T., ZHAO, Y. L., WANG, X., RENDTLEW-DANIELSEN, J. M., LIU, F., YANG, Y. G. 2014. Mammalian WTAP is a regulatory subunit of the RNA N6-methyladenosine methyltransferase. *Cell Research*, 24, 177-189.

PIRAYESH, S., ZAMANIZADEH, H. & MORID, B. 2015. Comparison of the production of fusaric acid produced by Fusarium oxysporum f. sp. lycopersici in different cultures with HPLC method. *International Journal of* Biosciences, 6**,** 355-359.

PORTA, C., PAGLINO, C., & MOSCA, A. 2014. Targeting PI3K/Akt/mTOR signaling in cancer.

Frontiers in Oncology, 4, 64.

PORTER, J. K., BACON, C. W., WRAY, E. M. & HAGLER, W. M. JR. 1995. Fusaric acid in Fusarium moniliforme cultures, corn, and feeds toxic to livestock and the neurochemical effects in the brain and pineal gland of rats. *Natural Toxins* 3, 91-100.

RANI, T. D., RAJAN, S., LAVANYA, L., KAMALALOCHANI, S. & BHARATHIRAJA, B. 2009. An overview of Fusaric acid production. *Advanced Biotechnology*, 8, 18-22.

REDDY, R. V., LARSON, C. A., BRIMER, G. E., FRAPPIER, B. L. & REDDY, C. S. 1996. Developmental toxic effects of fusaric acid in CD1 mice. *Bulletin of Environmental Contamination and Toxicol*ogy, 57, 354–360.

ROUNDTREE, I. A., LUO, G. Z., ZHANG, Z., WANG, X., ZHOU, T., CUI, Y., SHA, J., HUANG, X., GUERRERO, L., XIE, P., HE, E., SHEN, B., HE, C. 2017. YTHDC1 mediates nuclear export of N(6)-methyladenosine methylated mRNAs. *eLife*, 6, e31311.

RUIZ, J. A., BERNAR, E. M. & JUNG, K. 2015. Production of Siderophores Increases Resistance to Fusaric Acid in Pseudomonas protegens Pf-5. *PLOS ONE* 10, 1.

SACK, R. L. & GOODWIN, F. K. 1974. Inhibition of dopamine-b-hydroxylase in manic patients. A clinical trial and fusaric acid. *Archives of General Psychiatry*. 31, 649-654.

SANDLER, A., BEYER, U. & AMBERG, R. 1998. Systemic Fusarium oxysporum infection in an immunocompetent patient with an adult respiratory distress syndrome (ARDS) and extracorporal membrane oxygenation (ECMO). *Mycoses,* 41**,** 109-111.

SCHMITTGEN, T. D., & LIVAK, K. J. 2008. Analyzing real-time PCR data by the comparative C(T) method. *Nature Protocols*, 3, 1101-1108.

SEÇME, M., URGANCI, A. B. E., ÜZEN, R., ASLAN, A., TIRAŞ, F. 2023. Determination of the effects of fusaric acid, a mycotoxin, on cytotoxicity, gamma-H2AX, 8-hydroxy-2 deoxyguanosine and DNA repair gene expressions in pancreatic cancer cells. *Toxicon*, 231, 107179.

SHEIK-ABDUL, N. 2019. An investigation into the mitochondrial toxicity of fusaric acid

associated with aberrant energy metabolism and inflammatory responses. *Core.ac.uk*. Retrieved from https://core.ac.uk/download/pdf/304374553.pdf.

SEN, N. 2019. ER Stress, CREB, and Memory: A Tangled Emerging Link in Disease. *Neuroscientist*, 25, 420-433.

SHEN, W., PU, J., ZUO, Z., GU, S., SUN, J., TAN, B., WANG, L., CHENG, J. & ZUO, Y. 2022. The RNA demethylase ALKBH5 promotes the progression and angiogenesis of lung cancer by regulating the stability of the LncRNA PVT1. *Cancer Cell International,* 22, 353.

SHEPHARD, G. S. 2016. Current Status of Mycotoxin Analysis: A Critical Review. *Journal of AOAC International*, 4, 842-848. (Page 22, line 33).

SHI, H., WANG, X., LU, Z., ZHAO, B. S., MA, H., HSU, P. J., LIU, C. & HE, C. 2017. YTHDF3 facilitates translation and decay of N6-methyladenosine-modified RNA. *Cell Research*, 27, 315-328.

SHI, H., WEI, J. & HE, C. 2019. Where, When, and How: Context-Dependent Functions of RNA Methylation Writers, Readers, and Erasers. *Molecular Cell*, 74, 640-650.

SHIMSHONI, J., CUNEAH, O., SULYOK, M., KRSKA, R., GALON, N, SHARIR, B. & SHLOSBERG, A. 2013. Mycotoxins in corn and wheat silage in Israel. *Food additives & contaminants. Part A, Chemistry, analysis, control, exposure & risk assessment*, 30.

SINGH V. K., SINGH, H. B. & UPADHYAY, R. S. 2017. Role of Fusaric acid in the development of '*Fusarium* wilt' symptoms in tomato: physiological, biochemical and proteomic perspectives. *Plant Physiology and Biochem*istry, 118, 320-332.

SMITH, P. K., KROHN, R. I., HERMANSON, G. T., MALLIA, A. K., GARTNER, F. H., PROVENZANO, M. D., FUJIMOTO, E. K., GOEKE, N. M., OLSON, B. J., & KLENK, D. C. 1985. Measurement of protein using bicinchoninic acid. *Analytical Biochemistry*, 150, 76–85.

SOBRAL, M. M. C., FARIA, M. A., CUNHA, S. C. & FERREIRA, I. M. 2018. Toxicological interactions between mycotoxins from ubiquitous fungi: impact on hepatic and intestinal

human epithelial cells. *Chemosphere*, 202, 538–548.

SONI, P., GHUFRAN, M. S. & KANADE, S. R. 2018. Aflatoxin B1 induced multiple epigenetic modulators in human epithelial cell lines. *Toxicon*, 151, 119-128.

SPITALE, R. C., FLYNN, R. A., ZHANG, Q. C, CRISTALLI, P., LEE, B., L., JUNG, J. W., KUCHELMEISTER, H. Y., BATISTA, P. J., TORRE, E. A., KOOL, E. T. & CHANG, H. Y. 2015. Structural imprints in vivo decode RNA regulatory mechanisms. *Nature*, 519, 486–490.

SRIVASTAVA, S., SINGH, V. P. & RANA, M. 2020. Fusaric acid: a potent vivotoxin. *European Journal of Molecular and Clinical Medicine,* 7, 2020.

STACK JR, B. C., HANSEN, J. P., RUDA, J. M., JAGLOWSKI, J., SHVIDLER, J. & HOLLENBEAK, C. S. 2003. Fusaric acid: a novel agent and mechanism to treat HNSCC. *Otolaryngology--Head and Neck Surgery,* 131**,** 54-60.

STACK JR, B. C., YE, J., WILLIS, R., HUBBARD, M. & HENDRICKSON, H. P. 2014. Determination of oral bioavailability of fusaric acid in male Sprague-Dawley rats. *Drugs in Research and Development,* 14**,** 139-145.

STUPP, R., MASON, W. P., VAN DEN BENT, M. J., WELLER, M., FISHER, B., TAPHOORN, M. J., BELANGER, K., BRANDES, A. A., MAROSI, C., BOGDAHN, U., CURSCHMANN, J., JANZER, R. C., LUDWIN, S. K., GORLIA, T., ALLGEIER, A., LACOMBE, D., CAIRNCROSS, J. G., EISENHAUER, E. & MIRIMANOFF, O. R. 2005. Radiotherapy plus concomitant and adjuvant temozolomide for glioblastoma. *New England Journal of Med*icine, 352, 987–996.

STRIET, E., SCHWAB, C., SULYOK, M., NAEHRER, K., KRSKA, R. & SCHATZMAYR, G. 2013. Multi-mycotoxin screening reveals the occurrence of 139 different secondary metabolites in feed and feed ingredients. *Toxins,* 5**,** 504-523.

STUDT, L., JANEVSKA, S., NIEHAUS, E. M., BURKHARDT, I., ARNDT, B., SIEBER, C. M. K., HUMPF, H. U., DICKSCHAT, J. S. & TUDZYNSKI, B. 2016. Two separate key enzymes and two pathway-specific transcription factors are involved in fusaric acid biosynthesis in Fusarium fujikuroi. *Environmental Microbiology*, 18, 936-956.

SUBRAMANIAM, R., NASMITH, C. G., HARRIS, L. J., OUELLET, T. 2009. Insight into *Fusarium*-cereal pathogenesis. *Molecular Plant-microbe Interactions*. 319-336.

SUN, L., WANG, S., HU, C. & ZHANG, X. 2011. Down-regulation of PKHD1 induces cell apoptosis through PI3K and NF-κB pathways. *Experimental Cell Research*, 317, 932-940.

TERASAWA, F. & KAMEYAMA, M. 1971. The clinical trial of a new hypotensive agent, fusaric acid (5-butylpicolinic acid): the preliminary report. *Japanese Circulatory Journal*, 5, 339–357.

TOH, J. D. W., CROSSLEY, S. W. M., BRUEMMER, K. J., GE, E. J., HE, D., IOVAN, D. A. & CHANG, C. J. 2020. Distinct RNA N-demethylation pathways catalyzed by nonheme iron ALKBH5 and FTO enzymes enable regulation of formaldehyde release rates. *Proceedings of the National Academy of Sciences*, 117, 25284-25292.

TOWBIN, H., STAEHELIN, T., & GORDON, J. 1979. Electrophoretic transfer of proteins from polyacrylamide gels to nitrocellulose sheets: Procedure and some applications. *Proceedings of the National Academy of Sciences*, 76, 4350–4354.

USHIO, Y., KOCHI, M., HAMADA, J., KAI, Y. & NAKAMURA, H. 2005. Effect of surgical removal on survival and quality of life in patients with supratentorial glioblastoma. *Neurologia Medico-Chirurgica*, 45, 454–60.

VANHAESEBROECK, B. & WATERFIELD, M. D. 1999. Signaling by distinct classes of phosphoinositide 3-kinases. *Experimental Cell Research*, 253, 239-254.

VERDUGO, E., PUERTO, I. & MEDINA, M. Á. 2022. An update on the molecular biology of glioblastoma, with clinical implications and progress in its treatment. *Cancer Communications*, 42, 1083-1111.

VOSS, K., PORTER, J., BACON, C., MEREDITH, F. & NORRED, W. 1999. Fusaric acid and modification of the subchronic toxicity to rats of fumonisins in F. moniliforme culture material. *Food and Chemical Toxicology,* 37**,** 853-861.

WALKER, J. M. 1996. *The Protein Protocols Handbook*, Springer Science & Business Media.

WALKER, J. M. 2009. *The Protein Protocols Handbook* (3rd ed.). Humana Press.

WANG, J., ZHANG, J., MA, Y., ZENG, Y., LU, C., YANG, F., JIANG, N., ZHANG, X., WANG, Y., XU, Y., HOU, H., JIANG, S., ZHUANG, S. 2021. WTAP promotes myocardial ischemia/reperfusion injury by increasing endoplasmic reticulum stress via regulating m^6A modification of ATF4 mRNA. *Aging*, 13, 11135-11149.

WANG, L., ZHOU, K., FU, Z., YU, D., HUANG, H., ZANG, X. & MO, X. 2017. Brain development and AKT signalling: the crossroads of signalling pathway and neurodevelopmental diseases. *Journal of Molecular Neuroscience*, 61, 379-384.

WANG, S., ZHANG, J., WU, X., LIN, X., LIU, X. M., ZHOU, J. 2020. Differential roles of YTHDF1 and YTHDF3 in embryonic stem cell-derived cardiomyocyte differentiation. *RNA Biology*, 18, 1354-1363.

WANG, T., KONG, S., TAO, M. & JU, S. 2020. The potential role of RNA N6-methyladenosine in cancer progression. *Molecular Cancer*, 19, 88.

WANG, X., FENG, J., XUE, Y., GUAN, Z., ZHANG, D., LIU, Z., GONG, Z., WANG, Q., HUANG, J., TANG, C., ZOU, T., YIN, P. 2016. Structural basis of N6-adenosine methylation by the METTL3–METTL14 complex. *Nature*, 534, 575-578.

WANG, X., LU, Z., GOMEZ, A., HON, G. C., YUE, Y., HAN, D., FU, Y., PARISIEN, M., DAI, Q., JIA, G., REN, B., PAN, T. & HE, C. 2014. N6-methyladenosine-dependent regulation of messenger RNA stability. *Nature*, 505, 117-120.

WANG, X., ZHAO, B. S., ROUNDTREE, I. A., LU, Z., HAN, D., MA, H., WENG, X., CHEN, K., SHI, H. & HE, C. 2015. N(6)-methyladenosine modulates messenger RNA translation efficiency. *Cell*, 161, 1388–1399.

WANG, Y., LI, Y., TOTH, J. I., PETROSKI, M. D., ZHANG, Z., ZHAO, J. C. 2014. N6-methyladenosine modification destabilizes developmental regulators in embryonic stem cells. *Nature Cell Biology*, 16, 191-8.

WEI, C. M., GERSHOWITZ, A. & MOSS, B. 1975. Methylated nucleotides block 5′ terminus of HeLa cell messenger RNA. *Cell*, 4, 379-386.

WEN, A. Y., SAKAMOTO, K. M. & MILLER, L, S. 2010. The role of the transcription factor CREB in immune function. *Journal of Immunology*, 185, 6413-6419.

WIECHELMAN, K. J., BRAUN, R. D. & FITZPATRICK, J. D. 1988. Investigation of the bicinchoninic acid protein assay: identification of the groups responsible for color formation. *Analytical Biochemistry*, 175, 231-237.

WIEDMER, L., EBERLE, S. A., BEDI, R. K., ŚLEDŹ, P. & CAFLISCH, A. 2019. A Reader-Based Assay for m^6A Writers and Erasers. *Analytical Chemistry*, 91, 3078-3084.

WIENER, D. & SCHWARTZ, S. 2021. The epitranscriptome beyond m6A. *Nature Reviews Genetics*, 22, 31-119.

WINTER, G. & PEREG, L. 2019. A review of the relation between soil and mycotoxins: Effect of aflatoxin on field, food and finance. *European Journal of Soil Science*, 4, 882-897.

WU, J., GAN, Z., ZHUO, R., ZHANG, L., WANG, T. & ZHONG, X. 2020. Resveratrol Attenuates Aflatoxin B_1-Induced ROS Formation and Increase of m^6A RNA Methylation. *Animals (Basel)*, 10, 677.

WU, L., WU, D., NING, J., LIU, W & ZHANG, D. 2019. Changes of N6-methyladenosine modulators promote breast cancer progression. *BMC Cancer*, 19, 326.

WU, K., JIA, S., ZHANG, J., ZHANG, C., WANG, S., RAJPUT, S. A., SUN, L. & QI, D. 2021. Transcriptomics and flow cytometry reveals the cytotoxicity of aflatoxin B1 and aflatoxin M1 in bovine mammary epithelial cells. *Ecotoxicology and Environmental Safety*, 209, 111823.

WU, Y., HE, H., ZHENG, K., QIN, Z., CAI, N., ZUO, S., & ZHU, X. 2024. RNA M6A modification shaping cutaneous melanoma tumor microenvironment and predicting immunotherapy response. *Pigment Cell & Melanoma Research*, 37, 496–509.

WU, Z., XU, C., WANG, H., GAO, S., WU, S. & BAO, W. 2020. Transcriptome-wide assessment of the m6A methylome of intestinal porcine epithelial cells treated with deoxynivalenol. *Research Square*, 1–20.

XIAO, W., ADHIKARI, S., DAHAL, U., CHEN, Y. S., HAO, Y. J., SUN, B. F., SUN, H. Y., LI, A., PING, X. L., LAI, W. Y., WANG, X., MA, H. L., HUANG, C. M., YANG, Y., HUANG, N., JIANG, G. B., WANG, H. L., ZHOU, Q., WANG, X. J., ZHAO, Y. L. & YANG, Y. G. 2016. Nuclear m6A Reader YTHDC1 Regulates mRNA Splicing. *Molecular Cell*, 61, 507-519.

XIAO, X., LI, B. X., MITTON, B. A., IKEDA, A. K. & SAKAMOTO, K. M. 2010. Targeting CREB for cancer therapy: friend or foe. *Current cancer drug targets*, 10, 384 – 391.

YANG, Y., HSU, P. J., CHEN, Y. S. & YANG Y, G. 2018. Dynamic transcriptomic m^6A decoration: writers, erasers, readers and functions in RNA metabolism. *Cell Research*, 28, 616-624.

YANG, X., SHAO, F., GUO, D., WANG, W., WANG, J, ZHU, R., GAO, Y., HE, J. &LU, Z. 2021. WNT/B-catenin-suppressed FTO expression increases m6A of c-Myc mRNA to promote tumor cell glycolysis and tumorigenesis. *Cell death and Disease*, 12, 462.

YANG, Y., SHEN, F., HUANG, W., QIN, S., HUANG, J. T., SERGI, C., YUAN, B. F., LIU, S. M. 2019. Glucose is involved in the dynamic regulation of m6A in patients with type 2 diabetes. *Journal of Clinical Endocrinology and Metabolism*, 104, 665–673.

YANG, Z., ZHANG, S., XIONG, J., XIA, T., ZHU, R., MIAO, M., LI, K., CHEN, W., ZHANG, L., YOU, Y. & YOU, B. 2024. The m^6A demethylases FTO and ALKBH5 aggravate the malignant progression of nasopharyngeal carcinoma by coregulating ARHGAP35. *Cell Death Discovery,* 10, 43.

YE, F., WANG, X., TU, S., ZENG, L., DENG, X. LUO, W. & ZHANG, Z. 2021. The effects of NCBP3 on METTL3-mediated m6A RNA methylation to enhance translation process in hypoxic cardiomyocytes. *Journal of Cellular and Molecular Medicine*, 25, 8920-8928.

YIANNIKOURIS, A. & JOUANY, J. P. 2002. Mycotoxins in feeds and their fate in animals: a review. *Animal Research,* 51**,** 81-99.

YIN, E. S., RAKHMANKULOVA, M., KUCERA, K., DE SENA FILHO, J. G., PORTERO, C. E., NARVAEZ-TRUJILO, A., HOLLEY, S. A. & STROBEL, S. A. 2015. Fusaric acid induces a notochord malformation in zebrafish via copper chelation. *Biometals*, 28, 783-789.

ZAIN, M. E. 2011. Impact of mycotoxins on humans and animals. *Journal of Saudi Chemical Society,* 15**,** 129-144.

ZHANG, G., MI, W., WANG, C., LI, J., ZHANG, Y., LIU, N., JIANG, M., JIA, G., WANG, F., YANG, G., ZHANG, L., WANG, J., FU, Y. & ZHANG, Y. 2023. Targeting AKT induced Ferroptosis through FTO/YTHDF2-dependent GPX4 m6A methylation up-regulating and degradating in colorectal cancer. *Cell Death Discovery.* 9, 457.

ZHANG, L., ZHAO, H., ZHANG, X., CHEN, L., ZHAO, X., BAI, X. & ZHANG, J. 2013. Nobiletin protects against cerebral ischemia via activating the p-Akt, p-CREB, BDNF and Bcl-2 pathway and ameliorating BBB permeability in rat. *Brain Research Bulletin*, 96, 45-53.

ZHANG, Y., CHEN, W., ZHENG, X., GUO, Y., CAO, J. & ZHANG, Y. 2021. Regulatory role and mechanism of m6A RNA modification in human metabolic diseases. *Molecular Therapy Oncolytics*, 22, 52–63.

ZHANG, Y., GENG, X., LI, Q., XU, J., TAN, Y., XIAO, M., SONG, J., LIU, F., FANG, C. & WANG, H. 2020. m6A modification in RNA: biogenesis, functions and roles in gliomas. *Journal of Experimental and Clinical Cancer Res*earch, 39, 192.

ZHAO, M., ZHOU, A., XU, L. & ZHANG, X. 2014. The role of TLR4-mediated PTEN/PI3K/AKT/NF-κB signaling pathway in neuroinflammation in hippocampal neurons. *Neuroscience*, 269, 93-101.

ZHAO, Q., ZHAO, Y., HU, W., ZHANG, Y., WU, X., LU, J., LI, M., LI, W., WU, W., WANG, J., DU, F., JI, H., YANG, X., XU, Z., WAN, L., WEN, Q., LI, X., CHO, C. H., ZOU, C., SHEN, J. & XIAO, Z. 2020. m6A RNA modification modulates PI3K/Akt/mTOR signal pathway in Gastrointestinal Cancer. *Theranostics*, 10, 9528-9543.

ZHAO, Y., SHI, Y., SHEN, H. & XIE, W. 2020. M6A-binding proteins: the emerging crucial performers in epigenetics. *Journal of Hematology and Oncol*ogy, 13, 35.

ZHAO, Z., CAI, Q., ZHANG, P., HE, B., PENG, X., TU, G., PENG, W., WANG, L., YU, F. & WANG, X. 2021. N6-Methyladenosine RNA Methylation Regulator-Related Alternative

Splicing (AS) Gene Signature Predicts Non–Small Cell Lung Cancer Prognosis. *Frontiers in Molecular Biosciences,* 8, 657087.

ZHENG, G., DAHL, J. A., NIU, Y., FEDORCSAK, P., HUANG, C. M., LI, C. J., VÅGBØ, C. B., SHI, Y., WANG, W. L., SONG, S. H., LU, Z., BOSMANS, R. P., DAI, Q., HAO, Y. J., YANG, X., ZHAO, W. M., TONG, W. M., WANG, X. J., BOGDAN, F., FURU, K., FU, Y., JIA, G., ZHAO, X., LIU, J., KROKAN, H. E., KLUNGLAND, A., YANG, Y. G. & HE, C. 2013. ALKBH5 is a mammalian RNA demethylase that impacts RNA metabolism and mouse fertility. *Molecular Cell*, 49, 18-29.

ZHONG, L., LIAO, D., ZHANG, M., ZENG, C., XINCHUNG, L., ZHANG, R., MA, H. & KANG, T. 2019. YTHDF2 suppresses cell proliferation and growth via destabilizing the EGFR mRNA in hepatocellular carcinoma. *Cancer letters*, 442, 252-261.

ZHOU, P., WU, M., YE, C., XU, Q. & WANG, L. 2019. Meclofenamic acid promotes cisplatin-induced acute kidney injury by inhibiting fat mass and obesity-associated protein-mediated m^6A abrogation in RNA. *Journal of Biological Chemistry*. 294, 16908-16917.

ZOU, Z., SEPICH-POORE, C., ZHU, X., WEI, J. & HE., C. 2023. The mechanism underlying redundant functions of the YTHDF proteins. *Genome* Biology, 24, 17.

APPENDIX A

ELISA Assay

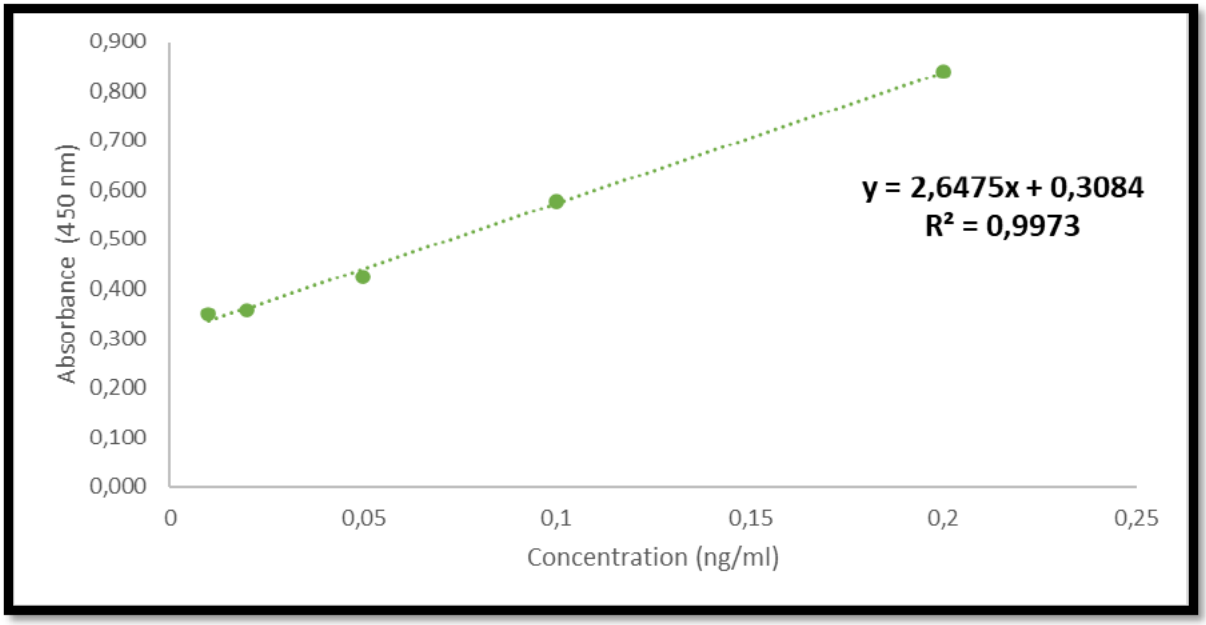

Figure 5.1: Standard curve representing the absorbance of different m6A concentrations in U87MG cells

Table 3: RNA concentrations for standardization

Sample	RNA concentration (ng/µl)	Volume of RNA (µl)	Final Concentration of Sample (ng/µl)	Final Volume (µl)
Control	2004,4	0,998	200	10
FA Treatment	866,8	2,307	200	10

APPENDIX B

BCA Assay

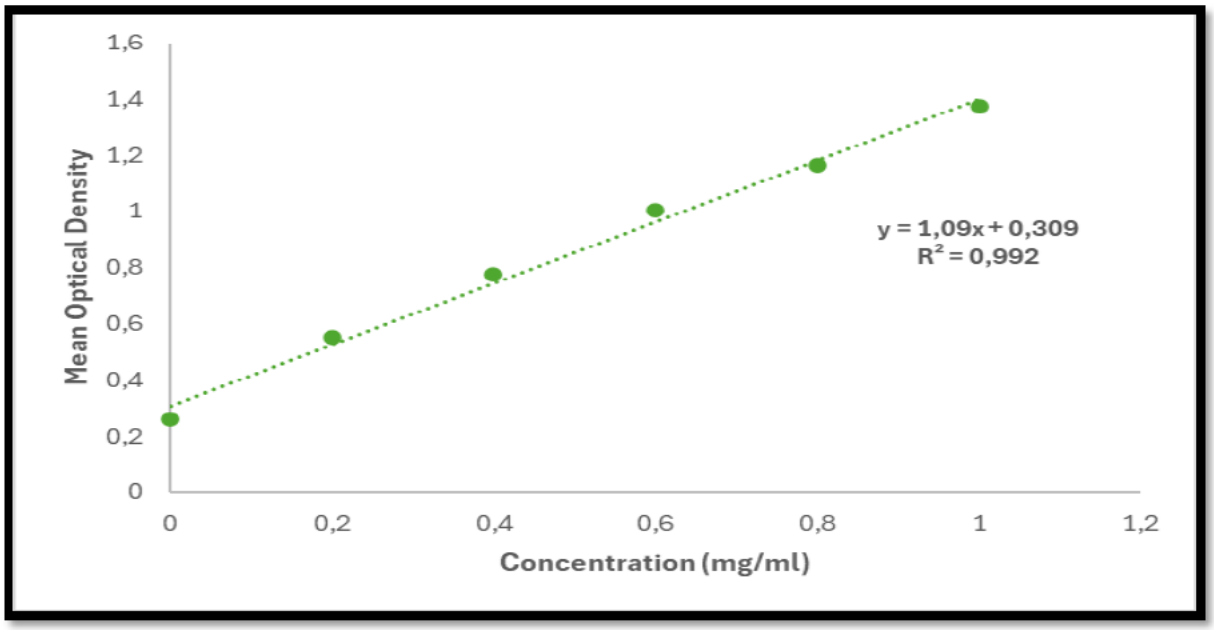

Figure 5.2: Standard curve representing the absorbance of different BSA concentrations used for protein concentration determination in each sample.

Table 4: Protein standardization (concentration = 1.5 mg/ml; Final volume = 150 µl)

Sample	Mean Absorbance	Protein Concentration (mg/ml)	Volume of Protein Stock (µl)	Volume of Cytobuster (µl)	Volume of Laemmli Buffer (µl)
Control	1,53	1,12	93,73	56,27	37,5
FA Treatment	1,66	1,24	84,87	65,13	37,5

APPENDIX C

UNIVERSITY OF KWAZULU-NATAL
INYUVESI YAKWAZULU-NATALI

18 October 2024

Mr Mcaylin Matadin (218027696)
School of Lab Med & Medical Sc

Dear Mr Matadin,

Protocol reference number: BREC/00007786/2024 Project title: Fusaric acid-induced brain toxicity: unravelling the molecular and epigenetic effects through m6A methylation
Degree: MMedSc

EXPEDITED APPLICATION
APPROVAL LETTER

A sub-committee of the Biomedical Research Ethics Committee has considered and noted your application.

The conditions have been met and the study is given full ethics approval and may begin as from 18 October 2024. Please ensure that any outstanding site permissions are obtained and forwarded to BREC for approval before commencing research at a site.

This approval is valid for one year from 18 October 2024. To ensure uninterrupted approval of this study beyond the approval expiry date, an application for recertification must be submitted to BREC on RIG on the appropriate BREC form 2-3 months before the expiry date.

Any amendments to this study, unless urgently required to ensure safety of participants, must be approved by BREC prior to implementation.

Your acceptance of this approval denotes your compliance with South African National Research Ethics Guidelines (2024), South African National Good Clinical Practice Guidelines (2020) (if applicable) and with UKZN BREC ethics requirements as contained in the UKZN BREC Terms of Reference and Standard Operating Procedures, all available at http://research.ukzn.ac.za/Research-Ethics/Biomedical-Research-Ethics.aspx.

BREC is registered with the South African National Health Research Ethics Council (REC-290408-009). BREC has US Office for Human Research Protections (OHRP) Federal-wide Assurance (FWA 678).

The sub-committee's decision will be noted by a full Committee at its next meeting taking place on 12 November 2024.

Yours sincerely,

[redacted]
Prof S Singh
Chair: Biomedical Research Ethics Committee